Development of methods to evaluate the performance of snowboard wrist protectors

Caroline Adams

A thesis submitted in partial fulfilment of the requirements of Sheffield Hallam University for the degree of Doctor of Philosophy

July 2018

Abstract

In snowboarding, the wrist is the most common injury site, as snowboarders often put their arms out to cushion a fall. This can result in a compressive load through the carpals coupled with wrist hyperextension, leading to ligament sprains or carpal and forearm bone fractures. Wrist protectors are worn by snowboarders in an effort to reduce injury risk, by decreasing peak impact forces and limiting wrist extension to prevent hyperextension during falls. There is no international standard or universally accepted performance specification that snowboarding wrist protectors should conform to, resulting in an inability to judge which designs offer the best protection. The aim of this project was to develop mechanical test methods to evaluate the protective characteristics of snowboarding wrist protectors.

Two new mechanical tests and accompanying surrogates were developed to characterise snowboarding wrist protectors. A quasi-static test to measure the rotational stiffness of protectors was developed. The test setup uses a surrogate attached to a bespoke rig mounted to standard material test equipment to facilitate the measure of angular wrist extensions over a range of torques. To ensure products were tested in a representative manner, three surrogate arms with increasing design complexity were developed and compared using the quasi-static test. A surrogate based on a 3D scan of a forearm was found to be the most representative and offer the best differentiation between products.
An impact test replicating injurious snowboard falls was developed to measure peak vertical force, energy absorption and wrist extension angle. The impact test mimics boundary conditions known to result in a wrist fracture by applying a load to an instrumented surrogate via a pendulum. Experimental tests validated that both setups can detect differences in protector design. Twelve products were tested with each setup, differences in quasi-static rotational stiffness; peak vertical force, time to peak and energy absorption during impact were observed between products. However, none of the tested products effectively lower the force below fracture threshold. Future research should focus on improving the bimodality of the surrogate and investigating the influence of protector design on injury risk for a range of inbound conditions.

Acknowledgements

No man is an island. This project would not have been possible without the support of numerous people who have travelled with me on this PhD journey.

Firstly, I would like to acknowledge the support of my supervisors: Nick Hamilton, Tom Allen and David James, you inspired me to persevere. Your patience, knowledge, enthusiasm and soldering assistance has been unwavering throughout the project. I would like to extend this thanks to all the members of the Centre for Sports Engineering Research, for your advice and willingness to be measured. Without the support and guidance of Terry Senior, the rigs would have never been developed.

To my fellow PhD students in Chestnut Court, it has been a privilege to share a portacabin with you all. Thanks for your friendship, engagement in scientific and not so scientific discussion and feedback. It has helped me grow as a researcher and kept me sane. Where else could I climb around a table, talk volleyball tactics and discuss regression analysis while eating obscene amounts of cake?!

To my family, friends and all those at The Crowded House Church, I am grateful for your unwavering encouragement and love. Your steadfast care has been amazing. You have supported me through two fractures, proofread drafts, fed me, sewn lines on wrist protectors and pointed me to our saviour and the cross, amongst countless other blessings.

Contents

10 Introduction

This thesis documents the development of new methods to evaluate the protective characteristics of snowboarding wrist protectors. This first chapter explains the motivation for the research and outlines the aim this body of work set out to achieve.

10.1 Motivation for Research

Snowboarding is a popular sport, enjoyed by an estimated 10-15 million people worldwide (Michel et al. 2013). Resorts, artificial and indoor slopes are spread across six of the seven continents. It has been an Olympic sport since 1998 (Russel, Hagel and Goulet, 2010), half-pipe, giant parallel slalom, parallel slalom, slopestyle and snowboard cross are all currently Olympic snowboard disciplines for men and women. The risk of sustaining an injury while snowboarding is higher than alpine skiing (Hagel, 2005) and injury rates are among the highest of all sports in the 9 to 19-year- old age group (Michaud, Renaud and Narring, 2001).

In snowboarding, the wrist is the most frequently injured region (K. Sasaki et al. 1999; Ekeland, Rødven and Heir, 2017; Costa-Scorse et al., 2017), with wrist fractures a common occurrence (Russell, Hagel and Francescutti, 2007). Snowboarders often attempt to cushion a fall with outstretched hands. In this scenario, impact loads can be transmitted along the upper extremity as an axial compression force and extension torque resulting in wrist hyperextension, which can lead to ligament sprains or carpal and forearm bone fractures (Whiting and Zernicke, 2008; Bartlett and Bussey, 2013).

Different preventative measures can be adopted: changing the biomechanical response of the body; altering how the applied load is distributed and reducing injury risk through the application of engineering design and appropriate regulation (McIntosh, 2012), including i) the design of ski areas, such as terrain park jumps (McNeil, Hubbard and Swedberg, 2012; Levy *et al.*, 2015) and ii) personal protective equipment (PPE) such as helmets (Kuhn *et al.*, 2017). PPE is worn in a variety of sporting contexts. In many cases, its design is stipulated by governing bodies or international standards (European Committee for Standardization, 2007; Parsons, 2014; International Organization for Standardization, 2016b). Governing bodies specify a series of parameters products should conform to when tested in a laboratory environment. Current safety standards to

assess PPE typically use surrogates as an artificial representation of humans, to enable products to be tested under injurious conditions.

Wrist protectors have been adopted amongst a limited number of snowboarders as a preventative measure to i) limit peak impact forces, ii) absorb or shunt the impact energy, and iii) prevent hyperextension (Hwang and Kim, 2004; Michel *et al.*, 2013). At present, a range of different designs are commercially available, but unlike other PPE, no standard exists stipulating protective performance parameters snowboarding wrist protectors should meet (Michel *et al.*, 2013). Unlike a wrist brace worn post-injury, wrist protectors (synonymous to wrist guards) aim to prevent wrist injuries. Whilst some studies have shown them to be an effective device in reducing the risk of injury (Machold, Kwasny and Eisenhardt, 2005; Russell, Hagel and Francescutti, 2007) others claim they have little effect or just transfer the load elsewhere (Chow, Corbett and Farstad, 1996; Hagel, 2005). There is little consensus as to which particular design features offer the most effective form of protection (Kim and Lee, 2011).

Previous research has sought to document the prevalence of injuries; facilitate a greater understanding of falls from a biomechanics perspective; validate the value of wrist protectors in the prevention of snowboarding upper extremity injuries. Following a call in 2013 (Michel *et al.*, 2013), the ISO/CD 20320 was set up to develop a standard for these products (International Organization for Standardization, 2016a). This PhD project is concerned with establishing mechanical tests and surrogates, to evaluate the protective performance of wrist protectors in scenarios representative of snowboarding falls.

For any surrogate, the aim is 'biofidelity', which is the term used to describe the exactness with which a given surrogate approximates the behaviour of a human when subjected to comparable loading conditions (Crandall et al., 2011). For this project, surrogate biofidelity includes but is not limited to shape, material characteristics, mechanical response and range of joint motion. The developed tests will attempt to achieve a compromise between biofidelic realism and a repeatable laboratory-based mechanical test. The developed tests will enable the effect of different design parameters on protective performance to be evaluated for a range of products across a range of loading scenarios.

As a member of the British Standards Institute (Bsi), this body of work will support the International Organization for Standardization in the implementation of ISO/CD 20320 'Protective clothing for use in Snowboarding -- Wrist Protectors -- Requirements and test methods'. This, in turn, will influence the design of next-generation wrist protectors, providing consumers with more transparency and ultimately decreasing the number of wrist injuries in the popular sport of snowboarding.

10.2 Aim and Objectives

The aim of this thesis is to develop test methods to evaluate the protective characteristics of snowboarding wrist protectors. This will be achieved through the following objectives:

1. To investigate current practices in protective equipment testing and determine performance criteria to evaluate snowboarding wrist protectors
2. To identify boundary conditions, the mechanical test should replicate to characterise snowboarding wrist protectors
3. To develop and validate mechanical tests to characterise snowboarding wrist protectors
4. To compare the protective characteristics of a range of wrist protectors using the developed methods

10.3 Thesis Structure

Based on the total design activity model of Pugh (1991) four stages were identified for this project: a) existing research, b) product design specification, c) test method development, d) evaluation of snowboarding wrist protectors. Figure 10.1 outlines each stage in the context of this thesis and how they each contribute to the project’s objectives.

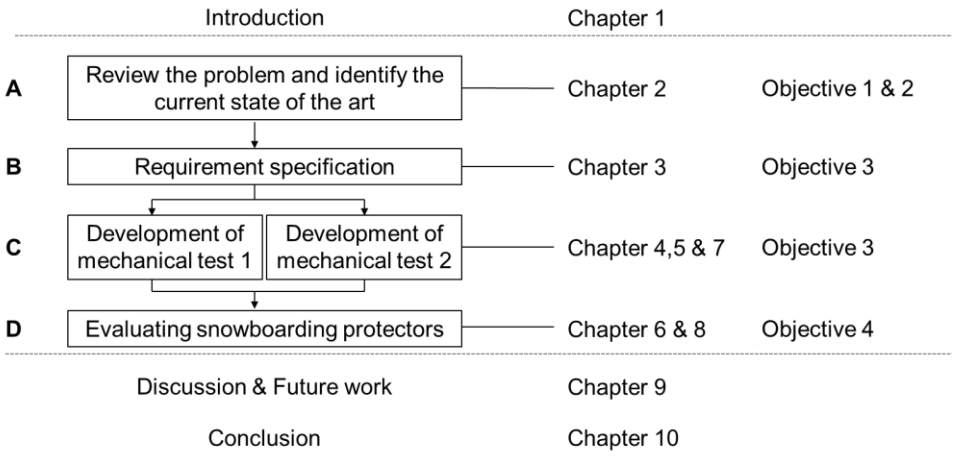

Figure 10.1 Thesis chapter structure linked to the design process model

11 Literature Review

11.1 Introduction

This chapter reviews the relevant literature in five sections. Section 2.2 outlines the research problem and need for prevention through examining wrist injury rates and patterns in snowboarding. Fracture mechanisms are reviewed in section 2.3, to aid in the prevention of wrist injuries, through an understanding of injury causation. Section 2.4 concerns the design of commercially available wrist protectors, to understand the current mechanisms used to prevent injury and identify protective performance criteria that tests should measure. Section 2.5 reviews the experimental recreation of falls to inform the selection of input parameters and boundary conditions the developed test should include. Section 2.6 reviews and evaluates test setups, including existing safety standards and mechanical surrogates, to help inform the development of new mechanical tests.

11.2 Wrist Injuries

The wrist is one of the most common fracture sites in the human body (Schuit et al. 2004). Wrist injuries place a significant burden on health services, in the United States Englander et al. (1996) predict that medical costs associated with fall injuries will reach $85.4 billion dollars by 2020. Sports injuries are some of the most common injuries in western societies, and their treatment can be difficult, expensive and time-consuming. The development of preventative strategies, such as the design of wrist protection through a new test method, are justified on medical as well as economic grounds (Parkkari et al. 2001).

11.2.1 Wrist anatomy

The wrist acts as a bridge connecting the hand to the forearm. The wrist complex consists of a collection of 15 bones surrounded by soft tissue structures; the distal ends of radius and ulna, eight carpal bones and the proximal portions of the five metacarpal bones (Kijima and Viegas, 2009). Both the bones and the soft tissue exhibit viscoelastic properties (Payne et al. 2015; Panjabi et al. 1973). The wrist is made up of four joints: radioulnar, radiocarpal, midcarpal, and carpometacarpal (Figure 11.1). Articular cartilage covers the ends of bones at the joints, providing a smooth substance enabling

the bones to slide against each other without causing damage. Relative to the forearm the hand is capable of 3 degrees of freedom (Figure 11.2). A biofidelic surrogate is recommended to evaluate the protective capacity of wrist protectors. Given the complexity of the joint with 3 degrees of freedom achieved through different rate-dependent materials, pragmatically a number of simplifications will be necessary when developing a surrogate.

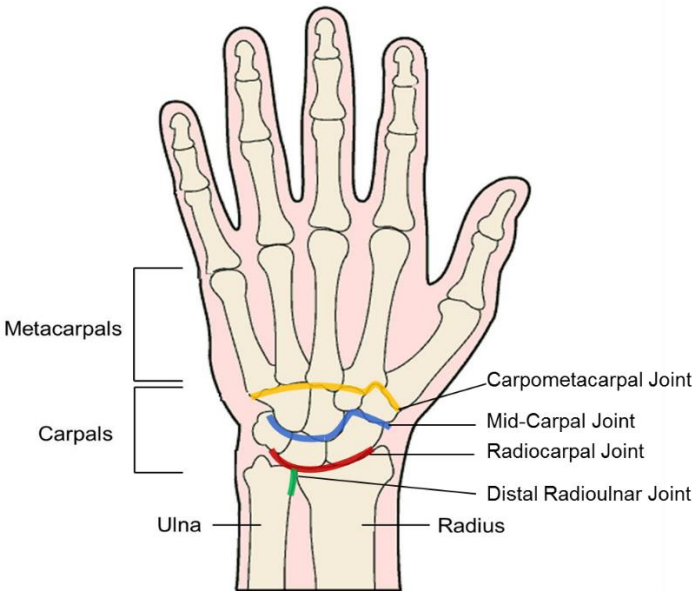

Figure 11.1: Wrist anatomy

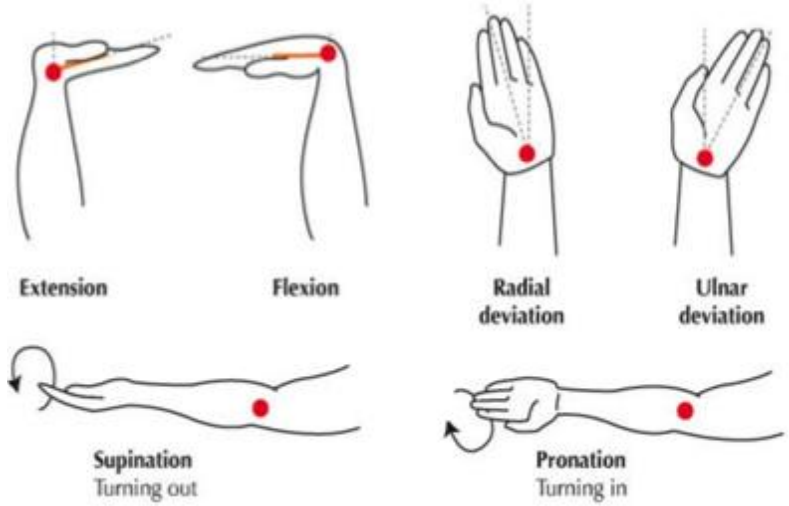

Figure 11.2: Wrist Motion (adapted from Medlej, 2014)

11.2.2 Injury Causality

Falls are a common cause of wrist injuries (Chiu and Robinovitch, 1998). Snowboarders, inline skaters and the elderly have all been identified as groups with a high proportion of fall-related upper extremity injuries. The annual incidence of distal radius fractures

for persons over 65 years is reported to be 7–10 per 1000 person-years (Kim and Ashton-Miller, 2003). Fall-related wrist injuries account for 37% of all inline skating injuries (Schieber *et al.*, 1996) and 69-93% of snowboarding injuries (Hagel, 2005). Individuals use their upper extremities to help manage a fall event, instinctively throwing their arms out to protect the head or torso. This action is associated with the potential risk for a wrist injury, a risk-benefit ratio that seems reasonable given the potential severity of head or hip injury in the absence of such a strategy (DeGoede, Ashton-Miller and Schultz, 2003). Directly falling onto a straight arm has been shown to increase the risk of injury (DeGoede, Ashton-Miller and Schultz, 2003) and is often considered to be the worst case. To protect the head and torso from hitting the ground, there needs to be a level of elbow and shoulder extension.

11.2.3 Wrist Fractures

Wrist injuries vary in severity and are generally classified as a sprain, contusion or fracture. Sprains can heal in a few weeks, whereas repairing a displaced fracture requires surgery and permanent inserts. In some instances, the pain never subsides, and there is a permanent loss of movement. A fracture occurs when the bone cannot support an applied force and fails. In the case of a fall onto an outstretched arm, a load is transmitted along the upper extremity as an axial compression force and torque (Figure 11.3). This may result in wrist hyperextension, wrist sprains or fractures (Whiting & Zernicke 2008; Bartlett & Bussey 2013). Hyperextension is defined as the extension of the wrist beyond its normal healthy range. Distal radius fractures are the most common forearm fracture and account for approximately 16% of all skeletal fractures (Porrino, 2015).

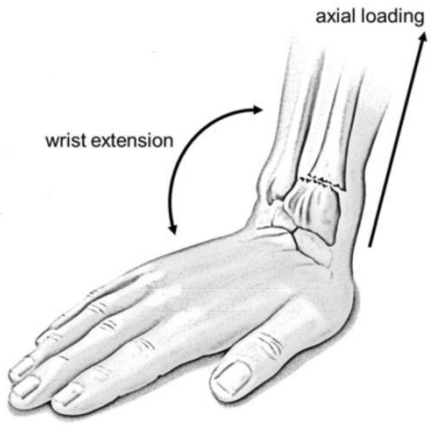

Figure 11.3: Wrist loading during fall (from Michel et al. 2013)

11.2.4 Wrist Injuries in Snowboarding

Upper-extremity injuries represent 35% to 45% of all snowboarding injuries (Russell, Hagel and Francescutti, 2007). A number of epidemiological studies present upper extremity injury rates rather than the anatomical location, so it is not always possible to obtain accurate wrist specific injury rates. Nevertheless, numerous studies have reported the wrist as the most affected site in snowboarding (Chow, Corbett and Farstad, 1996; K. Sasaki *et al.*, 1999; Kim and Lee, 2011). Distal radius fractures are the most common fracture in snowboarding (K Sasaki *et al.*, 1999; O'Neill, D, 2003; Wadsworth, Binet and Rowlands, 2012), with an injury rate of 0.28-0.31 per 1000 snowboarder daily visits (Matsumoto et al. 2004; Sasaki et al. 1999).

It is difficult to determine an absolute number of distal radius fractures per year amongst snowboarders, due to different reporting mechanisms used by different resorts and a limited number of publications. Assuming the injury rate per 1000 snowboarder days of 0.28-0.31 is relevant for the USA in 2016, it is possible to determine the approximate the number of distal radius injuries based on published statistics. Given that there were 54.7 million skier/boarder days during the 2016/2017 season in the USA (Statistica, 2018a) and snowboarders are reported to account for 35% of the snow sports population (Statistica, 2018b), the number of distal radius injuries that year was approximately 5000.

Snowboarding injuries tend to be caused by impacts resulting from falls, collisions or lift related incidences. When snowboarders experience a loss of balance, they are limited in regaining their stability as both feet are attached to the board through a non-release binding system. If incapable of stopping the fall, snowboarders often reach out with their arms in an effort to cushion the fall which can result in injury (Figure 11.4).

Figure 11.4: Forward and backward falls in snowboarding (from Yamauchi et al. 2010)

11.2.4.1 Risk Groups

The incidence and pattern of injury have been identified to differ between snowboarders by varying ability (Bladin et al. 2004; Yamauchi et al. 2010). Beginners with less than 5 days snowboarding experience are more prone to injury, due to the numerous falls involved in learning this new skill (Rønning *et al.*, 2001; Langran and Selvaraj, 2004). Wrist injury rates are highest in beginner snowboarders (Hagel, 2005), whilst intermediate, advanced and elite snowboarders are more susceptible to injuries affecting other regions (Ogawa et al. 2010; Idzikowski et al. 2000;Flørenes et al. 2012; Torjussen & Bahr 2006). This is likely due to the difference in speed and nature of manoeuvres being executed by snowboarders of different skill levels.

Adolescents have also been identified as a high-risk group susceptible to wrist injuries (Hagel, 2005; Dickson and Terwiel, 2011; Kim *et al.*, 2012) as growth plates, the area of cartilage at the end of children's bones are the last portion to harden, are particularly vulnerable to fracture. Concerns have been raised over the lasting impact of paediatric wrist injuries which can result in arrested bone growth and deformity (Brown and Deluca, 1992).

11.2.5 Summary

This section has put snowboarding wrist injuries in context, highlighting that fall-related wrist injuries are the most common injury in snowboarding. Wrist injuries have been seen to affect various demographics, beginners and adolescents have been identified as high-risk groups. Given the frequency of injuries coupled with the financial implications of healthcare, there is a need for prevention based on an understanding of injury mechanisms and causation. Therefore, the developed test method should facilitate the replication of a range of different fall scenarios and body masses.

11.3 Mechanism of injury

An understanding of fracture mechanisms is essential to quantify injury thresholds and identify the variables a successful wrist guard should mitigate, to aid in the prevention of wrist injuries.

11.3.1 Injury Threshold

To effectively mitigate the risk of injuries it is important to understand the human body's response to specific events including causal injury mechanisms and thresholds (Merkle 2013). Various studies on loading and functional range of movement (ROM) provide insight into the threshold values above which a fracture is likely to occur.

Reproducing falls to trigger fractures in participants would be unethical, hence studies using cadaveric forearms have attempted to determine the force required to fracture an adult radius. Different test setups including drop rigs and universal testing machines have been used to initiate fractures in cadavers. Despite cadaver testing being conducted under controlled laboratory conditions, there is considerable variation in fracture loads both between and within studies. Forces in the range of 1580-3600 N are needed to fracture a female adult radius and 2370-3773 N for males (Table 11.1). A preventative approach should aim to limit impact loads to 3340N (mean fracture force + standard deviation (SD), 2618 + 822N, Table 11.1), to reduce the incidence of snowboarding related wrist injuries.

A limitation of cadaver testing is the limited sample size and physical variation between samples. There are particular difficulties with obtaining cadaver specimens due to both ethical and social acceptance issues (Payne, Mitchell and Bibb, 2013). Available specimens tend to be biased towards the elderly population and no studies to date report the fracture loads of child or adolescent forearms. Mechanical properties differ between age groups as cortical bone strength has been shown to decrease with age (Helelä, 1969). As a large portion of the snowboarding demographic is made up of adolescents, this gap in fracture threshold data presents difficulties when trying to develop representative test setups. It is also apparent that a relationship between gender and injury response exists, with lower fracture loads reported for females. As almost 40% of snowboarders are female (SIA, 2011), preventative measures should be designed to meet the lower thresholds, to maximise the protective effect on the whole population.

Frykman (1967) and Lilienfeldt (1908) identified that fracture types vary depending on 2 factors: orientation of hand relative to the forearm and orientation of the forearm relative to impact surface. Distal radius fractures were produced when the wrist was positioned in 40-90° dorsal flexion and 0-35° radial or ulnar deviation (Frykman, 1967). Fractures of the proximal forearm occurred when the dorsal flexion angle was less than

40° and carpal bone fractures when the angle was greater than 90°. During a study, using cadavers Mayfield et al., (1980) observed varying injury patterns when different setups for ulna deviation and intercarpal supination were used. As different experimental setups and arm orientations can result in different fracture patterns; it is important to consider hand and arm orientation in the design of a surrogate when developing a test method to evaluate wrist protectors.

Table 11.1: Fracture Loads of Adult Cadaver Forearm

Gender	Sample Size	Mean Sample age (yr)	Experimental Setup	Fracture Site	Mean fracture load (N) ± SD (if recorded)	Reference
Female	18	74	Dynamic	Radius	1580 ± 600	(Myers et al. 1993)
	1	-	Dynamic	Radius	1863	(Frykman 1967)
	11	76	Dynamic	Radius	3180 ± 1000	(Myers et al. 1991)
	13	63	Quasi-static compression	Radius	1917 ± 640	(Frykman 1967)
	17	70	Quasi-static compression	Radius	3600 ±1160	(Horsman et al. 1983)
	12	85	Quasi-static	Radius	2008 ± 913	(Augat et al. 1996)
	10	84	Dynamic	Radius	1956 ±467	(Zapata et al. 2017)
Group mean ± SD				2300 ± 766		
Male	7	74	Dynamic	Radius	2370 ± 420	(Myers et al. 1993)
	7	76	Dynamic	Radius	3740 ± 532	(Myers et al. 1991)
	2	-	Dynamic	Radius	3874 ± 624	(Frykman 1967)
	9	59	Quasi-static compression	Radius	2769 ± 1266	(Frykman 1967)
	7	77	Quasi-static	Radius	3773 ± 1573	(Augat et al. 1996)
	4	74	Dynamic	Radius	3148 ± 452	(Zapata et al. 2017)
Group mean± SD				3279 ± 619		
Unknown	12	76	Quasi-static	Radius	1640 ± 980	(Spadaro et al. 1994)
	5	76	Quasi-static	Scaphoid	2410 ± 913	(Spadaro et al. 1994)
	5	47	Dynamic	Forearm	2821 ± 763	(Greenwald et al. 1998)
	20	-	Dynamic compression	Radius	2245	(Giacobetti et al. 1997)
	17	67	Dynamic	Radius	2648 ± 1489	(Augat et al. 1998)
	9	76	Dynamic - Incline	Radius with ulnar	2920 ± 1197	(Lubahn et al. 2005)
	11	76	Dynamic - vertical	Radius with ulnar	3896 ± 1991	(Lubahn et al. 2005)
	5	-	Dynamic - Incline	Radius Radius with ulnar scaphoid	1104 ± 119	(McGrady et al.2001)
	8	61	Dynamic	Radius	2141 ± 1229	(Burkhart et al. 2012)
Group mean± SD				2425 ± 798		
Overall mean ± SD				2618 ±822		

Unlike fracture force thresholds, specific values for injurious wrist extension angles have not been documented in the literature. Studies have focused on defining the functional range of movement and the necessary physiological range required to perform activities of daily living (Boone and Azen, 1979; Palmer *et al.*, 1985; Ryu *et al.*, 1991) rather than identifying the maximum possible angle that can safely be achieved under load. The range of wrist motion is reported to be 60-75° of extension to 60-82° of flexion for healthy adults.

During an on-slope study using an instrumented glove, Greenwald et al. (2013) observed wrist extension angles of 80.2 ± 15.8° (mean ± SD) at low loads as a result of a fall, without obtaining a fracture. Similarly, Schmitt et al. (2012) reported wrist extension values nearing hyperextension in a laboratory-based fall arrest study. The relationship between impact load, the angle of wrist extension and fracture is not well established in literature. Fractures may result from a combination of both the load and extension above certain thresholds. Frykman (1967) observed laboratory induced distal radius fractures in cadavers at extension angles as low as 40° when coupled with high loads (1917-2769 N), yet Greenwald et al. (2013) reported no fractures at angles above 80° with low loads (266 ± 232 N).

Peak impact force has been reported to contribute to fractures (Hwang *et al.*, 2006), but the contribution of other aspects such as strain rate or impact energy to injury incidence is poorly understood (DeGoede, Ashton-Miller and Schultz, 2003). Studies using cadavers provide insight into peak fracture load. As such, fracture load is most commonly reported in relation to injurious scenarios in literature. To mitigate injury risk wrist protectors must lower the impact force below the reported fracture force.

11.3.2 Summary

The wrist is a complex joint which can become damaged when subjected to injurious loading scenarios. A combination of applied compressive loads to a hyperextended wrist is believed to be the most common injury mechanism. Bone properties coupled with the nature of the fall and the resulting impact forces have been found to affect fracture loads. A preventative approach should aim to limit impact loads to 3340 N and limit the wrist angle below hyperextension, to reduce the incidence of snowboarding

related wrist injuries. The lack of adolescent-specific fracture thresholds has been identified as a limitation. Whilst this section has provided insight about the maximum injury thresholds, an understanding of kinematics and biomechanical loading surrounding fall scenarios is necessary for the development of a new test method.

11.4 Wrist protectors

Cadaver studies provide insight into the peak force wrist protectors should limit to prevent injury. This section will discuss the efficacy, protective mechanisms and design features employed in wrist protectors to reduce wrist injury

PPE has become an increasingly common method of injury prevention in a range of sporting contexts. In numerous cases, PPE is a requirement of governing bodies to ensure participant safety and prevent avoidable injuries including shin pads in association football, hockey and cricket (Marshall *et al.*, 2002). Generally, the design of PPE is regulated by a standards institution such as the International Organization for Standardization (ISO) to ensure that products on the market are safe and of sufficient quality. Such standards prescribe testing protocols and minimum performance requirements products should met. There is a range of snowboarding wrist protectors on the market (Figure 11.5): protectors of varying length; gloves/mittens with integrated protection; stand-alone protectors, yet no international standard or design regulations exist that these specific products should meet (Michel *et al.*, 2013).

Figure 11.5: Commercially available snowing boarding wrist protectors a) Glove with integrated protection b) stand-alone protectors of varying length

11.4.1 Protective Mechanisms

A range of approaches have been discussed in the literature as to how wrist protectors should function and protect the user from injury. Michel et al. (2013) argue that preventing wrist hyperextension and damping impact forces are the two fundamental functions of a wrist protector. This is in line with the requirements specified by the EN 14120 standard for roller sport wrist protectors (European Committee for Standardization, 2003b). Hwang *et al.*, 2006 suggest that impact force reduction is achieved through absorbing or shunting the impact energy to facilitate a time delay and thus level out the impulse curve. This is similar to the principles used in car design, where crumple zones are designed to reduce the initial force of the crash and redistribute it to keep the occupants safe. Staebler et al. (1999) identified that at sub failure loads wrist protectors have a load sharing function, transferring the applied load away from the palm directly to the mid-forearm, bypassing the carpus and distal radius.

In contrast to Michel *et al.* (2013), Maurel et al. (2013) argue that there is no basis in literature for the prevention of hyperextension reducing the risk of fracture. Chen et al. (2014) observed that the contact area between the scaphoid and distal radius is maximised when the wrist is fully extended and hypothesise that the risk of fracture is reduced when the wrist is fully extended, as the radiocarpal joint is more stable in this orientation. To date, there is no evidence to show that limiting hyperextension has negative consequences. A range of different approaches have been proposed to protect the wrist from injury, yet to date, no study has measured all these performance parameters for a range of commercial products.

11.4.2 Design of wrist protection

There is little consensus as to which wrist protector design is most effective at reducing injury (Kim and Lee, 2011; Wadsworth, Binet and Rowlands, 2012). There is a diverse range of products on the market with varying positions and materials for damping elements; differing strapping mechanisms; and different locations of splints: dorsal side only, palmar side only or both. The protector length varies across models but tends to run from above the knuckles to either low or mid forearm, positioning the wrist in slight

extension whilst still allowing full range of motion for the fingers and thumb (Cheng *et al.*, 1995).

Rigid splint elements on the palmar and dorsal side of the hand combined with palmar damping elements are the most commonly employed mechanisms in commercial products (Figure 11.6). The splints physically limit hyperextension as well as storing the kinetic energy, then release it over an extended period. The damping elements dissipate kinetic energy through deformation acting as a crumple zone, further reducing the transmitted force. Machold et al. (2005) suggest the following design criteria for optimised wrist protectors: the position of palmar padding; shape; length; stiffness; and fixation to the arm. To date, no study has evaluated the influence of these parameters on protective performance.

Figure 11.6: a) Dorsal splint b) Palmar damping element (adapted from Burton 2015; Decathlon 2015)

Staebler et al. (1999) noted that the position and fit of the palmar element resulted in differences in measured bone strain at sub fracture loads, suggesting that palmar plate design may affect load transfer to nearby anatomic structures. Splint stiffness is cited as a key design parameter, a design that is too stiff and does not bend under load, will generate areas of high stress at the proximal and distal ends of the protector, which has the potential to produce a fracture below or above the protector (Rønning *et al.*, 2001). Cheng et al. (1995) hypothesize that fractures proximal to the protector may be a result of splints transferring energy up the forearm. Furthermore, they postulate that the splint may act as a lever arm, multiplying the torque resulting from the fall by the length of the splint. Machold et al. (2000) found an increase in finger fractures in snowboarders

who wore protectors compared to those who didn't, which they suggest is due to the design of dorsal splints.

11.4.3 The effectiveness of wrist protectors

An effective wrist protector would prevent the user from wrist injuries; however, mixed results have been found in the literature concerning the protective capabilities of wrist protectors. Epidemiological and clinical studies have been conducted to compare injury rates in snowboarders wearing wrist protection against those who do not. Tests involving cadavers, mechanical surrogates and human volunteers have attempted to quantify the protective effect of wrist protectors.

11.4.3.1 Experimental studies

To date, no two studies have used the same wrist protectors or setup. Different products of different sizes, shape and materials have been tested in different ways. The results of experimental studies using cadavers, mechanical surrogates and participants will be reviewed in turn. A disagreement in the effectiveness of wrist protectors has been found by researchers using cadavers to determine protective capabilities of wrist protectors. Both Moore et al. (1997) and Lewis et al. (1997) observed differences in fracture severity between protected and unprotected groups, implying the protective benefits of wrist protectors. Conversely, when using comparable input parameters, three other studies using cadavers did not report a difference in injury severity when wrist protectors were used (Greenwald et al. 1998; McGrady, Hoepfner et al. 2001; Giacobetti et al. 1997). Variations exist in the cadaver samples with different ages and section methods being used. No cadaver studies testing commercially available wrist protection in the past fourteen years were found in the literature search, meaning the suitability and functionality of newer generation designs has gone virtually untested.

Different variations of surrogate arms have been used to mechanically test the performance of wrist protectors (Kim *et al.*, 2006; Schmitt, Michel and Staudigl, 2012; Maurel *et al.*, 2013). Schmitt et al. (2012) conducted the only snowboard specific wrist protector comparison to date characterising products based on their ability to reduce peak force and limit wrist angle extension. The authors tested fifteen products against the Inline skate EN 14120 standard which stipulates products should result in a peak force below 3 kN during an impact test and wrist extension angles between 35-55°

when subjected to a 3 Nm torque. The majority of products (67%) failed to attenuate the impact force to within the specified boundaries, whilst 56% of products failed to comply with the wrist extension angle requirement. The results from Schmitt et al. (2012) suggest that: the test standard is not necessarily applicable to snowboard specific equipment; snowboard wrist protectors are not fit for purpose or a combination of both. The results also imply that products are designed with greater consideration towards reducing hyperextension rather than the reduction of peak force. Both Kim et al. (2006) and Maurel et al. (2013) confirmed that wrist protectors protect the point of impact at the carpals through a reduction in peak force, although only Maurel et al.(2013) found this to be true at representative fracture loads.

At sub fracture loads, studies have been conducted using live participants to explore the effectiveness of snowboarding wrist protectors. Hwang & Kim (2004) found that palmar pads improved energy absorption by more than 38% compared with the bare hand but had no effect on the peak impact force. In a later study, utilising a different mass-spring-damper model, they reported that wrist protectors had no significant effect in terms of force transmission or energy storage and absorption (Hwang *et al.*, 2006). Whilst, Burkhart & Andrews (2010) found that wrist protectors demonstrate a protective effect in terms of reducing off-axis wrist accelerations and elbow accelerations in 2 axes. Experimental tests using cadavers, mechanical surrogates and participants have shown that in some cases commercially available wrist protectors exhibit protective capabilities.

11.4.3.2 Epidemiological studies

Numerous epidemiological studies conclude that wrist protectors can reduce the risk of wrist injuries among snowboarders (Idzikowski, Janes and Abbott, 2000; Rønning *et al.*, 2001; O'Neill, 2003; Machold, Kwasny and Eisenhardt, 2005; Russell, Hagel and Francescutti, 2007; Wadsworth, Binet and Rowlands, 2012). Yet, other epidemiological studies have reported adverse side effects from using a wrist protector claiming they transfer the impact to another body region, increasing the risk of injuries to the elbow or shoulder (Chow, Corbett and Farstad, 1996; Hagel, Pless and Goulet, 2005).O'Neill (2003), Waddington et al. (2013) and Rønning et al. (2001) found no association between wrist protector usage and an increased risk of proximal injuries. Based on the

majority of clinical studies, it appears that wrist protectors do play a role in reducing fall-related snowboarding wrist injuries.

Despite the effectiveness of wrist protectors reported in a number of experimental and epidemiological studies and the commercial availability of these products, the rate of wrist injuries has remained relatively constant. Michel et al. (2013) speculate that this could be due to the low usage of wrist protectors, with a reported usage rate between 1 and 18% for snowboarders who have sustained a wrist injury. Low levels of comfort; a belief that wrist protectors can trigger certain injuries; and general apathy towards the need for protection have been cited as the three main barriers to use (Bianchi *et al.*, 2012). A study by the Swiss Council for Accident Prevention observed that even though protector usage in Switzerland increased from 37% to 42% from 2003 to 2007, the proportion of wrist injuries remained unchanged (Swiss Council for Accident Prevention (bfu), 2012; Michel *et al.*, 2013). Despite the fact that wrist protectors have been shown to provide a protective effect, in some instances even when used, snowboarders have sustained wrist injuries (Cheng *et al.*, 1995; Idzikowski, Janes and Abbott, 2000). This raises questions about the design and protective capabilities of wrist protectors.

At present no study has systematically analysed a range of different protectors using a repeatable and comparable test approach, meaning current understanding about the effect of different wrist protector design elements is limited. These disparities between current approaches, further emphasise the need for a repeatable and representative test method. The use of a mechanical surrogate can be justified as it enables a consistent, repeatable method, which can characterise a range of products under the same parameters representative of injurious fall scenarios.

11.4.4 Summary

Studies have shown that wrist protectors are an effective method in reducing wrist injuries, yet injuries still occur. From a review of protective mechanisms, it can be concluded that to be an effective preventative measure; wrist protectors should meet the following performance criteria:

- Attenuate peak impact force

- Store, absorb and transfer impact energy safely away from the wrist joint without putting other regions at risk
- Stabilise the wrist and limit hyperextension
- Comfortable to wear to encourage higher usage rates

The development of a representative test and surrogate would enable the influence of design parameters on the protector's efficacy to be evaluated. Given the weaknesses associated with cadaveric studies and the ethical implications of participant-based studies a mechanical approach is necessary. The following section will provide insight into current approaches, to inform the design of the physical setup.

11.5 Injury Mechanics

The previous sections have identified the forces associated with wrist fractures and the way in which wrist protectors attempt to mitigate injury. To develop a test that represents injurious fall scenarios an understanding of the mechanics surrounding injury is necessary. Obtaining biomechanical information regarding injury scenarios is important (Bahr, R. & Krosshaug, 2005) yet ethically difficult due to its injurious nature (Krosshaug *et al.*, 2005). The biomechanics of sports injury scenarios have informed the development of a variety of mechanical test devices (Grund, Senner and Grube, 2007; Laing and Robinovitch, 2008; Ura and Carré, 2016).

This section will review the experimental recreation of falls to inform the selection of input parameters and boundary conditions for a representative test. To determine the kinetic and kinematic parameters associated with a snowboarding fall-induced wrist injury, ideally, an in-situ slope study involving snowboarders of various body sizes, replicating injurious falls instrumented with force and angle sensors, combined with motion capture would be required. Since this is neither ethical, repeatable or practical an alternative solution is needed. From existing literature boundary parameters can be selected from either cadaver studies resulting in fracture or from biomechanical data collected during low-level non-injurious falls in a laboratory.

11.5.1 Experimental laboratory-based fall studies

Biomechanical studies of controlled falls at sub-fracture loads in a laboratory enable the impact parameters to be measured. This is typically achieved by falling onto a crash mat

(Figure 11.7a) or by applying a load to the outstretched forearm using a dynamic pendulum (Figure 11.7b) (Chiu & Robinovitch 1998; Hsiao & Robinovitch 1998; Robinovitch & Chiu 1998; DeGoede & Ashton-Miller 2002; Kim & Ashton-Miller 2003; Lo et al. 2003; Schmitt et al. 2012; Choi & Robinovitch 2011; Tan et al. 2006; Hwang et al. 2006; DeGoede et al. 2002; Burkhart & Andrews 2010). Combinations of experimental and mathematical models have been used to study fall scenarios and to characterise the impact response of the body (Figure 11.7c).

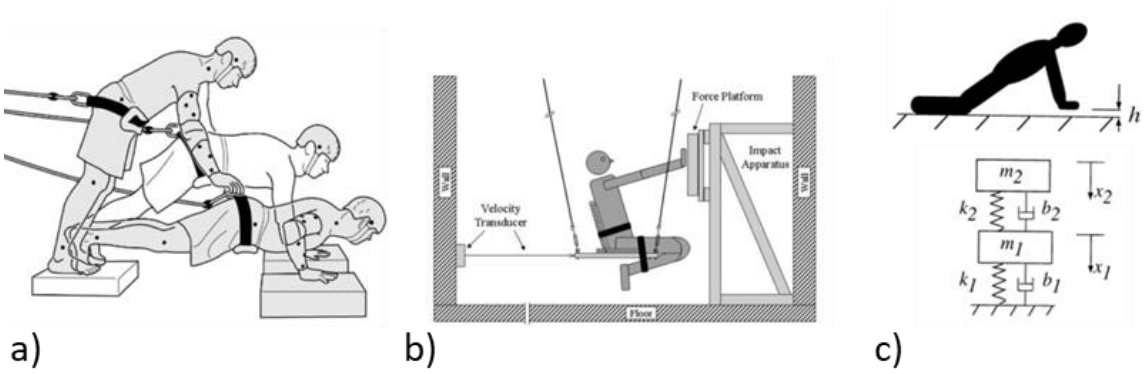

Figure 11.7: Experimental fall arrest setups a)Tethered cable (DeGoede and Ashton-Miller, 2002) b) Seated pendulum fall (Burkhart and Andrews, 2010) c) Experimental and mathematical model (Chiu and Robinovitch, 1998)

DeGoede et al. (2003) identified biomechanical factors that contribute to the risk of injury resulting from falls, presented in Table 11.2. Based on the modifiable factors in Table 11.2 two preventative strategies seem plausible: altering of fall kinematics or the use of protective equipment to modify the impact contact point, energy dissipation and surface conditions. The extrinsic factors can be used to inform the selection of boundary parameters.

Table 11.2: Biomechanical factors in falling (DeGoede, Ashton-Miller and Schultz, 2003)

Extrinsic Factors	**Intrinsic Factors**	
	Unmodifiable factors	***Modifiable factors***
Cause of fall	Bone properties	Configuration of head, torso and extremities during descent
Fall direction	Soft-tissue properties	Selected momentum arrest/ energy dissipation strategy before and during impact
Fall height	Maximum muscular rate of strength development	Body segment orientation and limb configurations at impact
Initial speed at the loss of balance	Reaction time	Velocity of body segment and its contact point with the ground at impact
Surface conditions (stiffness, coefficient of friction)	Movement time	Location of impact point relative to the whole-body centre of mass
		Values of pre-set muscular stiffness and damping about involved joints

11.5.1.1 Altering fall kinematics

Chou et al. (2001) and DeGoede & Ashton-Miller (2002) found that altering fall kinematics by flexing the elbows, can reduce and postpone the peak impact force. Peak hand impact force was found to reduce by 27-40% when participants actively tried to reduce their hand velocity during a simulated fall at sub fracture loads through elbow flexion (DeGoede and Ashton-Miller, 2002; DeGoede *et al.*, 2002). Whilst in a laboratory learning how to fall has been shown to reduce peak forces educational intervention techniques on the ski slope to alter fall kinematics were found to increase injury severity (Machold *et al.*, 2000).

Langran & Selvaraj (2002) observed that first day snowboarders who had taken professional instruction were three times more likely to be injured than those who had not. The authors hypothesise that this may be because snowboarders gain a false sense of skill once a small amount of experience has been gained, leading to an increase in risk-taking behaviour. Alternatively, this finding could be a reflection on the characteristics of those who opt to teach themselves rather than seeking instruction. Whilst in a laboratory context learning how to fall can reduce peak forces additional methods of intervention are necessary on the slopes. On the slopes falls are unexpected, and beginners are focused on learning the sport rather than arresting their falls. These findings highlight that additional preventative interventions in the form of PPE are necessary.

11.5.2 Extrinsic factors

11.5.2.1 Fall direction

Backward falls have been found to result in more wrist fractures (Davidson and Laliotis, 1996; Idzikowski, Janes and Abbott, 2000; Deady and Salonen, 2010; Yamauchi *et al.*, 2010), whilst Yamauchi et al., (2010) found that forward falls were more likely to result in shoulder dislocations and upper arm fractures. Tan et al., (2016) found that backward falls resulted in larger impact velocities of the distal radius during simulated falling compared to forward falls. However, Schmitt et al. (2012) conducted a study using a similar setup and noted no significant difference in impact velocity between forward and backward falls. Elbow flexion may be a contributing factor to the difference in fall direction injury pattern; limited elbow flexion treats the arm as a single segment known as ‘stiff-arming’. DeGoede and Ashton-Miller, (2002) observed forward stiff-arm falls resulted in higher peak forces than when the elbow was flexed, an effect that is likely to be observed in backward falls. Backward falls are the worst-case scenario that protective equipment should attempt to mitigate; therefore the developed impact test will attempt to mimic backward falls with a stiff-arm posture.

11.5.2.2 Mass of body acting on the wrist joint

When considering fall impacts, it is not sufficient to consider the full body mass or just the mass of the arm. Given the multi-segmented nature of the body, certain masses decelerate rapidly while others decelerate gradually. This pattern of deceleration is

equivalent to some proportion of the body's mass stopping abruptly at the point of impact (Lieberman *et al.*, 2010) and the term 'effective mass' is used to describe this proportion of body segment mass that contributes to an impact (Chi & Schmitt 2005; Lenetsky et al., 2015; Rousseau & Hoshizaki 2015). Simplifying the whole body into a rigid block of mass misrepresents the physical system, as body segments such as joints and muscles flex and deform on impact (Gruber *et al.*, 1998) reducing impact forces. Flexing the elbow when landing has been shown to reduce the effective mass and thus impact force (DeGoede and Ashton-Miller, 2002). In the case of falling onto an outstretched arm, Schmitt et al. (2012) define the effective mass as the mass that affects the wrist at the time of impact, comprised of the forearm, upper arm, and parts of the shoulder. A diverse range of values have been presented in the literature to describe the effective mass acting on the wrist during falls (Table 11.3).

Table 11.3: Overview of effective mass used in different studies

Experimental setup	**Effective Mass (kg)**		**References**
	Mean	**Range**	
Mechanical using cadavers	23	7.9-45.5	(Frykman, 1967; Lewis *et al.*, 1997; Moore *et al.*, 1997; Greenwald *et al.*, 1998; Lubahn *et al.*, 2005; Burkhart, Dunning and Andrews, 2012; Zapata *et al.*, 2017)
Biomechanics using participants	3	1.7-5.5	(Chiu and Robinovitch, 1998; DeGoede *et al.*, 2002; Schmitt *et al.*, 2012)
Mechanical using surrogates	3	2.5-3.5	(Maurel *et al.*, 2013; Thoraval *et al.*, 2013)

Given the variability in segment stiffness throughout the chain in different fall scenarios some variation in effective mass is expected, however differences in the region of 20kg have been reported between studies. The values presented by Schmitt et al., (2012), DeGoede et al., (2002) and Kim et al., (2006) are all within a similar range, yet these are significantly lower than those used in the cadaveric studies. However, no justification for effective mass choice was provided by Moore et al., (1997) or Lewis et al., (1997). An effective mass of 23kg was selected by Greenwald et al., (1998) as it corresponds to one-third of the average human body mass. The authors justify this choice as they state 23kg represents the portion of the upper body that would be directly above the arm in a backward fall, although there is no evidence to suggest this is an appropriate parameter.

11.5.2.3 Inbound velocity and fall height

A range of impact velocities have been used in previous studies to replicate fall scenarios. No impact velocity data exists for backward falls from standing as biomechanics studies have been limited to low level falls to ensure participant safety. The inbound velocities used in a number of the cadaver studies was determined by increasing the drop height until a fracture was observed (Frykman, 1967; Lewis *et al.*, 1997; McGrady, Linda Hoepfner, Young and Raasch, 2001; Burkhart, Andrews and Dunning, 2012). No justification is provided for the drop heights used in the mechanical studies.

Table 11.4: Overview of inbound velocity and drop height used in different studies

Experimental setup	Mean velocity (m/s)	Mean drop height (m)	References
Biomechanics using participants	1.60	0.33	(Chiu and Robinovitch, 1998; Robinovitch and Chiu, 1998; Chou *et al.*, 2001; DeGoede and Ashton-Miller, 2002; DeGoede *et al.*, 2002; Lo *et al.*, 2003; Schmitt *et al.*, 2012)
Mechanical using cadavers	3.54	0.69	(Frykman, 1967; Lewis *et al.*, 1997; Moore *et al.*, 1997; Greenwald *et al.*, 1998; McGrady, Linda Hoepfner, Young and Raasch, 2001; Lubahn *et al.*, 2005; Burkhart, 2012)
Mechanical using surrogates	2.24	0.27	(Hwang *et al.*, 2006; Thoraval *et al.*, 2012; Maurel *et al.*, 2013)

11.5.3 Summary

Biomechanics studies have emphasised that while bone strength establishes the ultimate threshold for fracture, a range of biomechanical factors alter the demand on bone. Altering fall kinematics and modifying the impact contact through protective equipment can aid in lowering the peak force.

When selecting parameters as input for a new wrist protector test, it is important to note the limitations of previous studies. The forces involved in biomechanics studies are lower than fracture scenarios, and it is not known if they are applicable at higher impact energies. Secondly, participants in these studies are anticipating the fall which may alter

their behaviour and force outcome. A weakness of cadaver tests to date is that they only utilised the forearm and did not consider this in relation to other limbs or the full body. Biomechanics investigations have considered the full body albeit at lower loads. Given that protective equipment should reduce the risk of injury rather than merely transferring it, a test method that considers more than just the wrist is preferable.

Despite these limitations, the knowledge of injury parameters developed in this section will inform the development of a mechanical test to facilitate the replication of fall scenarios at injurious load conditions. Backward falls have been found to result in more wrist fractures then forward with a high degree of variation existing between studies. Therefore, ranges of variable parameters have been identified for three boundary parameters:

- Effective mass (1.7-45.5kg)
- Inbound velocity (1.6-3.5 m/s)
- Fall height (0.3-0.7m)

Future chapters will justify the selection and magnitude of these parameters in more detail. There is a need to understand the application of these parameters in current tests of protective equipment.

11.6 Current test setups

The previous sections have identified the need for a mechanical test and surrogate to evaluate the protective characteristics of snowboarding wrist protectors repeatably. This section will review existing test setups, safety standards and surrogate design.

11.6.1 Test Setups

Test setups are necessary to measure the performance of existing products and inform the development of future equipment. It was reported by Norman, (1983) that users expect the testing of protective equipment to be conducted during the prototype development or production process. Whereas a great deal of the protective equipment used in sports has been developed on a trial and error basis with little, if any, objective laboratory evaluation of the degree of protection provided by the product. It is likely that the performance of snowboarding wrist protectors has gone untested, given that

there is presently no international standard governing the design of snowboarding wrist protectors; there is little motivation for manufacturers to invest in product testing.

Two approaches are typically used to impact test protective equipment. Moving a surrogate onto a rigid surface or moving a mass onto a surrogate fixed to a rigid surface. These test setups use a range of different orientations: vertically using a linear drop tower, horizontally by driving the surrogate into a plate, or angularly using a pendulum (Figure 11.8). A horizontal setup requires some form of external force input e.g. pneumatics, unlike the drop test and pendulum which can be driven by gravity, making them preferential.

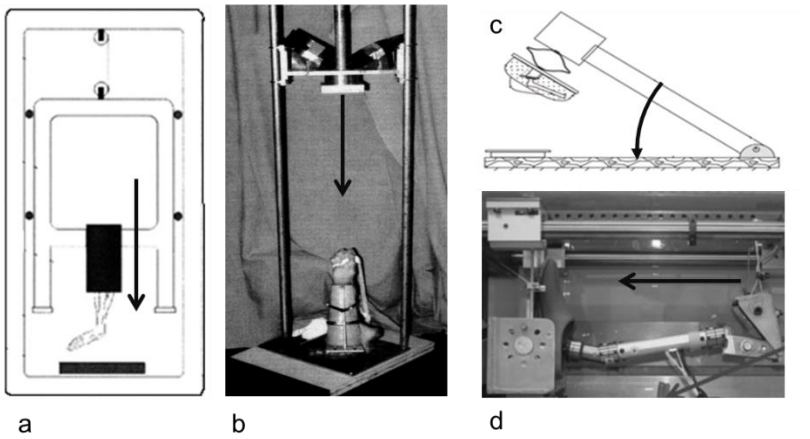

Figure 11.8: Sample of different impact test setups a) Cadaver dropped onto rigid surface (Lubahn *et al.*, 2005) b) load dropped onto rigidly mounted cadaver (Moore *et al.*, 1997) c) Hip surrogate mounted to pendulum impactor (Laing *et al.*, 2011) d) horizontal impact with pneumatic ram driving surrogate foot into impact surface (Van Tuyl, Burkhart and Quenneville, 2016)

Table 11.5 and Figure 11.14**Error! Reference source not found.** outline existing mechanical tests to determine the performance of snowboarding wrist protectors. The setups in Table 11.5 have only tested elements of wrist protectors, looking at either the palmar pad or the splints in isolation. Linear impact tests are commonly used to test the protectors' ability to reduce peak impact forces and absorb energy on impact (tests 2- 6 in Table 11.5). The test rigs, surrogates and inbound parameters differ between tests 2-6, but the fundamental principle is the same, to measure the peak force during an impact, to determine the damping provided by the wrist protector. No justification was provided for the boundary conditions used in the impact tests, in all cases the inbound energies used were lower than inbound energies reported in studies using cadavers.

The European Standard EN 14120 stipulates performance requirements that roller sport wrist protectors must meet in terms of damping behaviour and stiffness (tests 1 and 2 in Table 11.5, European Committee for Standardization, 2003). The standard stipulates that a protector designed for users >50kg should limit the peak force to 3 kN when subjected to a 5 J linear impact (Figure 11.9b). The standard also demands that products should limit wrist extension angles between 35-55° when subjected to a 3Nm torque (Figure 11.10c). Schmitt et al. (2012) used both the damping and stiffness tests from EN 14120 to evaluate the performance of snowboarding wrist protectors. The work of Schmitt et al. (2012) is the only study in the literature that has sought to characterise wrist protector stiffness.

Table 11.5: Mechanical test setups to measure wrist protector performance

Test	Surrogate	Instrumentation	Reference	Associated figure
1.	Simplified wooden arm	Force sensor, digital protractor	European Committee for Standardization, 2003; K.-U. Schmitt, Michel and Staudigl, 2012	11.11c 11-9e
2.	Spherical metal anvil	Force plate	European Committee for Standardization, 2003; K.-U. Schmitt, Michel and Staudigl, 2012	11.12b
3.	Rigid hand model made from body filler coupled with rubber to simulate soft tissue	Load cell, surrogate mounted accelerometer	Maurel *et al.*, 2013	11.13a 11-9c
4.	5^{th} % le Hybrid III dummy instrumented arm	Force plate, surrogate mounted load cell, potentiometer	Kim *et al.*, 2006	11-9a
5.	Cast polyurethane wrist model	Force plate, Flexible bend sensors, Force sensing resistors	Greenwald et al. (2013)	11-9d
6.	Solid resin forearm	Force plate	Thoraval *et al.*, 2013	Figure

based on wrist scans	11-9b

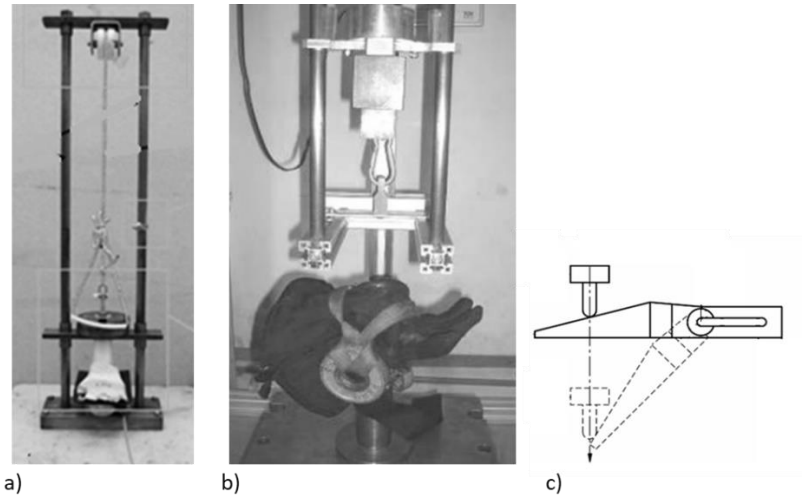

Figure 11.14: Mechanical test setups to measure wrist protector performance a) Maurel *et al.*, 2013 b & c) K.-U. Schmitt, Michel and Staudigl, 2012

The international standards for protective equipment, 13:340, are used to test PPE for various limbs across a wide range of applications (International Organization for Standardization, 2018). For the majority of standards, a rigid surrogate was used to represent the human body and subjected to a metal anvil at a specified input energy. Products were deemed acceptable if the mean transmitted force was below a set threshold in each case. While this enables a systematic way to characterise and compare protectors, it is disconnected from the context of their use. In reality, protectors are worn by humans with their complex geometries and non-rigid soft tissue structures.

Peak force is the measurement criteria specified in most standards however criteria such as deformation rate and load transfer could give richer information about the equipment's protective capability. Although the reviewed standards aim to protect limbs and joints, most test setups only measure impact attenuation from point impacts at specific locations. The stabilising of joints or reduction of certain movements which could aid in injury prevention are not considered.

Test standards for protective equipment have been criticised for: being formulated without proper scientific assessment; utilising test rigs with low biofidelity; and including subjective clauses about fit and comfort (Ankrah and Mills, 2003; Tsui, 2010). In many cases, it is unclear how the impact energies and force thresholds have been

derived. Ankrah & Mills (2003) argue that the football shin guard standard has been designed to protect the rig, rather than match the impact intensities encountered in the sport. Walker et al. (2010) state that the British Standard for cricket PPE is disconnected from the reality of gameplay, arguing that more representative test setups are necessary to provide a realistic indicator of the protection levels provided by PPE.

11.6.2 Surrogate Designs

Payne et al. (2015a) argue that human surrogates are critical in the development and testing of sports PPE due to the ethical restrictions of testing participants at injurious levels and the limitations of cadaveric tests. The following section provides an overview of surrogates currently used in product testing. Merkle et al. (2013) state that surrogates must closely represent anatomical structures, be composed of biomechanically representative simulant materials, and operate as a durable, repeatable test device capable of measuring tissue-level responses. To investigate injury mechanisms, support surgical repair and study grip strength, various attempts have been made to model the wrist joint both computationally and physically (Gíslason, Stansfield and Nash, 2010). Modelling the wrist has been achieved with varying degrees of anatomical and biomechanical accuracy. Physical and computation models will be discussed below.

11.6.2.1 Physical Models

Mechanical surrogates provide a physical interface for protective equipment to execute performance evaluations. Surrogates vary in levels of complexity but when instrumented are capable of providing a wealth of feedback through devices such as pressure films; load cells; accelerometers; and strain gauges (T Payne *et al.*, 2015b). Physical biofidelic human surrogates are necessary to test the effectiveness of real products rather than simply relying on what was intended or predicted by a computational model (T Payne *et al.*, 2015a). At present this field is limited, with largely simplified and non-anatomical models being presented in the literature.

Surrogates are either durable or frangible. Durable surrogates rely on instrumentation to assess responses and can repeatedly be used, whereas frangible surrogates are intended for one-time use and generally employ visible mechanisms to indicate injury risks. Payne et al., (2013) present the following criteria for surrogates used in the design and development of sports impact protection.

- Biofidelic exterior human geometries, to ensure that PPE is attached and aligned correctly before impact
- Biofidelic inertial properties, ensuring that the surrogate recoils accurately on impact
- Tissue structure biofidelity, i.e. the surrogate needs to represent the key human structural elements so that specific injury outcomes can be explored
- Tissue impact response biofidelity, i.e. the structures should have comparable strength and stiffness properties to approximate human behaviour on impact
- Instrumentation capabilities, to provide accurate feedback mechanisms to correlate the impact parameters to specific injury outcomes
- Durable, i.e. capable of providing consistent results from repeated impacts

The surrogates used in the mechanical tests outlined in Table 11.5 are shown below in Figure 11.15. Kim et al.(2006) used the forearm-hand complex of an enhanced airbag interaction (EAI) arm (Figure 11.15a), designed as an attachment for the 5th percentile Hybrid III female crash test dummy. This surrogate is primarily used to measure arm interaction during airbag testing (Duma *et al.*, 2003). The ability to instrument the EAI arm means that transmitted impact force can be measured simultaneously to the external impact force (determined using a force plate), which is not technically feasible in most cadaveric studies. The forearm is built around an inner metal core that attempts to replicate the bones; ligaments and muscle loads are not considered. This surrogate effectively replicates the range of motion of the human wrist; enables repeatable testing and can be instrumented with accelerometers and load cells. Its anatomical simplification and cost (£100,000 to build (AA, 2013)) can be seen as restrictions to widespread use. A practical limitation of this surrogate is the difficulty in mounting protective gloves, due to the hand posture with bent fingers.

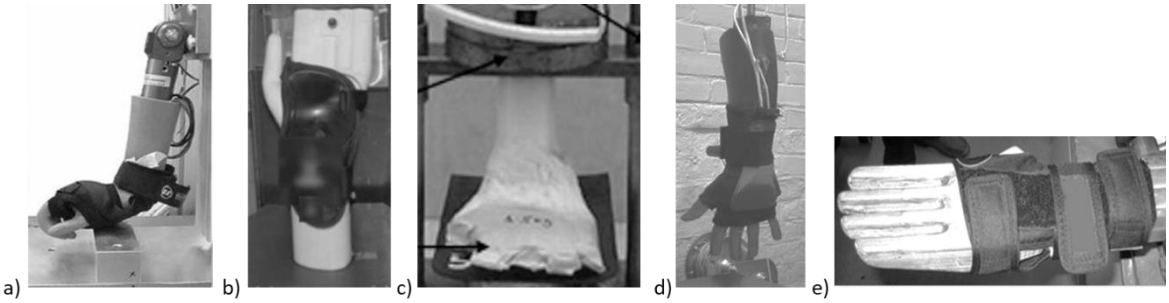

Figure 11.15: Mechanical surrogates used to test wrist protectors a) Kim *et al.*, 2006 b)Thoraval *et al.*, 2013 c) Maurel *et al.*, 2013 d)Greenwald, Simpson and Michel, 2013 e)Schmitt, Michel and Staudigl, 2012

The models used by Maurel et al. (2013), Thoraval et al. (2013) and Greenwald et al. (2013) are biofidelic in terms of hand geometry as they are based on casts or 3D scans of a human hand but do not consider muscle or soft tissue. The models used by Maurel et al. (2013) and Thoraval et al. (2013) are rigid and set at different wrist extensions angles to facilitate repeatable impacts onto the palm, limiting their use to evaluating palmar padding. The surrogates by Greenwald et al. (2013) and Schmitt, Michel and Staudigl, (2012) incorporate two solid sections connected with a single joint providing 1 degree of freedom replicating flexion-extension limiting biofidelity. To facilitate the testing of protective gloves Schmitt et al. (2012) modified the EN 14120 surrogate design to incorporate fingers (Figure 11.15e). The impact test specified in the EN 14120 (not pictured) uses a hemispherical anvil and a rectangular striker to measure damping behaviour. These geometric simplifications raise concerns about the fit of products during testing (Payne et al. 2013). The use of stiff steel anvils produces impact phenomena unrepresentative of the more viscoelastic human tissue response (Payne et al. 2015).

At present no mechanical surrogate exists that can facilitate the testing of wrist protectors integrated into gloves and simultaneously measure wrist extension angle during a dynamic impact. Five mechanical surrogate designs have been used previously to evaluate the performance of wrist protectors. While a crash test dummy forearm has the basic functionality to measure the protective capabilities of wrist protectors during a dynamic test, additional instrumentation and modifications to mount it onto a test rig would be required. Given the high cost of crash test dummy arms, an alternative lower cost bespoke instrumented surrogate will be developed.

Surrogates used in other injury prevention scenarios do exist. An instrumented surrogate knee known as the "Kandy" (Figure 11.16a), is a cast of a male's knee and contains three measurement points below the kneecap and along the tibial tuberosity to test knee pads. The protective knee pad is fixed to the surrogate knee and subjected to a load for a specified length of time while the force at each of the transducers is recorded (European Committee for Standardization, 2010). A similar approach using an instrumented surrogate could be developed to measure the force transfer along the forearm in the proposed impact test setup that will be developed as part of objective 3.

To test protective gloves designed for use in cold temperatures, the EN 511:2006 specifies a test to measure convective cold (European Committee for Standardization, 2006). Gloves are fitted to a thermal hand mannequin positioned in an environmental chamber. The thermal insulation of the glove is determined through the amount of power required to maintain a constant temperature between the surface of the hand and the surrounding chamber. Thermetrics produce thermal hand systems based on 75th percentile male hand dimensions that can be used to certify products to EN 511 (Figure 11.16b). The model includes an articulated thumb to reduce the hassle of mounting gloves to the surrogate. The techniques used by these two surrogates could assist in the development of a surrogate to test snowboarding wrist protectors.

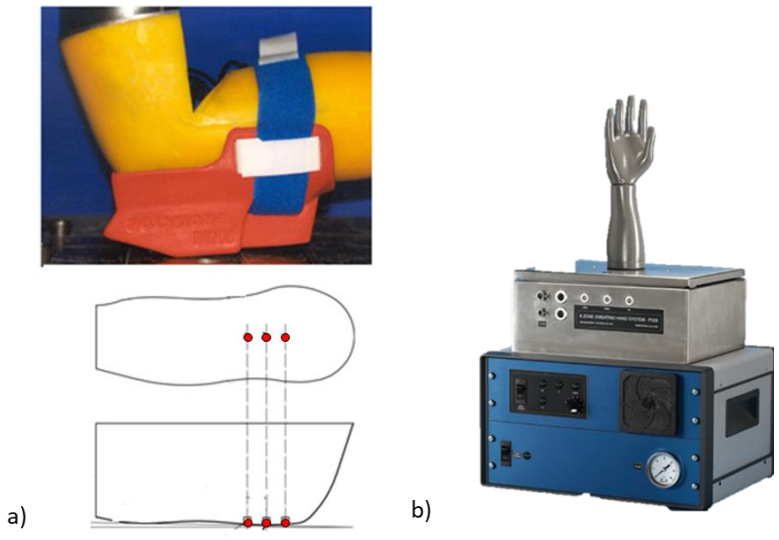

Figure 11.16: Instrumented surrogates a) BGIA "Kandy" test knee with transducers shown in red (European Committee for Standardization, 2010; Institut fuer Arbeitsschutz der Deutschen, 2015) b) Thermal hand system (Thermetrics, 2016)

11.6.2.2 Computational Models

Thoraval et al. (2013) proposed a new method to test protector performance based on the EN 14120 standard. Their approach utilised both computational and physical modelling (Figure 11.17). The solid resin forearm presented in Figure 11.17 was set at an angle of 55° in accordance with EN 14120. A complementary numerical model was developed by scanning the physical setup, applying material properties and fitting the wrist protector using spring elements in Pam-Crash software. The loads transmitted to the hand and forearm correlated well between the computational model and the physical rig.

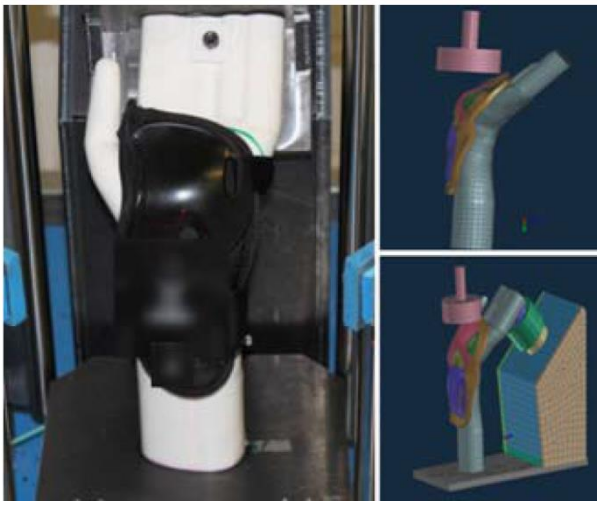

Figure 11.17: Physical and numerical model to evaluate protector performance (Thoraval *et al.*, 2013)

Validated computational models can be an effective tool for exploring joint kinematics, joint contact pressures and forces, soft tissue tensions and range of motion (Majors and Wayne, 2011). Computational wrist models fall under two main categories: finite element analysis (FEA) and rigid body modelling (RBM). Through advances in both knowledge and technology, computational models of the musculoskeletal system have gone through numerous iterations over the past 25 years (Gislason and Nash, 2012). Historically early models simplified the wrist joint to a 2-dimensional representation, by restricting the wrist position or fusing the bones together. Whilst such models were suited to specific applications and studies, their usefulness is limited to a particular case, as they cannot be used across a range of applications.

Mao et al. (2014) developed a 3D FEA model of a 10-year old child forearm in an attempt to characterise the mechanical responses of a backward fall. Their model

enables wrist protector models to be applied to the forearm, albeit directly to the bone and comparisons of stress contours across the structure to be obtained (Figure 11.18). As no paediatric data from cadaver tests are available, the authors adopted a scaling approach using values from adults to determine the relevant material properties. Validation of the model was not possible due to limited paediatric data which is contrary to Choppin and Allen, (2012) who state that user interactions and fully representative models need to be present for predictive models to provide realistic results.

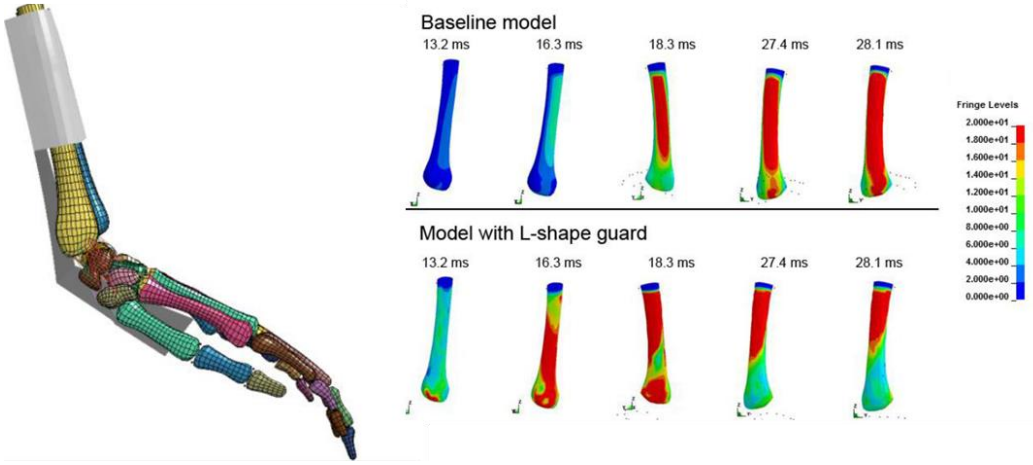

Figure 11.18: Wrist protector applied to the FEA model and stress contour comparison with and without protector (Mao, Cai and Yang, 2014)

Lehner et al. (2014) also used a combination of computer-aided engineering (CAE) tools to simulate falling scenarios and study the functional design of wrist protectors. The wrist joint and wrist protector designs were modelled in Computer-aided design software (CAD) and tested using FEA. The falls and loading situations were then simulated using a bespoke multibody system (MBS) to compare the performance of different protector designs (Senner, 2015). Through a series of laboratory studies, in which participants wearing a harness fell onto a crash mat, it was possible to obtain parameters such as impact force and wrist angle on impact enabling the validation of the MBS model (Schmitt et al. 2012).

Despite the limitations and assumptions inherent to computational models, this approach has shown promise. Majors & Wayne (2011) developed a 3D RBM model to study wrist range of motion when validated against a cadaver study the model reproduced 81% of the experiments within one standard deviation. Whilst

computational models are valuable; physical models are also needed to facilitate the performance testing of impact protection and support the validation of computational models. Payne et al. (2015a) argue that relying on computational analysis alone is unethical as it is necessary to test the physical product rather than relying on what was intended or predicted.

A major limitation of both computer and physical models is that their accuracy is largely dependent on the information that can be obtained from living and cadaver studies (Tsui, 2010). To date, numerous biomedical parameters related to simulating the wrist are ill-defined such as the fracture loads of adolescents; the relationship between peak load and hyperextension in a fracture; and the effective mass related to falling. As such, the developed test will be a pragmatic compromise between a true mechanical test and complete biofidelity.

11.6.3 Summary

The techniques presented provide a starting point for the characterisation of wrist protectors. Given the complexity of the wrist joint surrogates in literature lack biofidelity and fail to conform to the surrogate design principles outlined by Payne et al., (2013). To date, only Schmitt et al., (2012), based on EN 14120 standard, have tested a range of commercially available products. However, both the physical setup and test parameters used by Schmitt et al., (2012) lack a theoretical basis and consider only a single case rather than a range of parameters. This section has highlighted a gap in current research which limits the understanding of wrist protector efficacy and the effect of design elements.

11.7 Chapter Summary

From a review of the literature, the need for a representative test method and surrogate to evaluate the performance of a range of different snowboarding wrist protectors has been established.

Fall-related wrist injuries are the most common injury in snowboarders affecting various demographics. Given the frequency of such injuries, especially amongst

beginners and adolescents, there is a need for prevention based on an understanding of injury mechanisms and causation. Peak fracture force thresholds have been identified based on cadaveric studies. Whilst the samples used in these studies are not a true representation of the snowboarding population they serve as a useful starting point. Through a review of PPE design mechanisms, a set of protective performance criteria has been established. The field of fall biomechanics can also aid in the development of a test method, through the identification of the necessary parameters the test should consider in addition to peak force. Finally, by examining the current best practices in the field of mechanical testing and surrogate design, the limitations of current approaches have been identified and the need for a new method further emphasised.

Despite the existence of snowboard specific wrist protectors, fall-induced wrist injuries are still prevalent. Whilst some studies have demonstrated the protective capabilities of wrist protection at fracture load, no single test setup has evaluated the performance of a range of different products in a representative way. As such, there is a need for the development of a test method and surrogate to evaluate these products in an ethical, repeatable way.

Based on the findings of this literature review the idealised solution for a wrist protector test would utilise a validated biofidelic surrogate incorporating the hand, forearm elbow and shoulder. An idealised test would provide feedback on the injury event during a simulated fall throughout the whole upper extremity and identify the protective role played by the wrist protector. The developed test method will attempt to achieve a compromise between realism and a repeatable mechanical test due to numerous limitations. Namely: insufficient fracture thresholds for adolescents; mixed values reported for the proportion of body mass influencing the wrist at impact; incomplete understanding of the relationship between the forearm, elbow and shoulder during a fall; limited time; and limited funds.

12 Requirement specification for mechanical test methods

Previous research has identified that wrist protectors should: i) attenuate peak impact force; ii) absorb and transfer impact energy safely away from the wrist joint; iii) Stabilise the wrist and limit hyperextension. At present, there is no test set-up that can repeatedly assess wrist protectors based on these requirements. The limitations of existing approaches have been presented, highlighting the need for a new test method and surrogate. This chapter aims to identify the design requirements for new mechanical test methods. This aim will be achieved through the following objectives;

- To select appropriate boundary conditions related to injurious snowboarding falls
- To identify the design criteria for test setups

12.1 Test development approach

Most wrist protectors incorporate palmar pads for force attenuation and splints to reduce hyperextension. Testing to evaluate the protective pads in isolation and determine force attenuation is well established. However, no published approach has been established to quantify the rotational stiffness of wrist protectors, despite many products incorporating splints to reduce hyperextension. This project will take an incremental approach to developing new mechanical test setups. Firstly, a quasi-static test measuring the ability of wrist protectors to reduce hyper-extension will be developed as a preliminary tool to characterise products. As a quasi-static test cannot assess force attenuation properties of the palmar pad or rate effects of splints, a complementary approach employing an impact test will also be developed. Early identification of issues concerning the interaction of the wrist guard and surrogate during a quasi-static test will inform the development of an impact test.

The impact test will incorporate a measure of force transmission and the ability of wrist protectors to reduce hyperextension in a representative fall scenario. Figure 12.1 shows the necessary workflow to develop two complementary test setups. Wrist protector performance will be measured using both the quasi-static and dynamic impact setups.

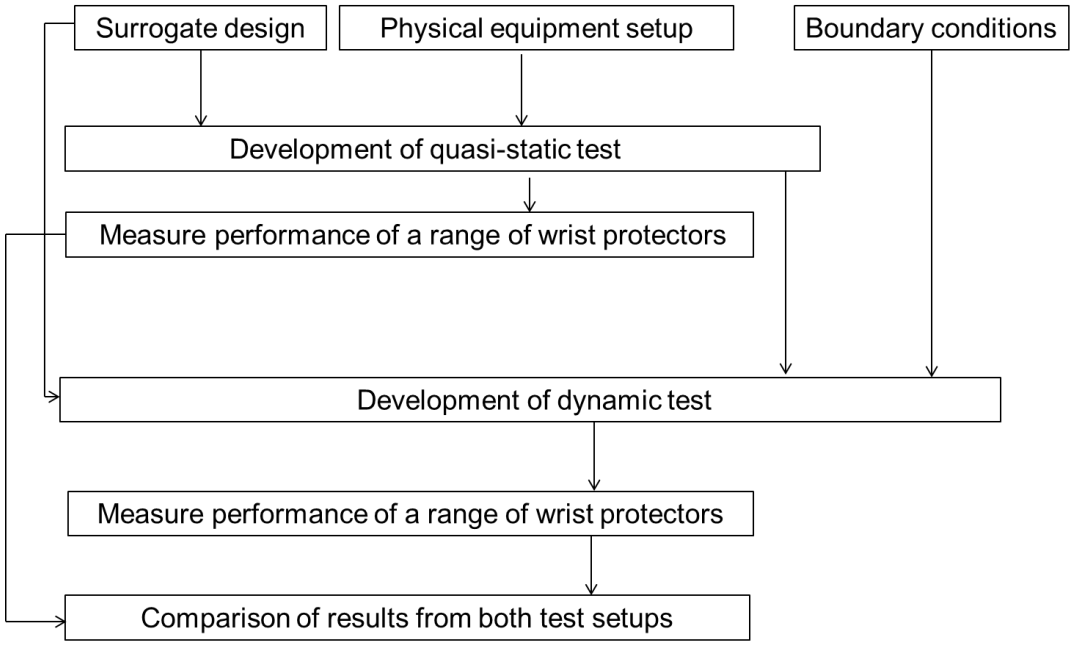

Figure 12.1: Test development approach

12.2 Boundary parameters

It is necessary to identify the requirements the system should adhere to in a product design specification (PDS), to facilitate the development of a test setup. Numerous factors should be considered when developing mechanical tests: boundary conditions (replicating injurious scenarios), physical test setup and physical constraints of university resources. Adopting a biomechanical approach with an understanding of injury mechanisms and human tolerance to load is important when designing injury prevention equipment (Odenwald, 2006; McIntosh, 2012). These parameters should be translated into input parameters and reproduced mechanically to test wrist protectors. Before a list of requirements can be established, it is necessary to identify the boundary parameters the test should replicate. The boundary parameters for the quasi-static test will be explored first, then the parameters specific to an impact test will be discussed.

12.2.1 Boundary parameters for quasi-static test

To inform the boundary parameters of a new quasi-static test setup, looking at other tests is beneficial. The EN 14120 (European Committee for Standardization, 2003b) has been identified as a suitable starting point for developing a dedicated snowboarding wrist protector standard (Schmitt, Michel and Staudigl, 2012). EN 14120 prescribes requirements for roller sports wrist protectors; requirement 5.9 stipulates that protectors

undergo a test to measure protector stiffness. This relates to protectors' ability to limit wrist hyperextension.

Protectors are deemed sufficiently stiff if the hand angle is between 35 to 55° when mounted to a simplified forearm surrogate and a 3Nm torque applied (European Committee for Standardization, 2003b). However, there is a lack of supporting literature to justify these thresholds. A study measuring wrist moment and hyperextension of snowboarders on a ski slope (Greenwald, Simpson and Michel, 2013) observed wrist extension angles of $76.8 \pm 15.8°$ (mean ± standard deviation) at wrist moments of 15.9 ± 20.7 Nm in snowboard falls which did not result in injury. The angles observed by Greenwald, Simpson and Michel, 2013 are higher than those in the roller sports standard, implying that higher thresholds could be more appropriate for snowboarders. The new quasi-static test should facilitate a wide range of torques and angles up to 90° to evaluate wrist protector products at representative boundary parameters.

12.2.2 Boundary parameters for impact test

To evaluate the protective capacity of wrist protectors using an impact test several parameters should be considered:

- Direction of fall
- Fracture force
- Time to fracture force (related to body/surrogate stiffness and surface compliance)
- Fall height and inbound velocity
- Mass of body acting on the wrist joint

Boundary parameters could be selected based on: cadaver studies (Frykman, 1967; Greenwald *et al.*, 1998; McGrady, Linda Hoepfner, Young and Raasch, 2001; Burkhart, Andrews and Dunning, 2013), or developing a mathematical model based on biomechanical data collected during low level non-injurious falls (Chiu and Robinovitch, 1998; DeGoede *et al.*, 2002; Hwang *et al.*, 2006) and scaling to a fracture scenario. As the purpose of the dynamic test is to characterise wrist protectors under injurious scenarios, cadaver studies will be used to ascertain the boundary parameters. The developed test will mimic backward falls with a stiff-arm posture as these falls have been identified as the worst cases.

12.2.2.1 Fracture force

Cadaver studies have identified the force required to fracture the distal radius. Table 12.1 shows thirteen different test setups including drop rigs and universal testing machines to initiate the radius fracture identified from the literature review. Due to the limited sample size and physical variation amongst specimens, there is considerable variation in the fracture loads reported both between and within studies. The mean fracture force from the reported cases is 2618 ± 822 N. Whilst a number of published studies examine fracture force they do not all contain sufficient information to facilitate the development of an impact test. To determine which published study the developed impact test should replicate numerous inclusion criteria were set:

- Force-time plots of the fracture impact scenario published
- Setup uses full cadaver forearm rather than bare bones
- Applied mass acting on the wrist joint reported
- Inbound velocity reported

Table 12.1: 13 studies with fracture loads of adult cadaver forearm

Reference	Gender	Experimental Setup	Fracture Site	Mean fracture load (N) ± SD (if recorded)
Frykman 1967	Female	Dynamic	Radius	1863
		Quasi-static compression	Radius	1917 ± 640
	Male	Quasi-static compression	Radius	2769 ± 1266
		Quasi-static compression	Radius	2769 ± 1266
Horsman et al. 1983	Female	Quasi-static compression	Radius	3600 ±1160
Myers et al. 1991	Female	Dynamic	Radius	3180 ± 1000
	Male	Dynamic	Radius	3740 ± 532
Myers et al. 1993	Female	Dynamic	Radius	1580 ± 600
	Male	Dynamic	Radius	2370 ± 420
Spadaro et al. 1994	Unknown	Quasi-static	Radius	1640 ± 980
		Quasi-static	Scaphoid	2410 ± 913
Augat et al. 1996	Female	Quasi-static	Radius	2008 ± 913
	Male	Quasi-static	Radius	3773 ± 1573
Giacobetti et al. 1997	Unknown	Dynamic compression	Radius	2245
Augat et al. 1998	Unknown	Dynamic	Radius	2648 ± 1489
Greenwald et al. 1998	Unknown	Dynamic	Forearm	2821 ± 763
McGrady et al.2001	Unknown	Dynamic - Incline	Radius	1104 ± 119
Lubahn et al. 2005	Unknown	Dynamic - Incline	Radius with ulnar	2920 ± 1197
		Dynamic - vertical	Radius with ulnar	3896 ± 1991
Burkhart et al. 2012	Unknown	Dynamic	Radius	2141 ± 1229
Zapata et al. 2017	Male	Dynamic	Radius	3148 ± 452
Overall mean ± SD			**2618 ±822**	

12.2.2.2 Time to fracture

Force time traces enable the approximation of loading rate. As shown in Table 12.2, of the thirteen cadaver studies presented, only four include force time plots. To extract data from the published graphs, each plot was manually digitised by converting the data points from the published image to pixels at approximately 0.4 ms intervals in Microsoft paint. Each data point was transformed into force time units enabling

comparison plots to be produced in Excel. An example of an original plot and the digitised version is shown in Figure 12.2. A comparison of all 4 force time traces with the peak forces aligned at 0 seconds is shown in Figure 12.4.

Table 12.2: Subset of cadaver studies that include force time plots

Experimental Design		**Boundary Conditions**				**Reference**
		Input variables		**Output variables**		
Equipment setup	***Sample***	***Applied mass (kg)***	***Inbound velocity (m/s)***	***Fracture force (N)***	***Time to peak (s)***	
Vertical drop test	Forearm	23	2.8	2802	0.024	Greenwald et al. 1998
Pendulum impactor	Forearm	32	3.1	4315	0.011	Frykman, 1967
Angular drop test	Forearm	Unknown	3.9	1104	0.019	McGrady, Linda Hoepfner et al. 2001
Powered horizontal setup	Radius and scaphoid bone	7	3.4	2266	0.008	T. A. Burkhart et al. 2013

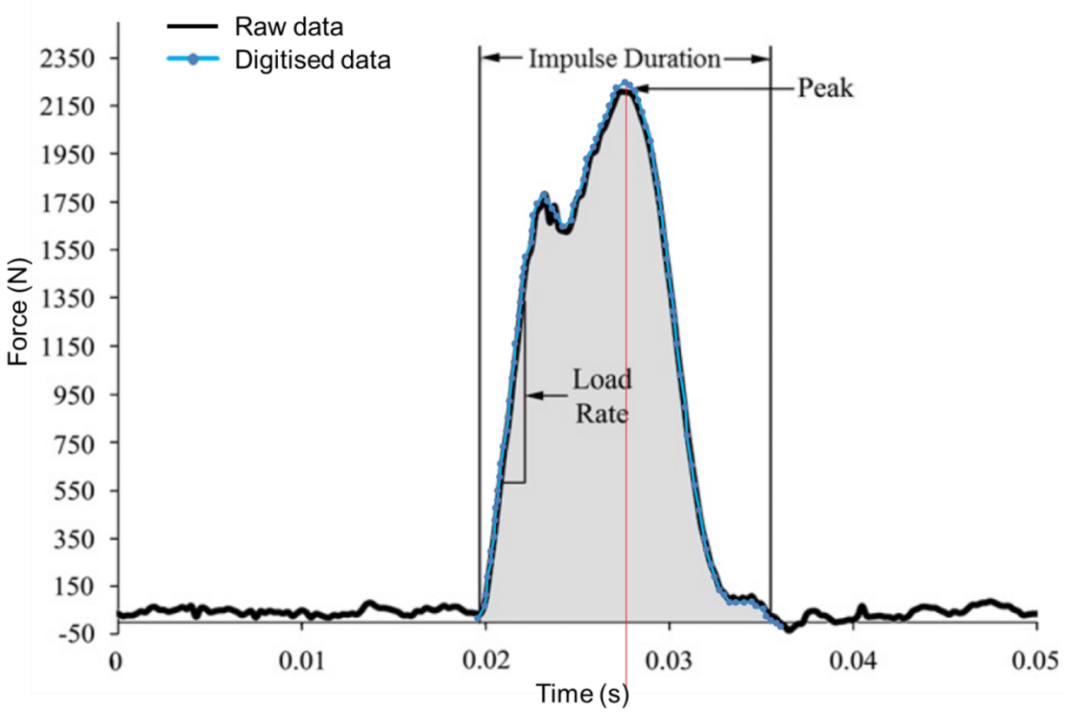

Figure 12.2: Digitised data overlaid on top of the original plot presented by Burkhart, Andrews and Dunning (2013)

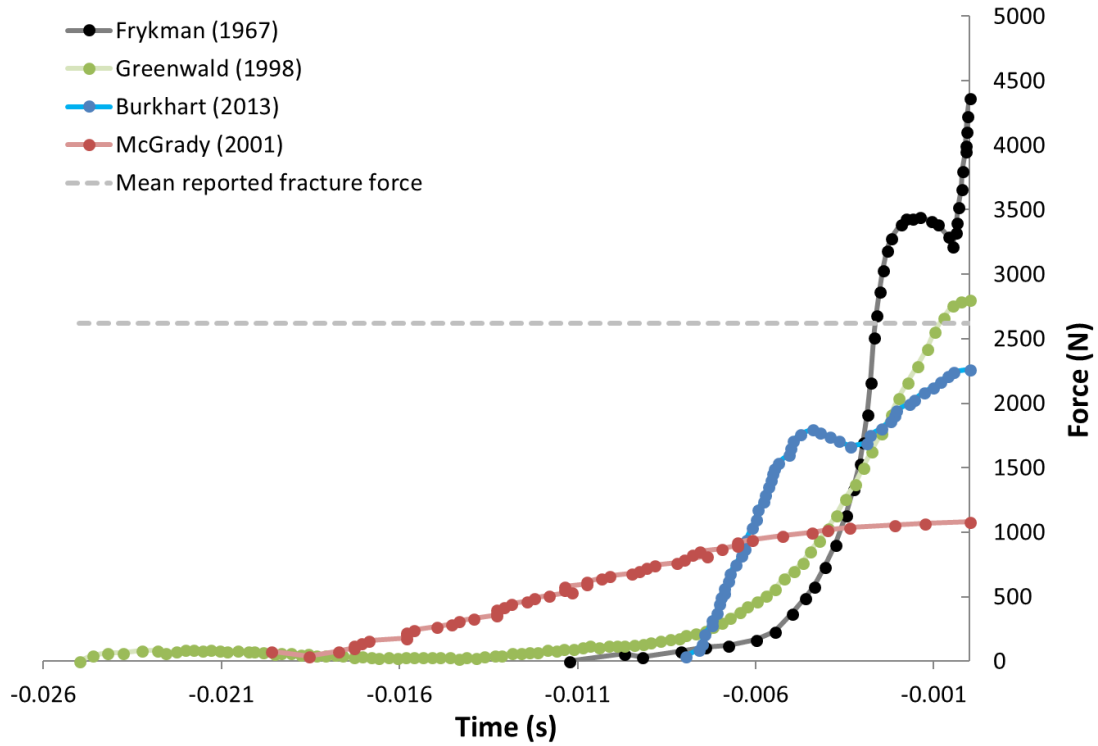

Figure 12.3: Comparison of digitised force time traces for 4 cadaver studies (Frykman, 1967; Greenwald *et al.*, 1998; McGrady, Linda Hoepfner, Young and Raasch, 2001; Burkhart, Andrews and Dunning, 2013)

McGrady, Linda Hoepfner, Young and Raasch, (2001) do not report the mass of the system. Therefore, it is not possible to design an impact test based on this work. Whilst the work of Burkhart, Andrews and Dunning, (2013) contains all the necessary

parameters; it replicates a different case as only the radius bone was used rather than the full forearm. Thus, the dynamic test can only be informed by the work of Frykman, (1967) and Greenwald et al., (1998).

In the work of Frykman, (1967) a moving mass is applied to a the palm of fixed cadaver (Figure 12.4a) through a pendulum, whereas Greenwald et al. (1998) set the cadaver forearm at an angle and dropped the cadaver onto a foam covered force plate (Figure 12.4b). The increased time to peak observed by Greenwald et al. (1998) (~0.015 s) is likely a result of the fingers of the cadaver contacting the force plate before the palm contacts the force plate, resulting in forearm compression, as shown in Figure 12.5. If the time to peak started from the point at which the force trace starts to increase before peak force, then the time to peak for the case measured by Greenwald *et al.*, (1998) would be ~ 0.009 s, similar to the 0.011 s measured by Frykman, (1967). Greenwald et al. (1998), used a foam pad on top of the force plate to represent snow, however Frykman, (1967) did not. This disparity in methods, likely accounts for the steeper loading rate gradient found by Frykman, (1967).

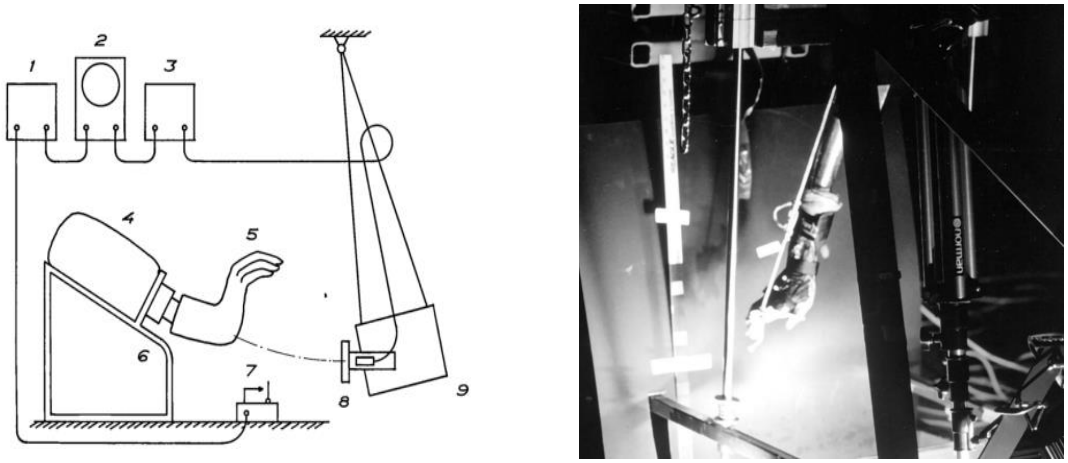

Figure 12.4: a) Frykman (1967) experimental setup with palmer impact **b)** Greenwald et al. (1998) experimental setup with forearm dropped onto a force plate

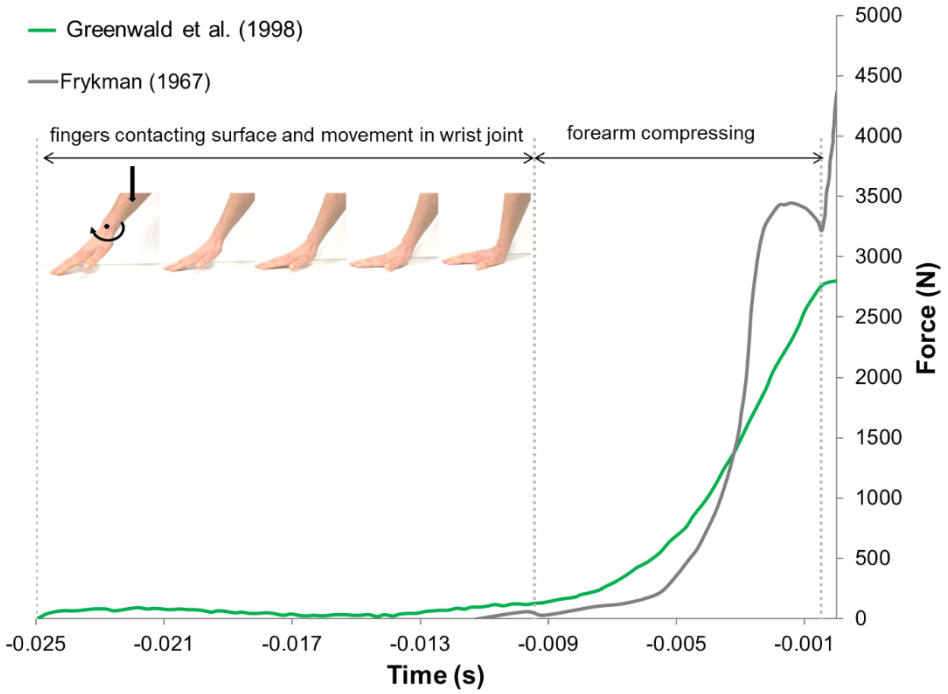

Figure 12.5: Comparison of time to peak between Greenwald et al. (1998) and Frykman (1967)

The developed setup will be informed by Greenwald et al. (1998). The fracture force for the published trace occurs at 2802 N which is similar to other published studies (2618 ± 822 N Table 12.1). The fracture force presented for Frykman (1967) is somewhat questionable and 1 kN above the range from other published studies (4315 N). The fracture force presented by Greenwald and colleagues is 2802 N, however the peak force of the system is higher as the velocity had not reached 0 m/s when the radius fractured as shown in Figure 12.6.

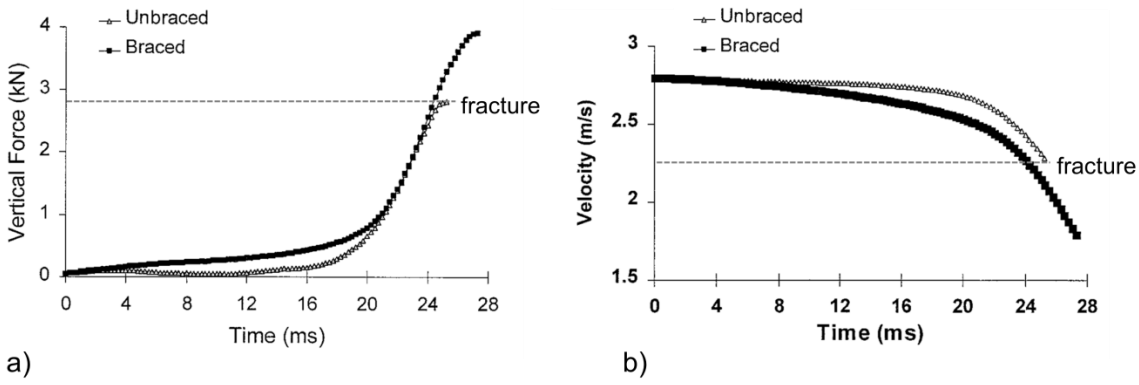

Figure 12.6: Plots from Greenwald et al. (1998)showing the incidence of fracture a) force time plot b) velocity time plot, only the unbraced condition is of interest

12.2.2.3 Compliance of system

The developed test set-up will involve a stiff impact rig and surrogate to allow the repeatable testing of wrist protectors under injurious loads. Rather, than attempting to duplicate the material properties of a frangible human arm where the repeatability is very hard to achieve. It is known that rigid body impacts result in short impact transients, not representative of the human body. It is, therefore, necessary to build some compliance into the system to simulate the dynamic stiffness. Typically, this is done by determining the system's stiffness from the gradient of a force displacement plot and replicating this within the experimental setup. However, as no displacement data is available, an alternative approach based on loading rate was used. The force time plot has been adjusted to start at 0 s and 0 N from the point where the force is continually increasing after the long lead time. Based on this adjusted force trace, the loading rate can be determined from the gradient of the curve during the linear ramp-up phase as shown in Figure 12.7. The loading rate is determined based on the adjusted data intercepting the origin. Therefore, the developed system should replicate this loading rate of 449262 N/s over 0.0045 s.

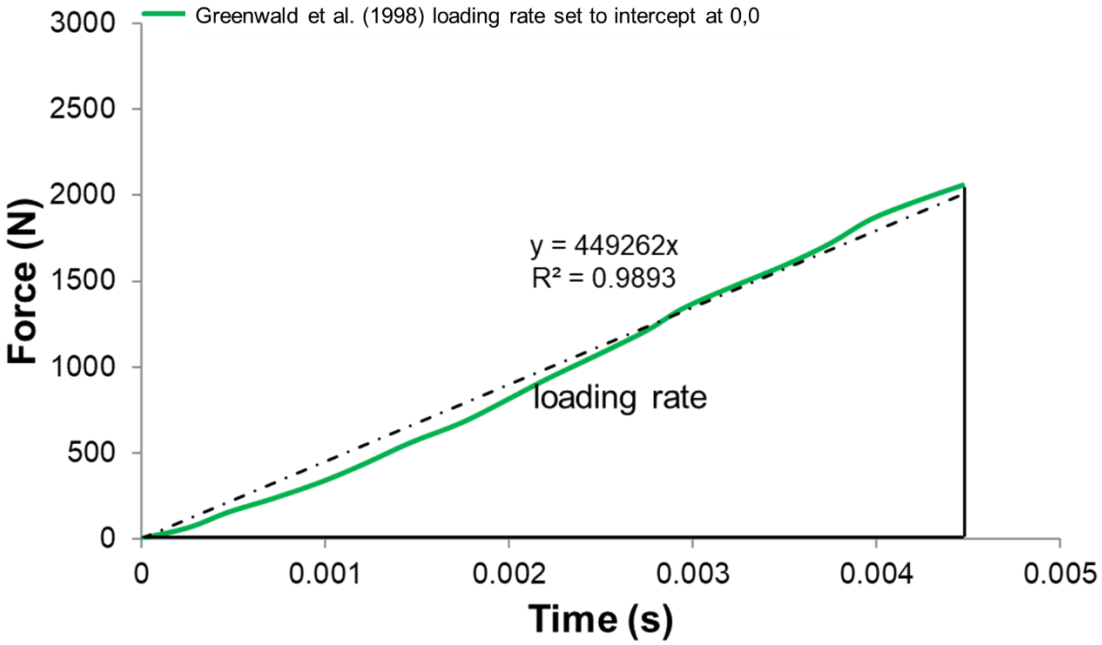

Figure 12.7: Force time curve for the Greenwald et al. (1998) fracture event adjusted to start at zero with linear loading rate

12.2.2.4 Fall height and inbound velocity

Cadaver studies give an indication of fracture load; however, the inbound test parameters such as velocity and mass tend not to be based on fall scenarios. No impact

velocity data exists for backward falls from standing, as this would put participants in at risk. It is possible to approximate the inbound velocity that would result from a backward fall from standing on a horizontal surface, by considering the body as an inverted pendulum. Impact velocity can be calculated based on fall heights derived from anthropometric data and the body position at impact.

From the work of Schmitt et al. (2012) it is possible to approximate the body position at impact. Figure 12.8a shows the arm angle of the participant during a simulated backwards fall. By digitising the reflective markers and simplifying the feet to shoulder segment as one line and the shoulders to the wrist as another, it is possible to determine the arm angle at impact. Assuming this arm configuration is constant throughout the entire fall (Figure 12.8b), the line from the heels to the wrist (L) can be used to simplify the fall into an inverted pendulum. Based on arm length and shoulder height, L and hence fall height and velocity can be determined using trigonometry and the conservation of energy (equations 1-5). Where L is an infinitely stiff rod, and the equivalent mass is a point mass at the end.

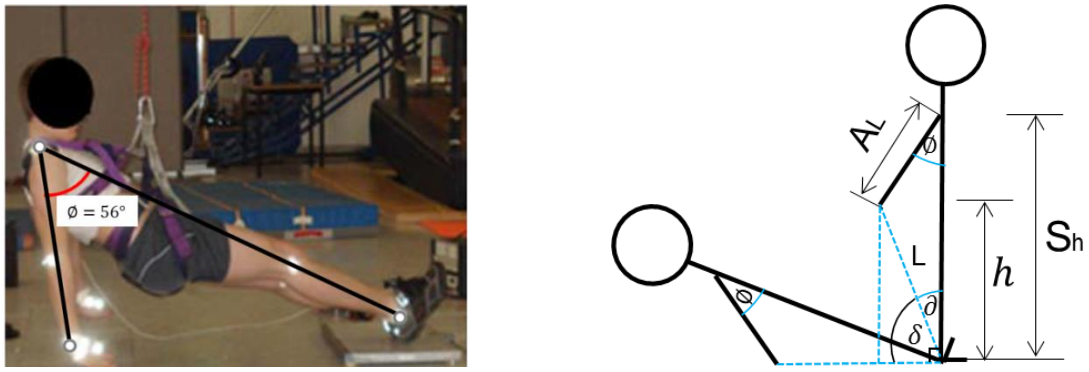

Figure 12.8: a) Arm angle from experimental backward fall scenario with a wrist drop height ~ 0.125 m (Schmitt *et al.*, 2012) **b)** Backward fall scenario. h- fall height, AL - arm length, L- distance from heel to the wrist, Sh -shoulder height

$$L = \sqrt{(Al^2 + Sh^2 - (2 * Al * Sh * \cos 56))} \quad (1)$$

$$\partial = \sin^{-1}\left(\frac{Al * \sin 56}{L}\right) \quad (2)$$

$$\delta = 90 - \partial \quad (3)$$

$$h = L * \sin \delta \quad (4)$$

$$v = \sqrt{2 * g * h} \quad (5)$$

Table 12.3 shows how fall velocity is determined for three different cases; 10-year-old child, 50th percentile male and 95th percentile male, assuming the arm angle position is always 56°. However, the fall height might be higher if snowboarders fall backwards down a slope rather than from horizontal. Whilst the velocity could be higher if snowboarders are moving prior to the fall.

Table 12.3: Inbound velocity for three different fall cases

Measurement	**10-year-old child (50th percentile)**	**50th percentile male**	**95th percentile male**
Shoulder height (m)*	1.08	1.44	1.55
Arm length (m)*	0.57	0.73	0.78
∅ (°)	56	56	56
Distance from heel to wrist (m)	0.90	1.20	1.28
∂ (°)	32	30	30
δ (°)	58	60	60
Fall height (m)	0.76	1.03	1.11
Inbound velocity (m/s)	3.86	4.50	4.67

* Anthropometric measurements (Alvin R Tilley and Henry Dreyfuss Associates, 2002)

The calculated velocities in Table 12.3 are higher than the reported impact velocities used in cadaver, biomechanics or mechanical studies, presented in Table 12.4. As the human body is not rigid, it is likely the inbound velocity would be lower. Snowboarders with flailing limbs and bent knees combined with the flexion of body segments will alter the inbound velocity.

In the first instance the dynamic study will aim to replicate the scenario presented by Greenwald et al. (1998). The work of Greenwald and colleagues is based on an inbound velocity of 2.8 m/s indicative of a 0.4 m fall. However, based on a 50th percentile male it is likely that fall height will be higher resulting in higher fall velocities. Whilst the setup will be designed to replicate Greenwald et al. (1998), adjustability will be built in, so products can be tested over a range of velocities.

Table 12.4: Reported velocities from other studies

Experimental setup	**Mean velocity (m/s)**	**Mean drop height (m)**	**References**
Mechanical using cadavers	3.54	0.69	(Frykman, 1967; Lewis *et al.*, 1997; Moore *et al.*, 1997;

			Greenwald *et al.*, 1998; McGrady, Linda Hoepfner, Young and Raasch, 2001; Lubahn *et al.*, 2005; Burkhart, 2012)
Biomechanics using participants	1.60	0.33	(Chiu and Robinovitch, 1998; Robinovitch and Chiu, 1998; Chou *et al.*, 2001; DeGoede and Ashton-Miller, 2002; DeGoede *et al.*, 2002; Lo *et al.*, 2003; Schmitt *et al.*, 2012)
Mechanical using surrogates	2.24	0.27	(Hwang *et al.*, 2006; Thoraval *et al.*, 2012; Maurel *et al.*, 2013)

12.2.2.5 Mass of body acting on the wrist joint

When transferring boundary conditions from biomechanics studies to mechanical test setups, an effective mass is used. Table 12.5 shows that to date published effective masses have ranged from 1.7 kg (DeGoede *et al.*, 2002) to 45.5 kg (Lubahn *et al.*, 2005) across study types. Some variation in effective mass between studies is expected due to the variability in segment stiffness throughout the chain but not to the extent that has been reported. Whilst the setup will be designed to match the 23kg case of Greenwald and colleagues; it should also be possible to test products over a range of masses. This will enable test parameters to be adjusted as biomechanics literature advances. It is not practical to develop a rig that accommodates masses as low as 3kg whilst maintaining structural integrity, but the setup will be designed to facilitate masses below 23kg.

Table 12.5: Overview of effective mass used in different studies (adapted from Schmitt et al. 2012)

Experimental setup	**Effective Mass (kg)**		**References**
	Mean	**Range**	
Mechanical using cadavers	23	7.9-45.5	(Frykman, 1967; Lewis *et al.*, 1997; Moore *et al.*, 1997; Greenwald *et al.*, 1998; Lubahn *et al.*, 2005; Burkhart, Dunning and Andrews, 2012; Zapata *et al.*, 2017)
Biomechanics using participants	3	1.7-5.5	(Chiu and Robinovitch, 1998; DeGoede *et al.*, 2002; Schmitt *et al.*, 2012)
Mechanical using surrogates	3	2.5-3.5	(Maurel *et al.*, 2013; Thoraval *et al.*, 2013)

The developed impact test setup will be based on the work of Greenwald et al., (1998) and match the test parameters presented in Table 12.6. In the case of velocity and mass

parameters, the system will be variable to enable a range of different fall scenarios to be tested.

Table 12.6: Boundary parameters for impact test

Test Parameter	Value
Fall direction	Backwards
Loading rate	483622 N/s over 0.0045 seconds
Inbound velocity	2.8 m/s [range 2.8- 5 m/s]
Effective mass	23 kg [range ≤ 23kg]

12.3 Product Design Specification

Pugh's (1991) method for total product design outlines 32 elements that should be considered when writing a PDS. Criteria irrelevant to the design of a one-off test device for a specific research application rather than a commercial product were excluded. Pugh (1991) suggests the design specification should outline the criteria the developed tests should meet to facilitate the evaluation of wrist protectors. General requirements relevant to both test setups are listed in Table 12.7, test specific criteria are outlined in Table 12.8 and Table 12.9. The quasi-static test will focus on characterising protectors up to hyper-extension angles of 90°, whilst the dynamic test will be based on the boundary parameters identified above.

Table 12.7: General Requirements relevant to both setups

Number	Requirement
Primary Requirements	
Performance	
1.1	Should facilitate the testing of both standalone protectors and protective gloves without permanent modification
1.2	Should utilise a surrogate incorporating fingers based on anthropometric dimensions
1.3	Should be able to differentiate between products
Timescale	
2.1	Both test rigs should be designed and built within 12 months
Cost	
3.1	Material costs for both test setups cannot exceed £1500
3.2	Man hours: The university's in-house design engineer will have limited time to dedicate to this project. Therefore the design should incorporate tasks that can be outsourced and are not time consuming where possible.

Product life span	
4.1	The test rigs should have a minimum life in service of 5 years
Size	
5.1	The test rigs should fit within the university laboratory ceiling height of 3m
Quality & Reliability	
6.1	The setup should be reproducible by other operators and institutions
Safety	
7.1	The test rig should not pose a risk to the investigator
Secondary Requirements	
Environment	
8.1	Facilitate testing at both room temperature and in a cold condition -25 to 25°
Maintenance	
9.1	Require minimal maintenance during service life
Installation	
10.1	The test rig should be mounted to existing fixtures/machines within the university's laboratories such as material testing machines or a drop hammer
10.2	The test rig should be easy to install in test houses should it be adopted as a standard
Ergonomics	
1.1	The system will be operated by one healthy adult

Table 12.8 Requirements specific to the quasi-static setup

Number	Requirement	Parameter
1.4	Should enable the measurement of wrist extension and applied torque	angles up to 90°

Table 12.9: *Requirements specific to the dynamic setup*

Number	Requirement	Parameter
1.5	Suited to the collection of multiple measurements: peak force, energy absorption and wrist extension angle at a sufficiently high frequency	
1.6	Should result in a peak force for the bare hand condition above the identified fracture threshold	>3440 (mean + SD from 22 reported cases)
1.7	Should replicate the loading rate of the Greenwald *et*	loading rate =

	al. (1998)	483622 N/s over 0.0045 s
1.8	Should replicate the inbound speeds associated with a backwards fall	2.8-5 m/s
1.9	Should replicate the impact mass associated with falls	5-23 kg
4.2	Withstand dynamic impacts	≥ 5.25 kN (1.5xfracture load)

12.4 Chapter summary

The aim of this chapter was to specify the design requirements for the two mechanical tests: quasi-static and impact. By identifying the boundary parameters associated with an injurious snowboarding fall and the physical constraints of university resources, a specification that outlines all the criteria the tests should meet has been developed. Through fulfilling these requirements, solutions that can evaluate the protective capacity of wrist protectors will be developed. This chapter contributes to Objective 3 in this PhD; to develop representative test methods to evaluate snowboarding wrist protector performance. Future chapters will discuss the development of the two test setups.

13 Development of Quasi-Static Test

13.1 Introduction

Previous chapters highlight the need for mechanical tests to evaluate snowboarding wrist protector performance. The aim of this chapter is to develop a quasi-static test to measure protector stiffness. This aim will be achieved through the following objectives:

- To critique the EN 14120 stiffness test
- To develop a test to quasi-statically measure wrist protector stiffness
- To evaluate the suitability of the experimental setup

13.2 Critique of EN 14120 stiffness test

The EN 14120 (European Committee for Standardization, 2003b) has been identified as a suitable starting point for developing a dedicated snowboarding wrist protector standard (Schmitt, Michel and Staudigl, 2012). There are marked differences between the two sports meaning this protocol should not be directly transferred to snowboarding products. In contrast to snowboarding the majority of in-line skating falls are in a forward direction onto a horizontal surface (Knox and Comstock, 2006). Snowboarders wear gloves over protection to keep them warm, whereas inline skate protectors feature a low friction plate on the palm to deflect the hand forward and limit the load experienced by the arm. To critique the EN 14120 test setup and identify the strengths and weaknesses of the approach proposed in the standard, the test was recreated.

13.2.1 Test Setup & protocol

Initial investigations recreating the EN 1410 test found several issues with the surrogate design and test setup. This finding is contrary to the requirement for clear and unambiguous standards (International Organization for Standardization, 2011). This body of work is described in detail in the author's publication Adams et al., 2016. The prescribed setup to apply the necessary torque is shown in Figure 13.1a. Information regarding the application of load or the distance between the wrist rotation axis and force application axis (distance 3) is not provided. The figure is misleading as measuring angles up to 55° would require a force application point closer to the wrist to maintain contact with the hand (Figure 13.1b).

The maximum values for distance 3 to enable angular displacement of 55° for each surrogate are shown in Table 13.1. However, it is not always possible to apply a load directly to the surrogate, due to the dimensions of the wrist protector. For longer protectors the load applicator would start in contact with the protector then slide onto the bare surrogate as the hand displaces, as shown in Figure 13.2. Interaction between the load applicator and protector could lead to unwanted protector movement, influencing the fit and potentially the test outcome. In addition to unclear diagrams, the EN 14120 stiffness test protocol is ambiguous and fails to specify how tightly protectors should be strapped, the number of repeats or the rate at which the load should be applied. This ambiguity could lead to inconsistent results between operators.

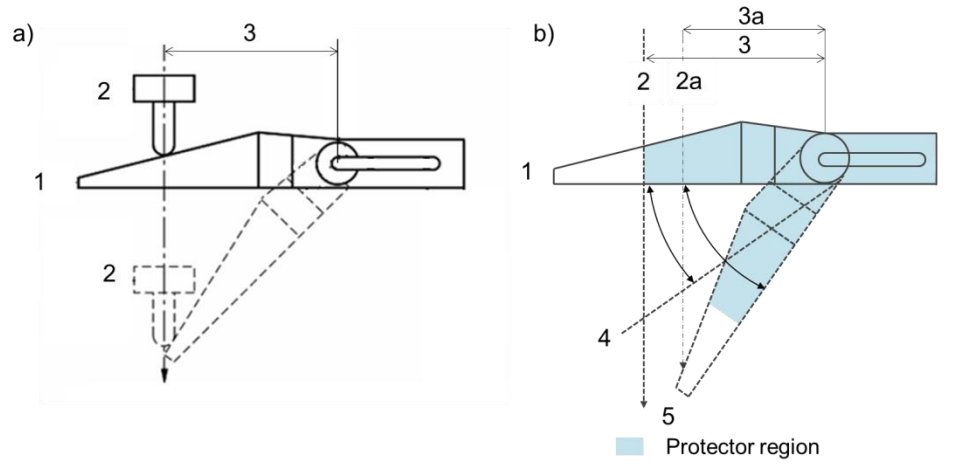

Key
1. Starting position
2. Point of force application from EN 14120
2a. Point of force application to maintain contact and achieve 55°
3. Distance between wrist rotation axis and force application axis from EN 14120
3a. Modified distance between wrist rotation axis and force application axis to achieve 55°
4. 35° from start position
5. 55° from start position

Figure 13.1 a) Schematic of EN 14120 stiffness test b) Modified test setup (adapted from European Committee for Standardization, 2003)

Table 13.1: Maximum distance between wrist rotation axis and force application axis for each surrogate size presented in EN 14120

	Surrogate Size		
	A	B	C
Distance 3 (mm)	88	99	110

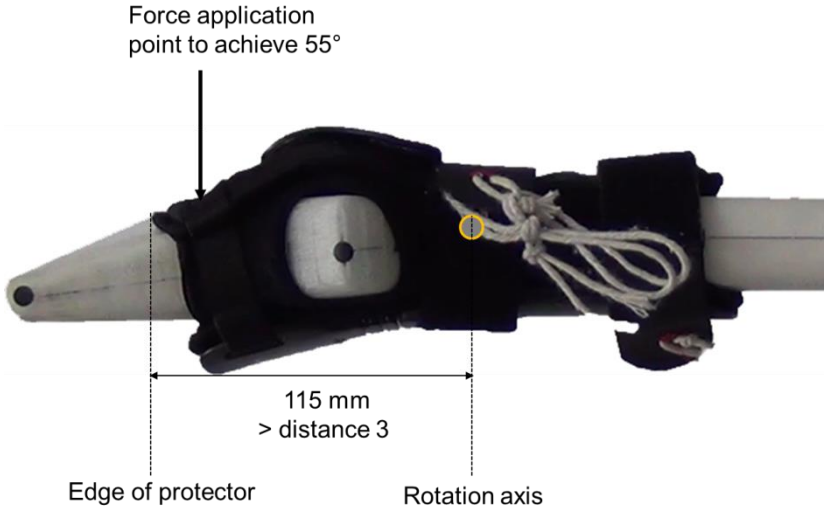

Figure 13.2: Size C surrogate wearing size medium Flexmeter protector

Another weakness of the EN 14120 standard is the value of the test parameters. As mentioned in the previous chapter, products are deemed to be adequate if protectors displace between 35 and 55° at a set torque (3 Nm for size C surrogate, European Committee for Standardization, 2003b). However, there is a lack of supporting literature to justify these thresholds. Therefore, a test setup that can facilitate a wide range of torques and angles is needed to evaluate wrist protectors at representative boundary parameters.

13.2.2 Surrogate Design

Numerous weaknesses were found with the EN 14120 surrogate design, concerning the shape, joint and size. The surrogate shape is simple, consisting of a rectangular cross-section forearm and a paddle-like hand with no fingers depicted in Figure 13.3. This limits the use of the surrogate for testing protectors integrated into gloves. To maintain protector alignment and attachment during testing, Payne et al, (2013) argued that surrogates with biofidelic geometries should be used when testing protective equipment. Schmitt et al., (2012) modified the EN 14120 surrogate design to incorporate fingers although no supporting dimensions were provided. The EN 14120 standard is unclear regarding the construction of the low friction hinge joint between the hand and wrist. In addition, the EN 14120 surrogate cannot be recreated based on the schematics and associated dimensions stated in the standard, and this represents a further weakness. Three thickness dimensions are not provided (marked as x,y and z on Figure 13.3), whilst there is a discrepancy for four other measurements g,h, i and j between the

dimensions presented in the standard and the accompanying figure. Based on the figure g < h and i<j, however the presented values do not adhere to this.

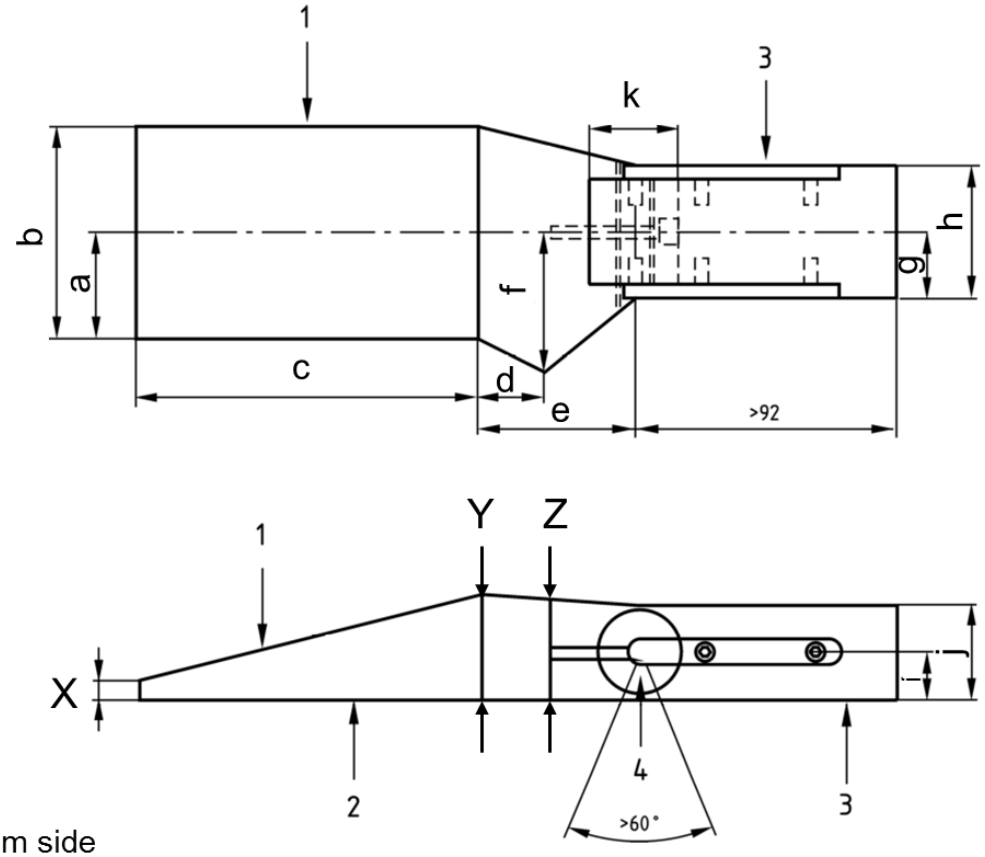

Key
1. Palm side
2. Back side of palm
3. Wrist
4. Joint (low friction coefficient cylinder)

t

Figure 13.3: EN 14120 surrogate x,y,z are missing dimensions and g,h, i and j are presented incorrectly (adapted from European Committee for Standardization, 2003b)

Typically, protectors are sold based on hand size. Therefore, it is unclear why the standard differentiates surrogate size based on user mass. Table 13.2 presents the EN 14120 surrogate sizes and their equivalent user groups based on anthropometric data selected from the specified user mass. To monitor the suitability of EN 14120 surrogate dimensions, a comparison between surrogate sizes and published data was made in Table 13.3. Due to limited published data for child and youth hands, only three of the surrogate dimensions can be cross-referenced to published datasets.

Table 13.2: EN 14120 Surrogate sizes and torque requirement with equivalent user group based on anthropometric data (Pheasant, 2001; Alvin R. Tilley and Henry Dreyfuss Associates, 2002; European Committee for Standardization, 2003b)

	EN 14120 Surrogate Size		
	A (users <25 kg)	**B** (users 25-50 kg)	**C** (users >50 kg)
Torque requirement (Nm)	2	3	3
Equivalent user group	<50th percentile age 8	50th percentile age 8-14	>50th percentile age 14
EU hand size	-	7	9

Table 13.3 :Comparison between surrogate size and anthropometric dimensions based on equivalent user groups (Alvin R Tilley and Henry Dreyfuss Associates, 2002)

Measurement (mm)		**EN 14120 Surrogate Size** **A** (users <25 kg)	**B** (users 25-50 kg)	**C** (users >50 kg)
Hand length (c+e)	Surrogate	153	172	191
	Anthropometric dimensions based on equivalent user groups	<137	137-172	>172
Hand breadth exc thumb (b)	Surrogate	65	73	81
	Anthropometric dimensions based on equivalent user groups	<63	63-79	>79

EN 14120 surrogate A is larger than the dimensions for the largest user in the <25 kg category. Whilst, EN 14120 surrogate B appears to be a good approximation for users between 25-50 kg, based on measurements of hand length and breadth. As EN 14120 surrogate C is suitable for all users > 50 kg, direct comparisons with published data are difficult. By examining a series of measurements for different user groups > 50 kg, a deeper understanding of the relevance of the surrogate size can be established (Table 13.4).

Table 13.4: Surrogate size C compared to 50th percentile male(Alvin R. Tilley and Henry Dreyfuss Associates, 2002)

Measurement (mm)	**Hand breadth (exc thumb)** B	**Hand breadth (with thumb)** (f-a)+b	**Wrist breadth** g	**Wrist depth** i	**Hand length** c+e
Surrogate size C	81	94.5	50	35	191
5th percentile female	69	81	51	31	152
50th percentile female	76	91	58	38	172
50th percentile male	89	104	69	43	191
95th percentile male	99	117	76	50	213
Range of anthropometric measurements	69-99	81-117	51-76	31-50	152-213
Median of anthropometric measurements	83.3	98.3	63.5	40.5	182

The dimensions of EN 14120 surrogate C tend to be similar to the median of the four different user groups, with the exception of wrist breadth. The EN 14120 surrogate wrist breadth measure is smaller than the four published sizes. Based on the above table surrogate size C appears to be a good compromise for a wide range of users >50 kg. To keep standards simple there is a need to limit the number of surrogate sizes, but the use of hand size rather than body mass is preferable.

Several issues were identified during the EN 14120 critique: test setup, test protocol, boundary conditions and surrogate design. To overcome these issues and enable products to be tested over a range of angels a new quasi-static test setup is needed.

13.3 Development of test method to quasi-statically measure wrist protector stiffness

This section describes the development of a new method to characterise the stiffness of snowboarding wrist protectors.

13.3.1 Concept Design

Based on the critique of the EN 14120 stiffness test and the design requirements outlines in Chapter 3, ideation sessions with input from the university's design engineer resulted in the development of 5 concepts (Figure 13.4). Concept a uses a motor embedded within the surrogate to drive rotation through the wrist joint. Concept b is the simplest concept where increasing mass is applied to the hand to generate angular displacement. Concepts c,d and e facilitate angular displacement over a range of loads through mounting the surrogate to a universal testing machine. Such machines incorporate load and displacement instrumentation, can use a range of load cells and be used with speeds up to 500 mm/min. They are typically used for material testing and are commonly found in universities and test facilities.

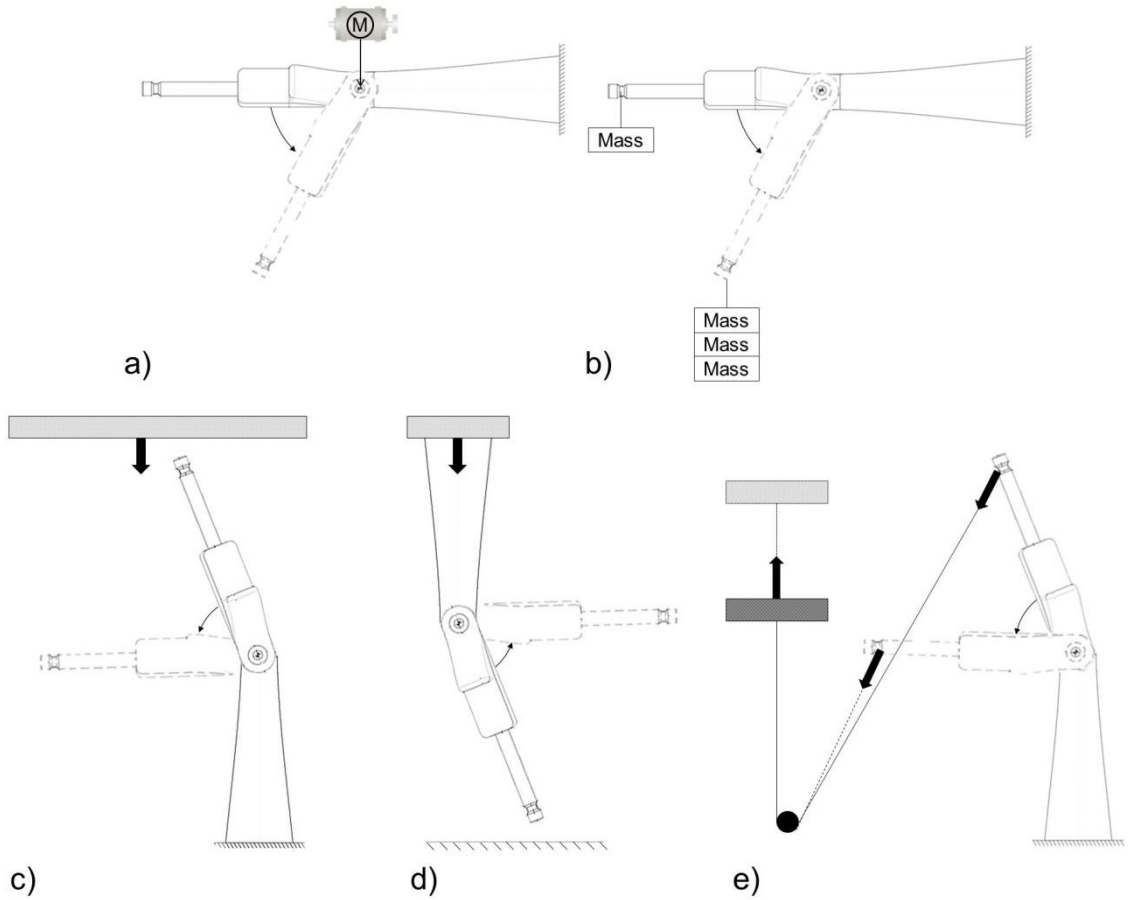

Figure 13.4: Concept design **a)** Motorised axle within wrist joint **b)** Variable masses applied to the hand **c)** Compression set-up with moving plate applied to fixed surrogate **d)** Compression set-up with moving surrogate applied to rigid surface **e)**Extension set-up with load applied to hand via pulley through upward displacement

13.3.2 Concept Selection

All five concepts meet the criteria outlined in the product design specification. Therefore, in order to determine which concept should be taken forward to further development and manufacture a decision matrix was established. The criteria were informed by the product design specification and discussions with the design engineer responsible for the construction of the setup. As can be seen in Table 13.5 these criteria are based on manufacturability, potential for instrumentation and usability. Each of the five concepts is rated on a scale of 1-3 for its feasibility to meet the design criteria, where a score of 1 means it would poorly satisfy the criterion, and 3 means it fully satisfies the criterion.

Table 13.5: Concept selection matrix

Criteria	**Concepts**				
	Stand alone		**Mounted to universal test machine**		
	a	**b**	**c**	**d**	**e**
Easy to manufacture - Uses off the shelf components - Can be mounted to existing test setups within the university	1	3	2	2	3
Easy to operate	3	1	3	2	3
Easy to instrument	1	1	3	3	3
Total	5	5	8	7	9

Concept e scored the highest based on the design criteria. This concept involves fixing the surrogate in a vertical position and applying a torque via load cell (built into the universal testing machine) through a pulley and cable system. Concept c which uses a plate fixed to the load cell rather than a pulley and cable also score well. However, concept e was considered preferable as it would involve using pulley and cable components which are regularly available rather than the manufacture of a bespoke plate and fixture. Therefore, a test setup based on concept e was further developed and manufactured.

13.3.3 Detail Design

Based on the load cell and pulley concept presented in the previous section a surrogate and rig was developed. In contrast to the EN14120 setup, the new method faciliates testing over a range of loads, facilitating an understanding of the relationship between hand angle and torque, for representative conditions. The following section outlines the design and development of the surrogate and rig. and their associated subassemblies.

13.3.3.1 Surrogate

The EN 14120 surrogate size C was used with subtle modifications., as despite its flaws it has previously been shown to be sufficient at detecting differences between products (Schmitt, Michel and Staudigl, 2012). Assumptions were made for the three hand dimensions missing from the standard (x = 15 mm, y = 38 mm, z = 40 mm Figure 13.3), based on approximations from the other dimensions. A low friction hinge was constructed from a countersunk bolt combined with nylon washers and a nut, which connected the hand and arm as shown in Figure 13.5. Mounting holes were added into the arm to enable it to be fixed to the bespoke rig. The surrogate was designed using CAD software (PTC Creo, USA). The arm was made from solid polyamide (tensile modulus 1650 MPa ± 150 (Materialise, 2017)) using laser sintering (Materialise, UK). The hand was made from polyamide (tensile modulus 3309 MPa (NatureWorksLLC, 2018)) using fused deposition modelling (Makerbot, USA).

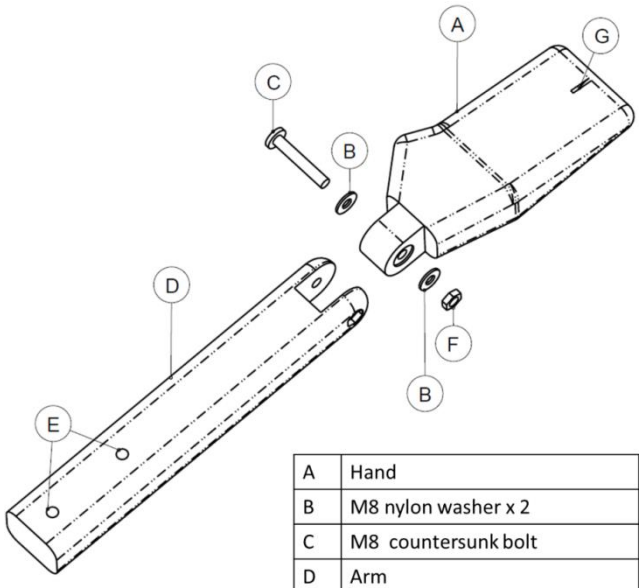

A	Hand
B	M8 nylon washer x 2
C	M8 countersunk bolt
D	Arm
E	Rig mountings
F	M8 nut
G	Cable hole to attach hand to rig

Figure 13.5: Exploded view of modified EN 14120 surrogate

13.3.3.2 Rig development

A bespoke rig was designed and developed that could be mounted onto an existing uniaxial test machine housed within the university (Instron 3367). A number of different fixtures can be added onto the test machine via the fixture mounts as shown in Figure 13.6. As none of the standard fixtures offered a suitable way to mount the surrogate onto the machine, a bespoke rig was designed to hold the surrogate and pulley that could be mounted to the Instron via the base of the flexture fixture (Figure 13.6. c). The rig was constructed from a series of Bosch Rexroth Aluminium 40 x 40 mm struts (Rexroth, 2017). The dimensions of the rig were selected based on the length of the surrogate arm size C specified in EN 14120.

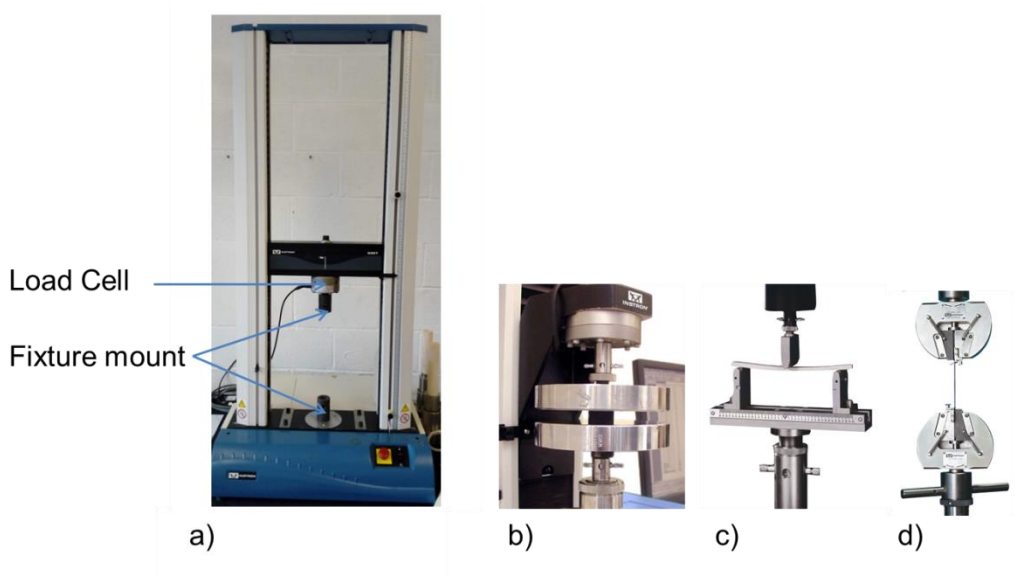

Figure 13.6 Instron setup **a)**3367 Uniaxial test machine **b)** Compression plates **c)** Flexture fixture for 3 point bend test **d)** Grips for tensile testing (Instron 2017)

Figure 13.7 shows the developed rig constructed from a series of Bosch Rexroth Aluminium 40 x 40 mm struts (Rexroth, 2017). Through vertical displacement of the load cell, a torque was applied around the wrist joint pulling the hand backwards. Due to difficulties associated with horizontally mounting the surrogate and applying a linear load, the surrogate was mounted vertically. The load was applied via a galvanized steel cable (diameter 2 mm) coupled with a low friction pulley (Harken, 2017). The cable runs vertically from the load cell through the pulley to the hand. The top of the cable was connected to the load cell via a cable lock (Rize Enterprises, USA). The bottom of the cable was connected to the distal end of the fingers, via a karabiner attached to a second cable looped around the surrogate. Tensile testing of the cable was conducted to confirm that the cable would not stretch during testsing. A tensile test of the cable

resulted in a strain of <0.01 at 80 N (maximum load in validation tests), confirming extension of the cable would not influence the results of the protector test. Through the use of removable fixings, the surrogate can be easily removed from the rig.

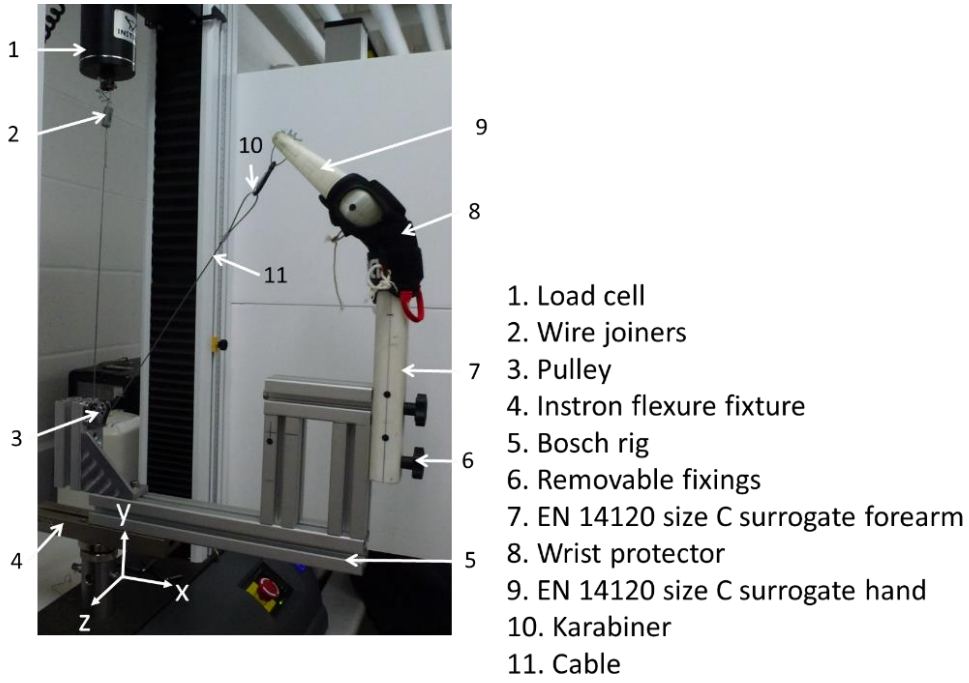

Figure 13.7: Bespoke test setup mounted to Instron machine

13.4 Experimental validation of new test method

To validate the suitability of the test setup, the stiffness of three commercially available wrist protectors was measured.

13.4.1 Test Protocol

The protocol is based on the approach in the EN 14120 with some modifications. Three adult left-hand wrist protectors were tested. Two snowboarding protectors were chosen, as they represent different design approaches, whilst the roller sports protector acted as a comparison that was certified to EN 14120. A short snowboarding wrist protector - Burton, Impact wrist guard (Figure 13.8a); a long snowboarding wrist protector - Demon, Flexmeter double wrist guard (Figure 13.8b); and an EN 14120:2003 certified skateboarding wrist protector - Oxelo, Black skateboard wrist guard (Figure 13.8c). The wrist protector characteristics are presented in Table 13.6. Based on protector dimensions, the two snowboarding protectors will be referred to here as short and long snowboarding protector. The snowboarding protectors were size medium, whilst the

roller sports protector was size large. Sizes were selected based on what fitted the EN 14120 surrogate, as there is no standard sizing used across manufacturers.

Figure 13.8: Tested wrist protectors

Table 13.6: Wrist protector characteristics

Wrist Protector	**Short snowboarding**	**Long snowboarding**	**Skateboard**
Construction			
Palmar	Three splints and palmar pad	One splint and skid plate	One splint
Dorsal	Two splints	One splint	One splint
Splint dimensions (width x length x thickness) mm			
Palmar	8 x 70 x 7	70 x 205 x 6	35 x 155 x 8
Dorsal	10 x1 45 x 6	70 x 210 x 10	30 x 135 x 7
Number of straps	2	2	3
Mass (g)	76	160	72

The standard does not stipulate how tightly protectors should be strapped. To determine whether strapping tightness influences protector stiffness three different strapping conditions were tested; tight, moderate and loose. The protector was tightened by hanging a weight of known mass (tight = 3 kg, moderate = 2 kg, loose = 1 kg) from the Velcro strap and rotating the arm horizontally until the protector was fitted. The position of the strap and buckle at each condition was marked on the protector (Figure 13.9). It was not possible to test the skateboard protector at a moderate tightness due to

the design of the straps, so eight different conditions were tested (Table 13.7). Five repeat trials were performed on each protector for each strapping condition, resulting in 40 tests in total. If the protector slipped during testing and clear movement was observed by the investigator, the trial was void and restarted until five complete trials were obtained for each condition.

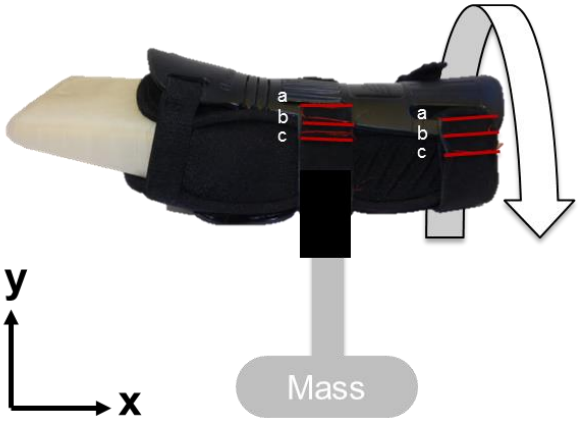

Figure 13.9: Procedure used to strap protector onto surrogate a-tight, b-moderate, c-loose

Table 13.7: Test conditions

Condition	Protector	Strapping
1	Short snowboarding	Tight
2		Moderate
3		Loose
4	Long snowboarding	Tight
5		Moderate
6		Loose
7	Skateboard	Tight
8		Loose

For each trial, the surrogate was mounted to the rig and the protector strapped to the desired tightness. The protectors were found to hold the hand slightly backwards in an extended position, the angle between the vertical and the resting position of the hand was defined as the neutral angle (Figure 13.10). The neutral angle was measured using a digital inclinometer before connecting the cable to the hand. A manually applied preload of ~1 N removed any slack from the cable, although this sometimes caused the hand to rotate slightly further backwards. Therefore, the start angle ($\theta_{t=0}$) was also measured before initiating the trial, if the difference between the neutral and start angle was $\geqslant$5° the, trial was restarted.

Figure 13.10: Hand pulled back to neutral angle by wrist protector

Upward displacement of the load cell at 200 mm/min applied a torque to the wrist joint, via the cable until a vertical force of 80 N was reached. The hand angle at the end of the test was measured using the inclinometer ($\theta_{t=end}$). An 80 N vertical force was equivalent to 10-14 Nm torque, depending on the end angle (see equations 7-8 below). Load and displacement were recorded at 10 Hz and transferred to spreadsheet files for analysis. Trials typically lasted between 60 to 80 seconds.

13.4.2 Data Analysis

The *Rotational stiffness* of the protector was defined as the ratio of torque to hand angle (Nm/°). Load cell force and displacement data coupled with start and end angles were used to determine hand angle and torque throughout the trial. As the cable was pulled at a constant rate the angular displacement of the hand was also constant. Based on the known start and end angle the rate of angular displacement was determined, enabling the hand displacement angle (θ_t) to be calculated for each time step. The recorded load was in the vertical axis rather than perpendicular to the hand, as required to calculate torque. Therefore, it was necessary to determine the load application angle (ϕ_t) and hence perpendicular load throughout the trial (Fp_t). Using trigonometry, the load application angle was calculated from the hand angle and fixed lengths AC, AD, BC and CD as shown in Figure 13.11 using equations 4.1-4.5.

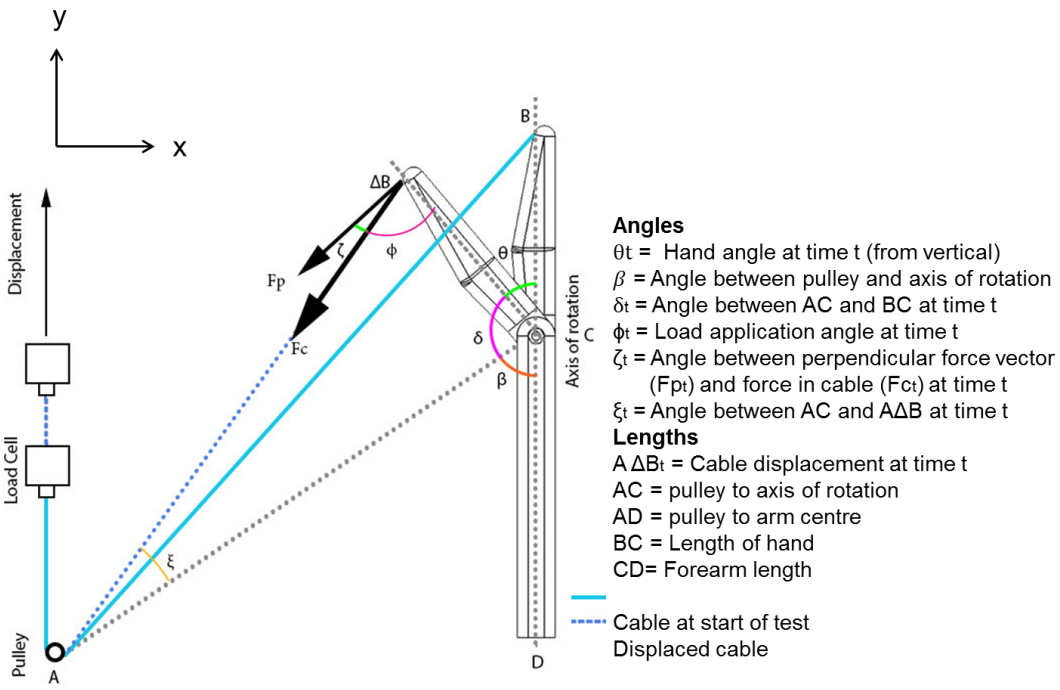

Figure 13.11: Test analysis schematic

$$\beta = \sin^{-1}\left(\frac{AD}{AC}\right) \tag{4.1}$$

$$\delta_t = 180 - \beta_t - \theta_t \tag{4.2}$$

$$A\Delta B_t = \sqrt{((BC^2 + AC^2) - 2(BC * AC * \cos\delta_t))} \tag{4.3}$$

$$\xi_t = \sin^{-1}\left(\frac{BC * \sin\delta_t}{A\Delta B}\right) \tag{4.4}$$

$$\phi_t = 180 - \xi_t - \delta_t \tag{4.5}$$

During the trial the angle between the cable and the hand changes from an acute angle to an obtuse angle, shown in Figure 13.12. Therefore, it is necessary to use Equations 4.6a or 4.6b to determine ζ the angle between the perpendicular force vector (Fp) and the measured force in the cable (Fc).

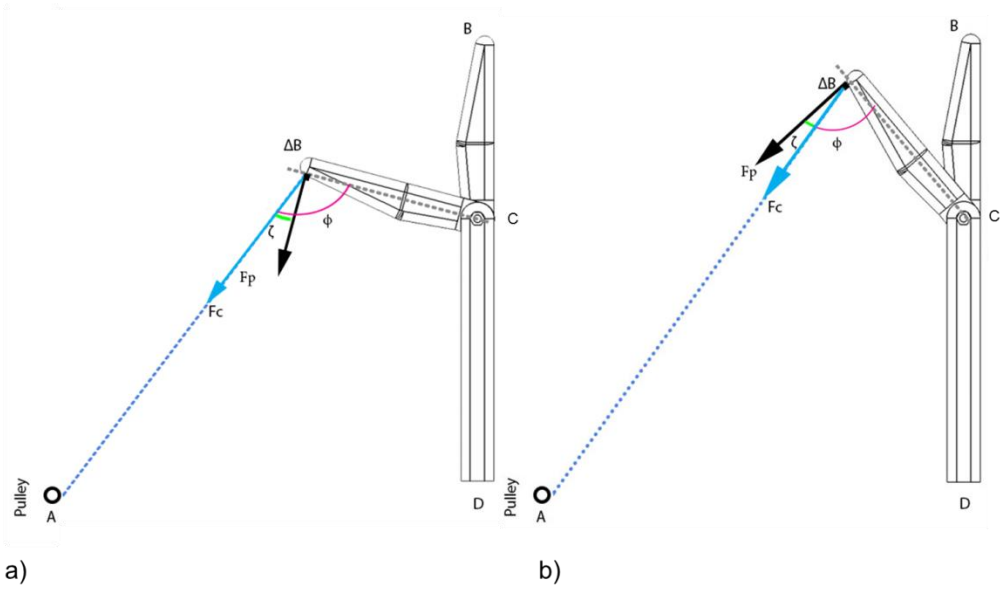

Figure 13.12: a) **ζ** when angle between hand and cable is > 90 **b) ζ** when angle between hand and cable is < 90

$$\zeta_t = \phi_t - 90 \ \ (\text{if } \phi_t > 90) \tag{4.6a}$$

$$\zeta_t = 90 - \ \phi_t (\text{if } \phi_t < 90) \tag{4.6b}$$

Fp_t was determined based on ζ_t and Fc_t using force vectors.

$$Fp_t = \text{Fc}_t * \cos \zeta_t \tag{4.7}$$

The torque was calculated by:

$$\text{Torque} = Fp_t * \text{BC} \tag{4.8}$$

Regression techniques were used to model the relationship between hand angle and torque based on the data from the five repeat trials per condition. For each condition four different functions were considered: linear, power, exponential and 2nd order polynomial (Ratkowsky, 1983) using the Matlab curve fitting app (MathWorks, 2015). The function with the lowest sum of squared error (SSE) and highest R^2 adjusted was selected as the best representation of the data. R^2 adjusted is a measure of fit that is adjusted for the number of predictor terms in the model.

13.4.3 Results

Figure 13.13 shows that all conditions resulted in non-linear growth relationships between angle and torque. An exponential function ($f(x) = ae^{(bx)}$) provided the best fit for all strapping conditions for the short snowboarding and skateboard protectors. A

power function $\left(f(x) = ax^{(b)}\right)$ best represented the long snowboarding protector for all three strapping conditions. As the test ended when 80 N was reached the measured end angle was dependent on protector stiffness. For the long snowboarding and skateboard protectors hyperextension angles of 90° were not reached before 80N was applied.

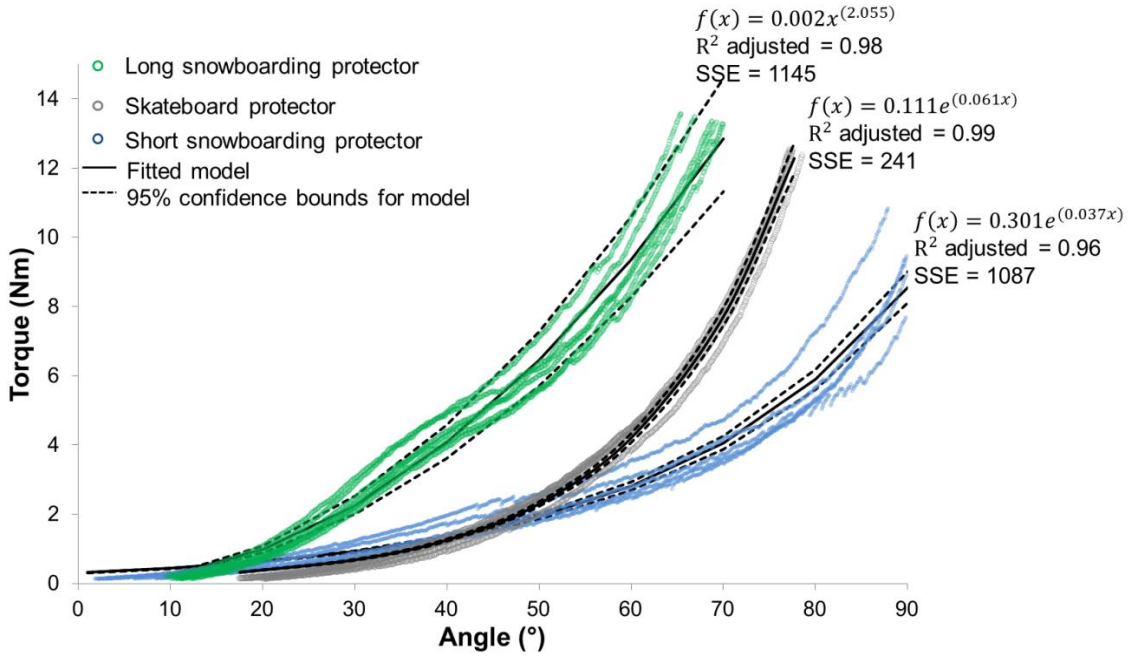

Figure 13.13: Raw data and fitted model based on five repeats for each protector loosely strapped

The mean and standard deviation values for start and end angles are presented in Table 13.8. Typically, the standard deviation for repeat trials of the same condition was lowest for the end angle (6 of 8 conditions). For all three protectors, the standard deviation of the end angle was smallest in the tightly strapped condition. The mean standard deviation for the end angle across all eight conditions was 1.2° (<1.8% of the mean measured end angle). Figure 13.14 shows the relationship between hand angle and torque for all three protector designs, at three strapping conditions. Distinctive differences can be seen for the different protector designs. The long snowboard protector exhibited the highest rotational stiffness at torques above 1Nm. The same models of snowboard protector were tested by Schmitt, Michel and Staudigl (2012) their results are included in Figure 13.14 as a comparison.

Tighter strapping resulted in lower end angles for both snowboarding protectors. Distinctive differences are observed for the short snowboard protector for each strapping condition. For the other two protectors the differences between strapping conditions are smaller, as shown by the overlapping boundaries in Figure 13.14. The black line represents the pass range for the EN 14120 test; the short snowboarding protector only meets the requirements when tightly strapped. For the long snowboarding protector, the tight strapping condition is outside of the EN 14120 pass threshold, whilst the skateboard protector is at the upper end of the threshold for both strapping conditions.

Table 13.8: Mean ± standard deviation for start angle, end angle, torque at end angle and angle at 3 Nm from the function

Protector	**Strapping**	**Start angle** (°) (Mean ± SD)	**End angle** (°) (Mean ± SD)	**Torque at end angle** (Nm) (Mean ± SD)	**Angle at 3 Nm** (°) equivalent to EN 14120	**Fitted model parameters** a	b
Short Snowboard	Loose	4.4 ± 2.8	91.1 ± 1.6	10.2 ± 0.4	61.1	0.301	0.037
	Moderate	3.5 ± 2.2	89.5 ± 1.6	10.5 ± 0.3	58.5	0.336	0.037
	Tight	3.9 ± 1.8	87.8 ± 0.8	10.9 ± 0.2	53.7	0.395	0.037
Long Snowboard	Loose	10.9 ± 1.0	70.1 ± 2.9	13.2 ± 0.3	32.2	0.002	2.055
	Moderate	11.5 ± 0.8	65.8 ± 0.8	10.6 ± 0.3	32.7	0.002	2.161
	Tight	12.3 ± 1.7	64.1 ± 0.5	13.6 ± 0.02	33.7	0.001	2.021
Skateboard	Loose	18.9 ± 1.3	77.7 ± 0.5	12.5 ± 0.1	54.7	0.111	0.061
	Tight	20.5 ± 1.4	78.5 ± 0.5	12.4 ± 0.1	53.9	0.107	0.060

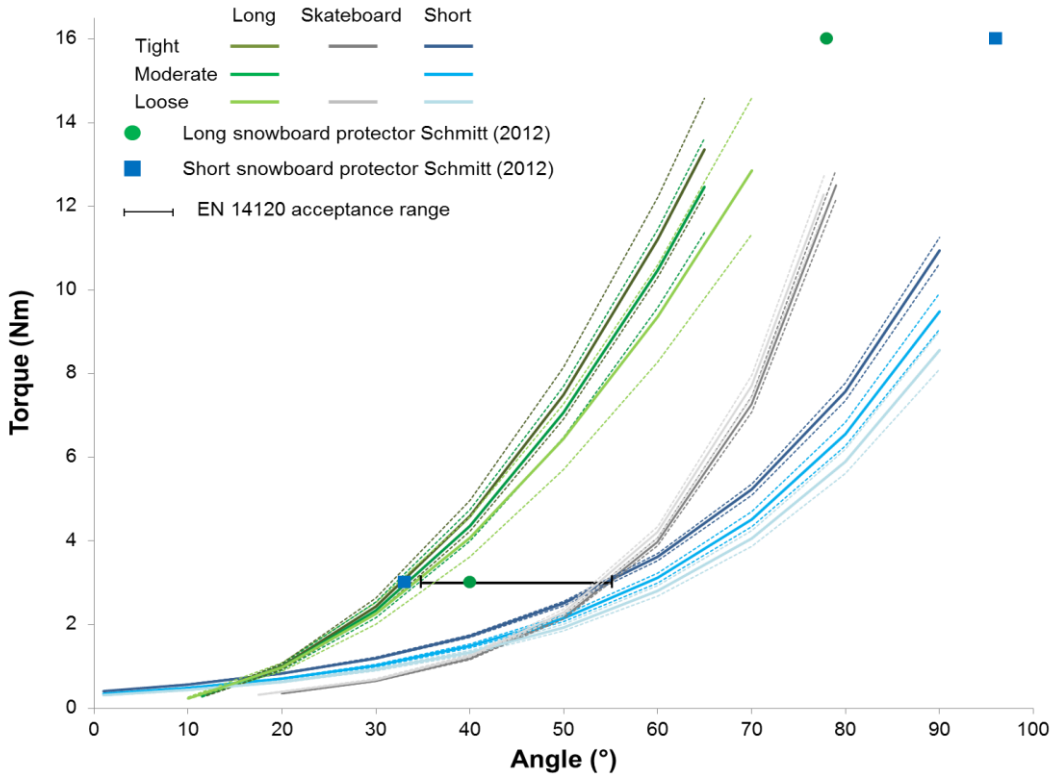

Figure 13.14: Strapping and protector comparison (dotted lines show 95% confidence intervals)

13.4.4 Discussion

Based on the above findings three conclusions are drawn: (1) the proposed test setup enables stiffness characteristics of wrist protectors to be measured over a range of loads. (2) The proposed method can distinguish differences in rotational stiffness between wrist protector designs. (3) Strapping tightness influenced the rotational stiffness of the protectors.

Three protectors based on different design principles were tested and different stiffness characteristics observed using the proposed test. For a given torque the long snowboard protector resulted in smaller hand angles, demonstrating it had a higher rotational stiffness than the other products. This is expected, based on its long dual splint construction, compared to the other products which had shorter and narrower splints (Table 13.6). The short snowboard protector and the skateboard protector resulted in similar hand angles, and hence rotational stiffness at 3 Nm. The skateboard protector exhibited a higher rotational stiffness than the short snowboard protector, at higher torques. Both designs have dorsal splints of the same length but different splint

constructions, indicating that a combination of design factors affect a protectors' ability to resist hand extension.

The proposed method also detected differences in end hand angle for different strapping conditions. At the tightest strapping condition, the short snowboarding protector meets the EN 14120 requirements (hand angle of 54° at 3 Nm). However, at the moderate and loose strapping conditions it failed for being too flexible and not limiting the hand angle enough (
Table 13.8). This highlights the importance of defining strapping tightness when testing wrist protectors. A product could be deemed suitable by one operator, but not another, simply due to strapping differences.

The same models of short and long snowboard protector were tested by Schmitt, Michel and Staudigl (2012), yet their results were notably different (Figure 13.14). At 3 Nm an angle of 33° was measured by Schmitt, Michel and Staudigl (2012) for the short snowboard protector, in contrast to 61° (loose), 59° (moderate) and 54° (tight) measured in this study. Schmitt, Michel and Staudigl (2012) measured a hand angle of 40° at 3 Nm for the long snowboard protector, yet this study found the protector to have a higher rotational stiffness with lower hand angles; 34° (loose), 33° (moderate) and 32° (tight). The maximum torque measured in this study was 13.6 Nm, so a direct comparison against the 16 Nm results measured by Schmitt, Michel and Staudigl (2012) was not possible. Discrepancies in protector performance between the two studies at 3 Nm could be due to a combination of factors: different hand dimensions for the three unspecified values (Figure 13.3); different loading rates; and different strapping tightness. This disparity further emphasises the need for a consistent and repeatable test protocol to measure wrist protector performance.

The proposed setup enables wrist protector stiffness characteristics to be quantified. However, several tests had to be repeated as the protector slipped or the strapping came undone. Additional tests were required for 75% of the tested conditions. Over half of the void trials occurred in the loosely strapped condition. The poor fit between the surrogate and protector was likely to contribute to this unwanted movement during the test. Whilst the EN14120 surrogate has a thumb representation it is only a small protrusion and in some instances the protector slipped off it during the test (Figure

13.15). The fit between the surrogate arm and protector was poor due to the overly simplified cuboidal shape of the forearm. The use of non-representative geometries is a weakness of the EN 14120 surrogate design. Modifying the surrogate to incorporate a larger thumb protrusion, more representative geometries and a higher friction surface should reduce variation in fitting protectors and improve consistency of the test.

Figure 13.15: Protector slipped off thumb during trial

The current test protocol loaded protectors to 80N, only the short snowboard protector reached the maximum possible angle of the setup, equivalent to 90° hyperextension at this load. For future studies the protocol should be modified so the end condition is set based on displacement; this would enable the loads associated with hyperextension to be measured for all protectors. Fitting mathematical functions to experimental data was found to be an adequate way to represent the experimental data. However, it is possible that certain protector designs will not conform to common functions, so an alternative solution is recommended for future studies.

13.5 Chapter Summary

This chapter makes significant progress towards addressing the third of the project's objectives: to develop and validate mechanical tests to characterise snowboarding wrist protectors. Based on a critique of the EN 14120 stiffness test and the design requirements outlined in chapter 3, a new test setup to characterise the stiffness of snowboarding wrist protectors was developed. Unlike the work of Schmitt, Michel and Staudigl (2012), the proposed method facilitates angular measurements over a range of torques. Experimental tests validated that the method can distinguish differences in rotational stiffness between wrist protector designs. Preliminary results show that differences in protector performance exist between products of different designs. The results were shown to be dependent on how tightly the protectors were strapped to the surrogate. Therefore, strapping tightness should be accounted for in future work.

The proposed setup and protocol provides a method to evaluate the rotational stiffness of wrist protectors. It could be used to further understanding of the relationship between protector design and performance. The use of standard material testing equipment means the setup can feasibly be implemented into existing test houses. This approach can aid manufacturers in the design and development of future products, evaluating different splint element designs. A limitation of this setup is the use of the EN 1412 surrogate. Its lack of fingers does not allow the assessment of products integrated into gloves. Also, there is no evidence to suggest that the simplified design (shape and size) of the surrogate was based on anthropometric data. Another limitation is the use of a relatively low magnitude load applied quasi-statically. Future efforts should focus on: testing all products to 90° of hyperextension; modifying the design of the surrogate; testing a range of commercially available products and transferring key learnings into the development of a dynamic test. Future chapters will aim to overcome these limitations.

14 Development of more representative surrogates

14.1 Introduction

Chapter 4 highlighted the need for a new surrogate to perform quasi-static testing of snowboarding wrist protectors. The aim of this chapter is to develop alternative surrogates to overcome the issues identified in the previous chapter. A well-designed surrogate is considered to be based on anthropometric dimensions; enable testing of both stand-alone protectors and those integrated into gloves; and detect differences between products in a repeatable manner. This aim will be achieved through the following objectives:

- To develop two alternative surrogates
- To investigate the effect of surrogate design on the measured rotational stiffness of snowboarding wrist protectors

The work presented in this chapter is also described in the author's publication (Adams *et al.*, 2018).

14.2 Surrogate development

Two new surrogates of increasing biofidelity were developed. The first new surrogate, referred to as geometric from this point onwards, is a simplified geometric representation more biofidelic than the EN14120 surrogate in its shape and size. The second new surrogate, referred to as scanned, is the most biofidelic being based on a 3D scan of a human hand and arm. To enable comparison all three surrogates, correspond to EN 420 sizes 8 and 9, use the same single axis low friction hinge construction and were made from solid polyamide (tensile modulus 1650 ± 150 MPa using laser sintering (Materialise, UK).

14.2.1 Geometric surrogate

The geometric surrogate, shown in Figure 14.1 is based around basic geometric profiles developed for use and replication in the draft version of ISO/CD 20320 standard for snowboarding wrist protectors (International Organization for Standardization, 2016a). The geometric surrogate was developed by members of the Centre for Sports Engineering Research at Sheffield Hallam University in collaboration with the Swiss council for Accident Prevention to support the ISO standard development. The ISO/CD 20320 draft standard is based around hand sizes, unlike EN 14120, where surrogate sizing was based on body mass. The ISO/CD 20320 draft stipulates 3 surrogate sizes

based on hand circumference and hand length: Surrogate A for hand size 6, surrogate B for hand size 8 and surrogate C for hand size 10, based on EN430 hand sizing (European Committee for Standardization, 2003a).

From the EN 420 hand length and circumference, it was identified that size 8 is equivalent to 15th percentile adult male (Peebles and Norris, 1998; Pheasant, 2001; Alvin R Tilley and Henry Dreyfuss Associates, 2002; European Committee for Standardization, 2003a). Therefore, the size B surrogate is based on eleven anthropometric dimensions scaled to the 15th percentile (Table 14.1). Simplifications of the hand and forearm resulted in a scalable design constructed from basic geometric profiles that can be communicated as an engineering drawing and reproduced. The forearm shape is based on segmentation principles developed by Yeadon (1990) using a circular cross section at the elbow (cross section 1 Figure 14.1) and a stadium shape at the wrist (cross section 2 Figure 14.1). The hand is formed of a series of extrusions and sweeps blending circular profiles into a representative shape which fits the anthropometric data.

Table 14.1: Geometric Surrogate dimensions (International Organization for Standardization, 2016a)

Dimension on Figure 14.1	**Description**	**Measurement for size B**	**Reference**
A	Hand Width	82	(Pheasant, 2001)
B	Hand thickness	30	(Pheasant, 2001)
RC	Radius of palm	115	-
D	Distance between fingers	11	Proportion of hand width
E	Half hand width including thumb	50	(Pheasant, 2001)
F	Hand thickness at thickest point	47	(Pheasant, 2001)
G	Wrist width	57	(Peebles and Norris, 1998)
H	Hand Length	182	(European Committee for Standardization, 2003a)
I	Clamp position	170	-
J	Palm length (wrist crease to crotch digit 2&3)	100	(Alvin R Tilley and Henry Dreyfuss Associates, 2002)
K	Wrist crease to thumb crotch	56	(Alvin R Tilley and Henry Dreyfuss Associates, 2002)
L	Back of elbow to wrist crease length	273	-
M	Minimum arm length	180	-
N	Forearm Girth (diameter)	69	(Peebles and Norris, 1998)
O	Diameter of test fingers	12	-
Circumference	Circumference of the hand	200	(Peebles and Norris, 1998)

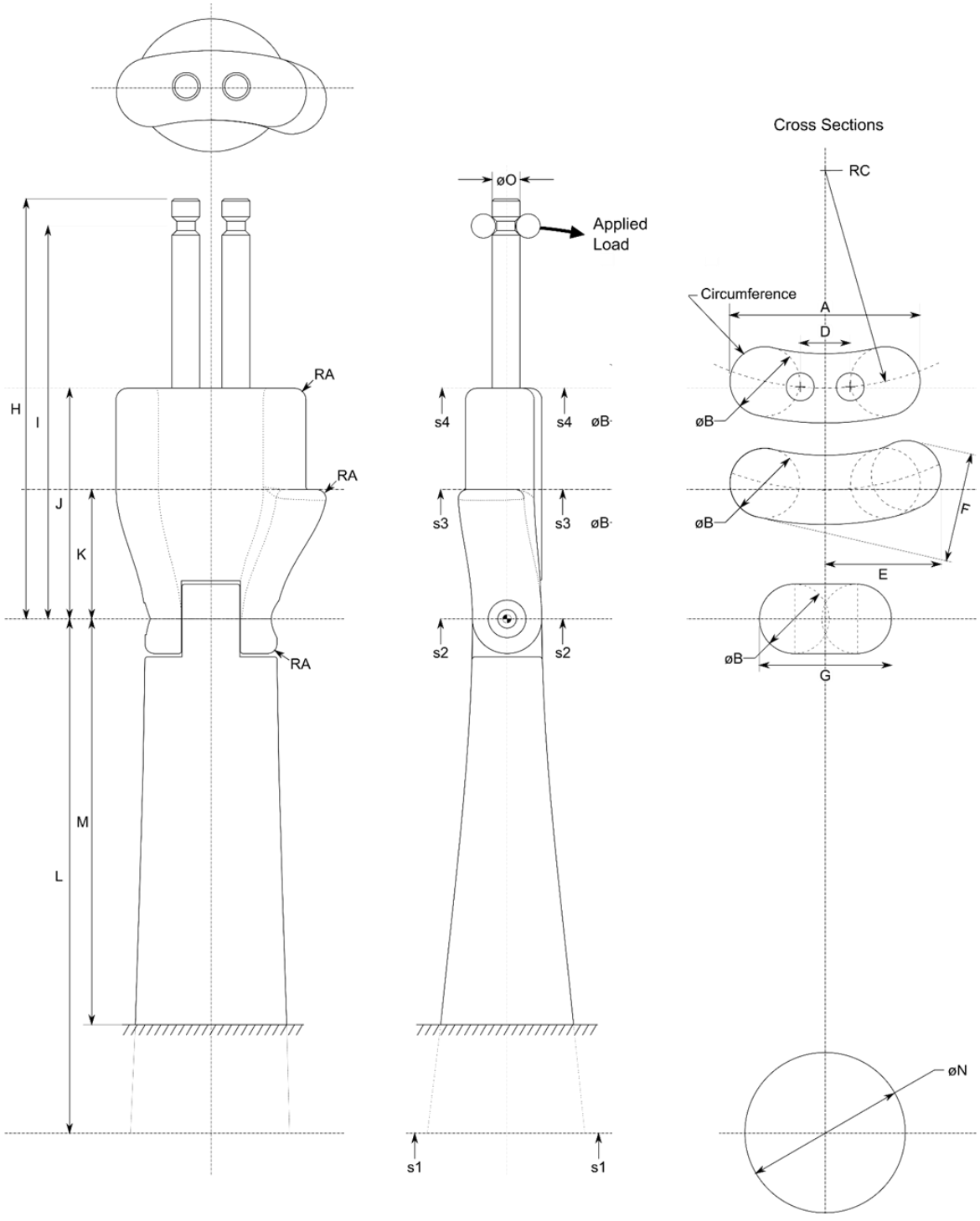

Figure 14.1: Geometric surrogate dimensions (International Organization for Standardization, 2016a)

To limit protector movement during testing, a more pronounced thumb protrusion (Figure 14.2 item D), than then the one used in the EN 14120 surrogate was incorporated into the geometric surrogate design. A full length rigid thumb would make mounting protectors onto a surrogate too difficult. To allow testing of products integrated into gloves, two steel rods (ø12 x 80 mm) representing digits three and four

were incorporated into the surrogate. To allow displacement from the testing device to apply a torque to the wrist an external clamp was mounted over the surrogate and protector to attach to the cable (Figure 14.2b-c, Figure 14.3). At the end of the forearm, 180 mm from the wrist pivot (distance M), a mounting block was incorporated.

A	Hand
B	60mm holes for fingers x2
C	Fingers
D	Hook like thumb protrusion
E	M8 countersunk bolt
F	M8 nylon washer x2
G	Arm
H	Rig mountings
I	Rig mounting block
J	M8 nut
K	M6 Eye bolt
L	M6 nut
M	Plate to mount inclinometer onto
N	Clamp to connect to fingers
O	Threaded bolt to vary clamp distance dependent on protector design

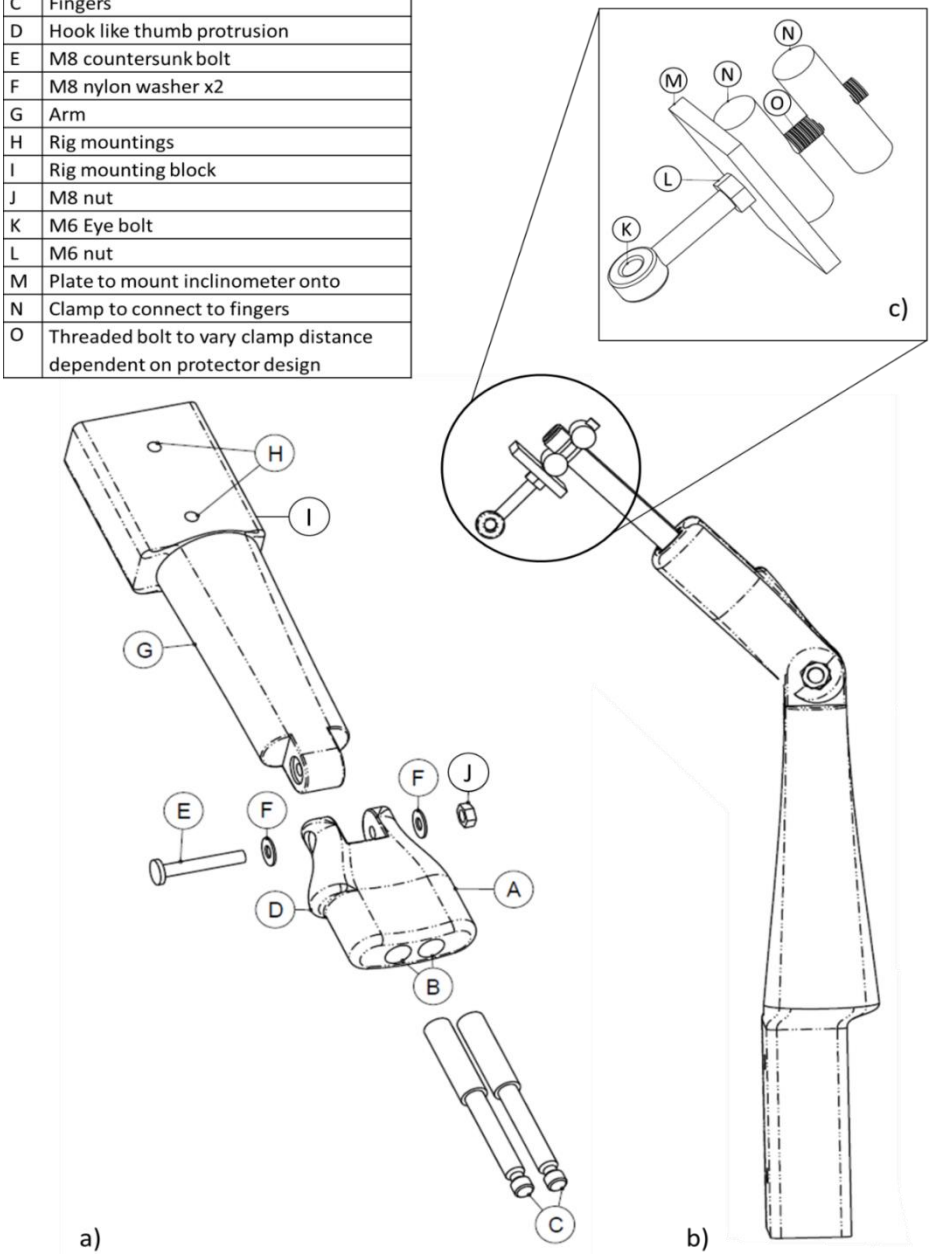

Figure 14.2:a) Exploded view of geometric surrogate b)External clamp mounted to surrogate fingers c) Detailed view of clamp

Figure 14.3: External clamp mounted to surrogate wearing protective glove via clamp attached to steel rods

14.2.2 Scanned surrogate

2D anthropometric measurements are insufficient at capturing detailed shape variations needed for realistic body models (Allen, Curless and Popović, 2003), resulting in geometric simplifications with assumptions about shape (Williams, 2007). To increase the fidelity of the surrogate, a 3D scan of a hand and forearm was used to define the exterior form. The following sections outline the process required to develop the scanned surrogate.

14.2.2.1 Selecting participant

A participant with hand measurements close to published 50th percentile data (equivalent to hand size 8/9) was identified from a convenience sample of ten British males, based on nine manual measurements of each upper extremity (Table 14.2 and Figure 14.4). Both arms were measured for each participant by a level one accredited ISAK kinanthropometrist, thus 20 upper extremities were measured. A metal anthropometric tape measure (Lufkin Executive Thinline 2 m, W606PM), was used for circumference measurements and digital callipers (Mitutoyo CD-6”B) for length and breadth measurements. The nine manual measurements were selected based on the work of Hsiao, Whitestone, Kau, & Hildreth, (2015) and Williams (2007) who evaluated glove fit and related dimensions for the design of protective gloves.

Table 14.2: Manual measurements used to identify suitable participant

Upper extremity measurements	
Hand	**Wrist and forearm**
a) Hand circumference	f) Wrist Circumference (over bony protrusions)
b) Hand breadth (excluding thumb)	g) Wrist Circumference (at wrist crease)
c) Hand length	h) Wrist width
d) Middle finger length	i) Forearm Circumference
e) Palm length	

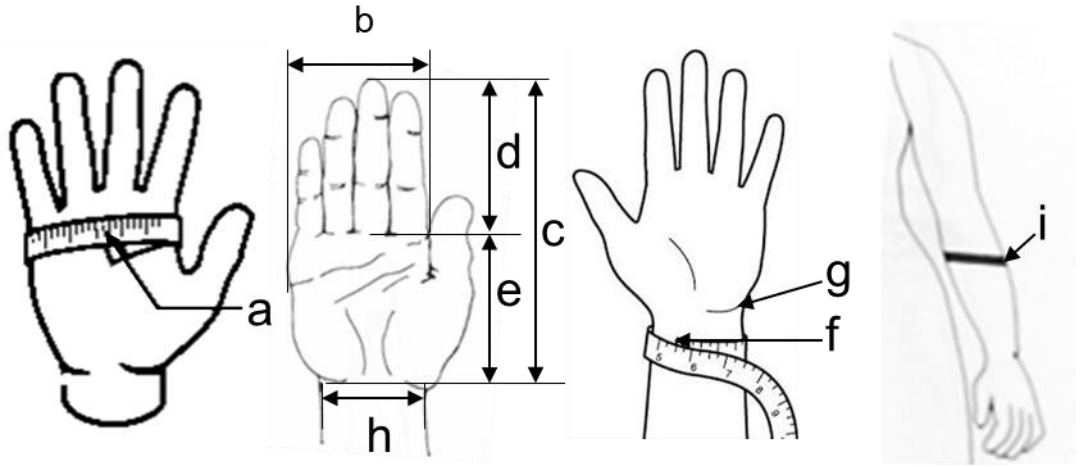

Figure 14.4: Hand and forearm measurements, letters correspond to Table 5-2

Ethical approval was obtained from the Faculty of Health and Wellbeing Ethics Committee, Sheffield Hallam University, UK (HWB-S&E-69). Upper extremity measurements were then compared to the general population, to identify which participant arm was closest to 50th percentile across all nine measures. As no participant conformed to 50th percentile measures for all measurements, data filtering was required. The data was filtered in 2 phases, initially any upper extremity that fell outside of the 5-95th percentile range on any measure was excluded. Four upper extremities remained after the initial screening: 01L, 08L, 08R and 09R (Figure 14.5). The difference between each upper extremity and published 50th percentile data (Peebles and Norris, 1998) was determined for each measure and the summed squared error (SSE) across all measures was calculated. The participant upper extremity with the lowest total SSE was deemed the most appropriate forearm for 3D scanning (Figure 14.5). The selected upper extremity, 08L, had the lowest sum squared error, 917mm. Five of the 9 measurements were equivalent to published 50th percentile measurements, the largest differences from

the 50th percentile measurements were the wrist and forearm circumferences (Table 14.3).

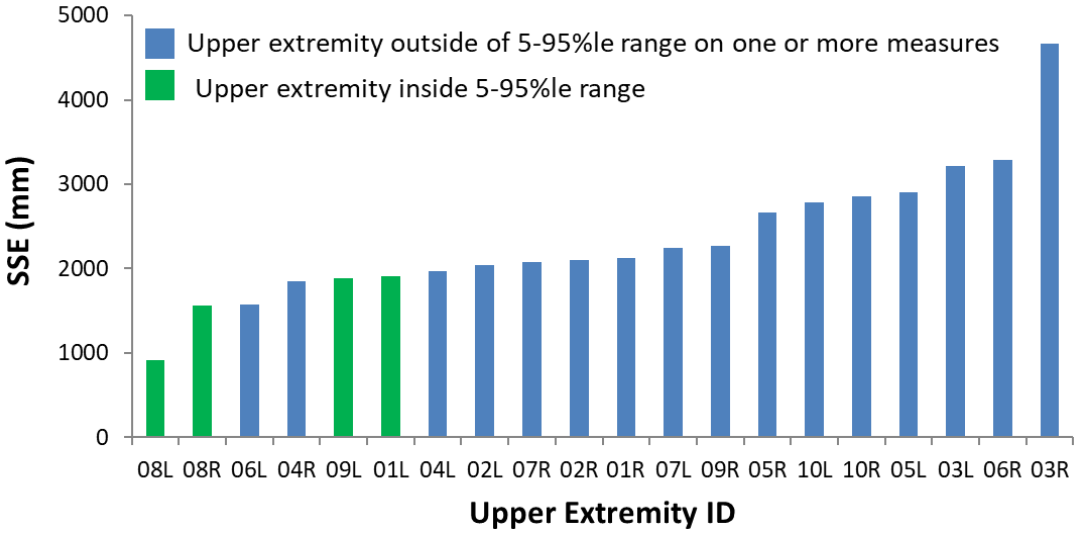

Figure 14.5: SSE for all participants

Table 14.3: Percentage difference between published 50th percentile (Peebles & Norris 1998) and selected upper extremity

Measurements (mm)	Percentile of selected participant
Forearm Circumference	80
Wrist Circumference (over bony protrusions)	10
Wrist Circumference (at wrist crease)	15
Wrist width	50
Hand Circumference	50
Hand Breadth (no thumb)	50
Hand Length	50
Middle finger length	50
Palm length	15

14.2.2.2 Development of scanned surrogate

Shape data for the hand and forearm was obtained by scanning the identified participant using 3dMDbody5 (3dMD, USA). The system consists of five modular units, each containing three machine vision cameras and two infrared projectors, accompanied by four light boxes (Figure 14.6a). All modular units collect data simultaneously. Thus, capture time is very short, ~1.5 ms, thereby minimising risk of movement artefacts. For identification of landmarks in post processing visual markers were positioned on the wrist (radial styloid and ulnar styloid) and the elbow (medial epicondyle and lateral epicondyle). The participant lay in a supine position on a box in the centre of the

capture volume with their left arm raised upwards perpendicular to their trunk (Figure 14.6b). The arm was held straight with the palm facing inwards parallel to the sagittal plane, the fingers were slightly apart, and the thumb held outwards in a neutral position.

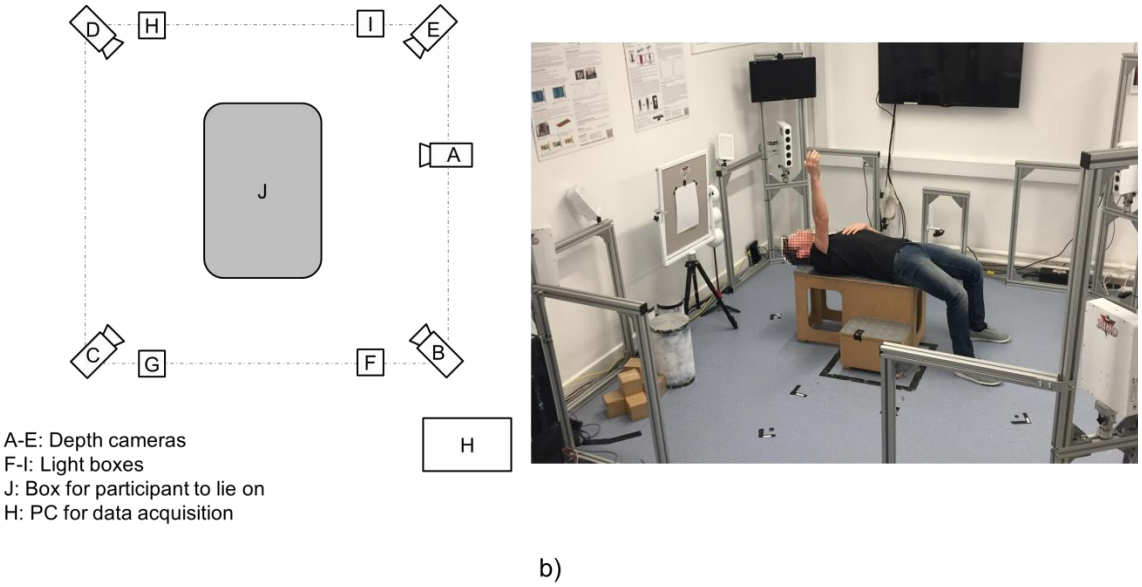

Figure 14.6 a) Scan setup not to scale **b)** Participant scanning position

The surface data was exported as an object file (.obj) and postprocessed in 3D imaging software (Geomagic studio 9,3D systems, USA) to refine the raw point cloud data (Figure 14.7). The wrist markers were used to identify the wrist joint and create an axis for the surrogate's hinge joint. The elbow markers were used as a forearm boundary and all data beyond this region was removed. The final data was converted into a watertight solid and exported for CAD software (PTC Creo, USA).

Figure 14.7: Scan prior to post processing in Geomagic with excess point cloud data and rough surfaces

The part was split into two components; hand and forearm prior to the hinge joint being created, as shown in Figure 14.8. The thumb was cut just above the metacarpophalangeal joint, providing a protrusion rather than a full thumb to ensure

protectors could be easily mounted onto the surrogate while maintaining their position during testing. At the end of the forearm, 180 mm from the wrist pivot (distance M), a mounting block was incorporated. The same clamp setup as the geometric surrogate was used for the application of displacement. Digits 3 and 4 were replaced with two steel rods (ø12 x 140 mm) protruding 80mm from the hand.

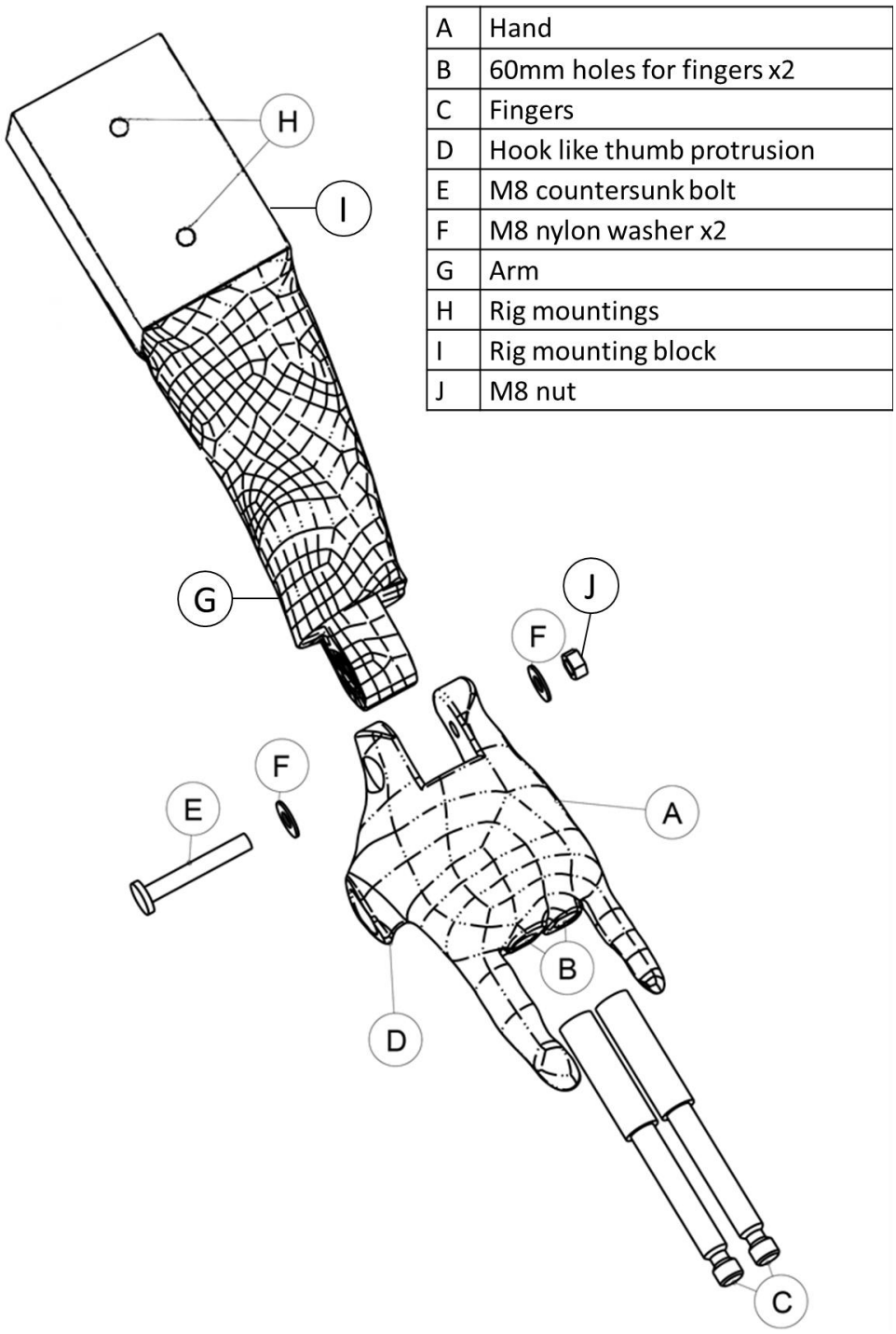

Figure 14.8: Exploded view of scanned surrogate

14.3 Investigation of the effect of surrogate design on the measured rotational stiffness of snowboarding wrist protectors

To investigate the influence of surrogate design, the rotational stiffness of three wrist protectors was compared across the three surrogate designs (Figure 14.9). All three surrogates correspond approximately to EN 420 sizes 8 and 9; a summary of their measurements is given in Table 14.4. The scanned surrogate was developed first with 4 fingers; however pilot studies found this was not practical, making it difficult to put gloves on. Therefore, based on this learning the geometric surrogate only has two fingers, which are sufficient to test gloves without adding unnecessary complexity.

Figure 14.9 Surrogate designs that were compared **a)** EN 14120, **b)** geometric, **c)** scanned

Table 14.4: Summary of surrogate measurements in relation to standard sizes

Measurements	**50th percentile male** (Peebles and Norris, 1998)	**Size 8 / 9 measurements** (EN 420)	**Surrogate**		
			EN 14120	**Geometric**	**Scanned**
Hand length (mm)	190	182/192	191	182	192
Hand circumference (mm)	223	203/229	220	200	207
Maximum forearm circumference (mm)	-	-	167	197	240
Total Volume (mm^3)	-	-	893,970	900,212	1,110,321

14.3.1 Method

The experimental procedure was a modified version of the method specified in chapter 4. The modifications made were: the end of test was based on a displacement of 90° rather than load; torque at 4 specific hand angles were measured, rather than fitting mathematical functions to the data; the trigonometry calculations were adapted for the use of the clamp on the geometric and scanned surrogates. The same models of protectors tested in chapter 4 were used for this study, short snowboarding wrist protector, long snowboarding wrist protector and an EN 14120:2003 certified roller sports wrist protector. Having shown the influence of strapping tightness in the previous chapter, each protector was strapped by attaching a 2 kg mass to the strap and rotating the surrogate about its long axis until the protector was securely fitted.

The same test protocol outlined in chapter 4 was used. Upward displacement of the load cell at 200 mm/min applied a torque to the wrist joint, until a hand extension angle ~90° was reached (displacement value required to achieved 90° determined through pilot testing). Eight repeat trials were performed on each protector on each surrogate, resulting in seventy-two trials for the nine test conditions. The protector was re-positioned and re-strapped between trials.

14.3.1.1 Data Analysis

As outlined in the previous chapter, load cell force and displacement data coupled with start and end angles were used to calculate the hand angle and extension torque. Due to the addition of the clamp the force required to determine the torque is perpendicular to the moment arm CE rather than BC shown in Figure 14.10, so an alternative set of equations are needed. Equations 5.1-5.10 were used to determine extension torque for each hand angle.

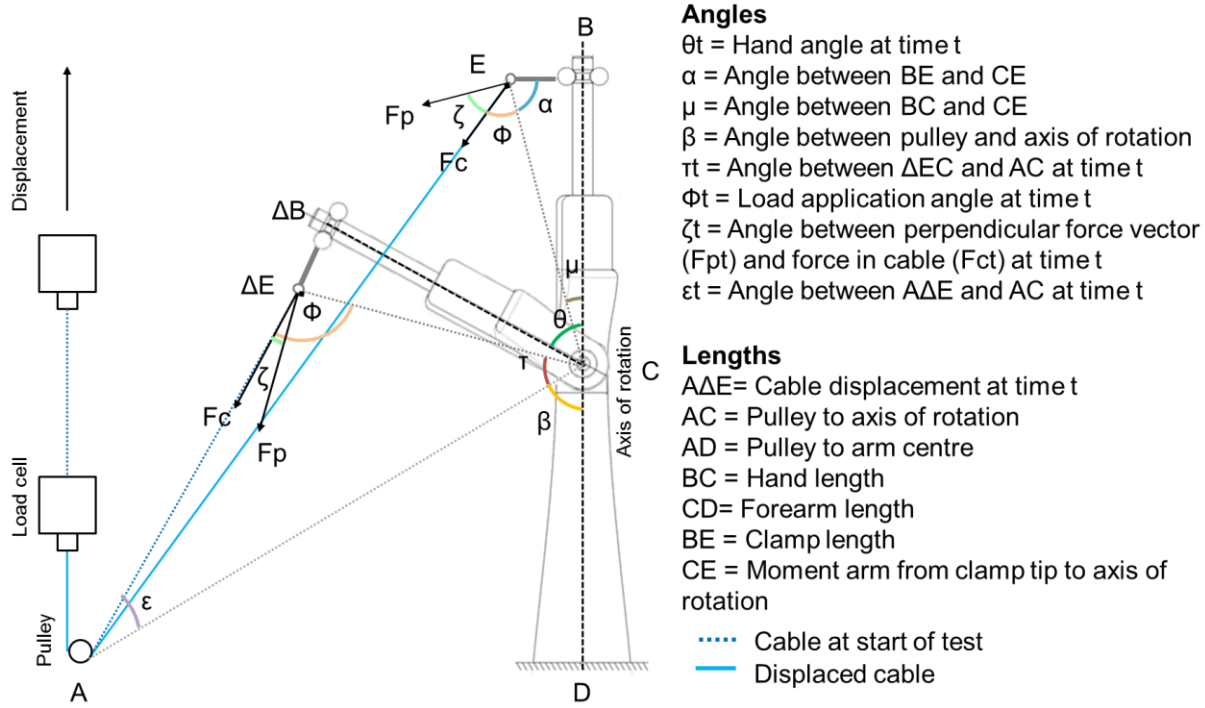

Figure 14.10: Test analysis schematic

$$\alpha = \cos^{-1}\left(\frac{BE}{CE}\right) \tag{5.1}$$

$$\mu = \sin^{-1}\left(\frac{BE}{CE}\right) \tag{5.2}$$

$$\beta = \sin^{-1}\left(\frac{AD}{AC}\right) \tag{5.3}$$

$$\tau_t = 180 - \beta - \theta_t \tag{5.4}$$

$$A\Delta E_t = \sqrt{((CE^2 + AC^2) - 2(CE * AC * \cos\tau_t))} \tag{5.5}$$

$$\xi_t = \cos^{-1}\left(\frac{AC^2 + AE^2 - CE^2}{2 * AC * AE}\right) \tag{5.6}$$

$$\phi_t = 180 - \xi_t - \tau_t \tag{5.7}$$

During the trial the angle between the cable and clamp moment arm changes from an acute angle to an obtuse angle. Therefore, it is necessary to use Equation 5.8a or 58b to

determine ζ_t the angle between the perpendicular force vector (Fp) and the measured force in the cable (Fc).

$$\zeta_t = 90 - \phi_t (\text{if } \phi_t < 90) \quad (5.8a)$$

$$\zeta_t = \phi_t - 90 \ (\text{if } \phi_t > 90) \quad (5.8b)$$

Fp_t was determined based on ζ_t and Fc_t using force vectors.

$$Fp_t = \mathrm{Fc}_t * \cos \zeta_t \quad (5.9)$$

The torque was calculated by:

$$\mathrm{Torque} = Fp_t * \mathrm{CE} \quad (5.10)$$

The relationship between hand angle and torque was examined for four cases: 35°, 55°, 80° and 90°. Angles 35° and 55° are the pass threshold in EN 14120 when 3 Nm is applied, whilst 80° and 90° are representative of wrist hyperextension angles measured in non-injurious on-slope falls (Greenwald, Simpson and Michel, 2013).

The torque at the prescribed angles was determined by interpolation using a first order polynomial through a range of angles ± 2.5 at all angles except end angle 90°, where only -2.5° was used. Each of the eight repeats were analysed and a mean and standard deviation obtained. The data was divided into thirty-six sets (3 surrogates x 3 protectors x 4 angles), this was subdivided into twelve groups (e.g. same protector, same angle on three different surrogates). Statistical analysis was conducted to determine if differences in torque between the three surrogates at the same extension angle exist for each of the twelve groups.

The statistical analysis was conducted using SPSS (IBM SPSS Statistics for Windows, USA). Normality and homogeneity of variance were established by Shapiro–Wilk and Levene tests performed with the significance level set at $P < 0.05$. Relevant statistical analyses were applied and post hoc analyses were conducted to assess where the significant differences between pairs of surrogates occurred. One-way ANOVA and Bonferroni post hoc were used if data were normally distributed and had equal variance;

Welch ANOVA and Games Howell post hoc if data were normally distributed and had un-equal variance; Kruskal-Wallis and Mann-Whitney tests with a Bonferroni correction (effects reported at a 0.0167 level of significance) were used as a non-parametric equivalent to one-way ANOVA. Effect sizes were calculated using Pearson's correlation coefficient, as described by Field (2009). The magnitudes of the correlations were interpreted using Cohen's thresholds where: < 0.1, is trivial; 0.1 to 0.3 is small; 0.3 to 0.5 is moderate; and >0.5 is large (Cohen, 1988). To compare the repeatability of the three surrogates the coefficient of variation (CV) was determined for each protector on each surrogate at the four angles of interest.

It was not possible to obtain full measurement sets for all four angles in two cases: 35° for the roller sports protector mounted on the Geometric surrogate and 90° for the Long snowboard protector mounted to the Scanned surrogate. When the Roller sports protector was mounted on the Geometric surrogate the start angle of the hand exceeded 35° (47.5 ± 2.2°). Similar behaviour was observed in an earlier study, different protectors designs hold the hand at a different neutral angle (Adams *et al.*, 2016). The Long snowboard protector mounted on the Scanned surrogate exceeded the limit of the load cell (500 N) before the hand could be displaced to 90°, resulting in an extension angle of 84 ± 0.2° at the end of the test. In these cases, alternative statistical tests to compare two surrogates rather than three were used, independent t-test if data were normally distributed or Mann–Whitney test if data were not normally distributed.

14.3.2 Results

Significance test results and effect sizes for each pair of surrogates with each protector mounted on them at four angles are presented in Table 14.5. Statistically significant differences exist in torque between the three surrogates in 78% of all tested cases. All cases except one demonstrate a moderate to large effect size. In all cases the Geometric and Scanned surrogates were significantly different ($p<0.005$) with large effect sizes. EN 14120 and the Geometric surrogate were significantly different in 80% of measured instances; EN 14120 surrogate and the Scanned surrogate were significantly different in 55% of measured instances.

Table 14.5: Inferential statistics, significance test results and effect sizes between surrogates for torque measurements at four different angles. EN - EN 14120, Geo - Geometric, Scan - Scanned

Protector	Angle	P			Effect Size		
		EN - Geo	EN - Scan	Geo - Scan	EN - Geo	EN - Scan	Geo - Scan
Roller sports	35	-	0.202 [e]	-	-	-0.31	-
	55	0*[c]	0.029 [c]	0* [c]	-0.84	-0.57	-0.84
	80	0*[c]	0.021 [c]	0* [c]	-0.84	-0.6	-0.84
	90	0.097 [b]	0.019*[b]	0.003*[b]	0.51	-0.76	-0.8
Short snowboarding	35	0.003*[b]	0.547 [b]	0.032*[b]	0.74	-0.26	-0.62
	55	0*[b]	0.161[b]	0.009*[b]	0.83	-0.46	-0.73
	80	0.001*[b]	0.007*[b]	0.001*[b]	0.81	-0.73	-0.83
	90	0.162 [b]	0* [b]	0* [b]	-0.46	-0.88	-0.87
Long snowboarding	35	0.004*[a]	0.006*[a]	0*[a]	0.77	-0.61	-0.86
	55	0*[c]	0*[c]	0*[c]	-0.84	-0.84	-0.84
	80	0.001* [c]	0*[c]	0.001* [c]	-0.84	-0.84	-0.84
	90	0*[d]	-	-	0.97	-	-

*Notes: Statistical tests performed: [a]One way ANOVA, [b]Welch ANOVA, [c] Kruskal-Wallis, [d]independent t-test, [e]Mann–Whitney U test, * indicates a significant difference. Magnitude of effect measured using Pearson's correlation coefficient.*

Table 14.6 presents the coefficient of variation for each protector on each surrogate at the four angles of interest and the mean coefficient of variation for the three surrogate designs. The EN 14120 and Geometric surrogate have similar mean coefficients of variation of 22% and 20% respectively, while the Scanned surrogate had a higher mean coefficient of variation of 30%. Figure 14.11a shows the first order polynomial functions and the mean torque for the four angles across eight repeats for one condition. Figure 14.11 b-d shows the torque-angle relationship across all three arms for each protector. In all cases, torque increased with hand extension angle.

Table 14.6: Coefficient of variation (CV) for each protector on each surrogate at the 4 angles of interest

		CV (%)		
Protector	**Angle**	**EN 14120**	**Geometric**	**Scanned**
Roller sports	35	84	-	60
	55	45	26	34
	80	18	30	28
	90	12	42	27
Short snowboarding	35	25	24	47
	55	16	16	38
	80	14	10	27
	90	13	9	23
Long snowboarding	35	23	30	24
	55	8	12	15
	80	6	8	5
	90	6	15	-
Mean CV for each arm based on all cases (%)		22	20	30

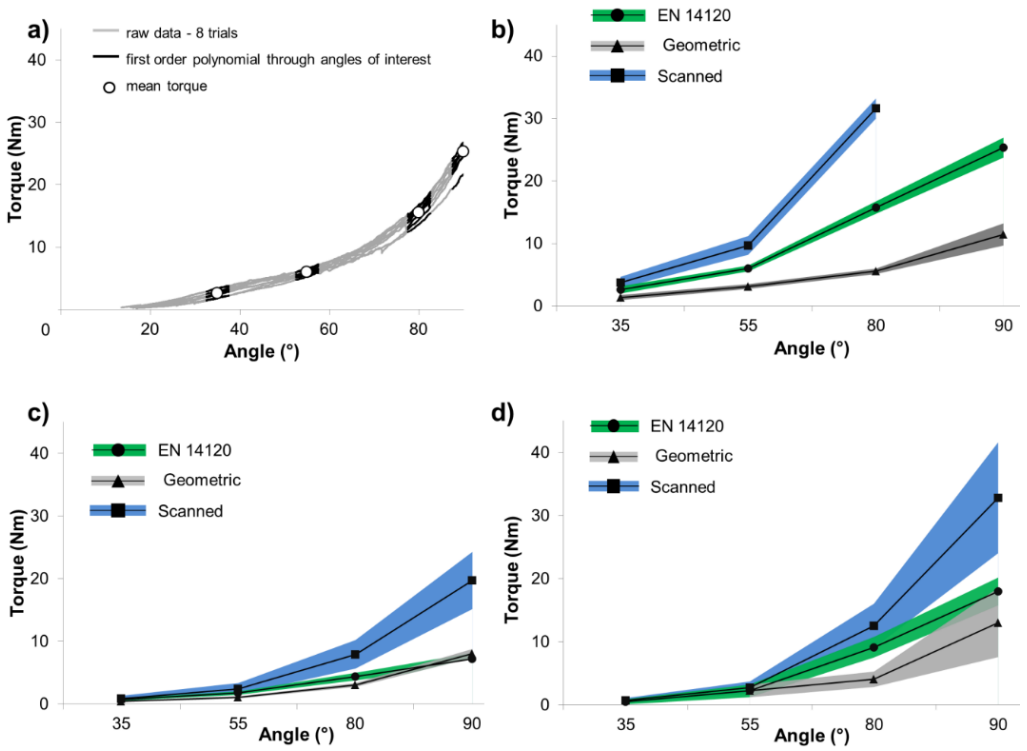

Figure 14.11: a) Raw data and mean torque at angles of interest for long snowboarding protector on EN:14120 surrogate, surrogate comparison for: **b**) long snowboarding, **c)** short snowboarding protector, **d)** roller sports protector where boundary represents mean ± standard deviation

Figure 14.12 shows that ranking order of protector rotational stiffness was generally consistent across surrogates, except for three conditions. In 90%, of cases the Long snowboarding protector exhibited the highest rotational stiffness, requiring a larger torque to reach each hand angle. In contrast, the Short snowboarding protector tended to exhibit the lowest rotational stiffness (83% of cases), with the Roller sport protector showing intermediate behaviour. Exceptions include, i) the EN 14120 surrogate at 35°, ii) the Scanned surrogate at 35°, in both cases the Short snowboarding protector required a similar torque (+0.3 Nm) marginally more torque (0.3 Nm) than the Roller sports protector and iii) the Geometric surrogate at 90°, where the Roller sports protector required slightly more torque (1.6 Nm) than the Long snowboarding protector.

From Figure 14.12 it can also be seen that the relative difference in rotational stiffness between protectors changed between surrogates. The smallest differences in protector rotational stiffness were measured when using the Geometric surrogate. For example, consider the Short and Long snowboarding protector at a hand angle 80°. For these two protectors mounted to the EN 14120 the difference in torque was 11.4 Nm, a difference

of 2.5 Nm when mounted to the Geometric surrogate and 23.7 Nm difference for the Scanned surrogate.

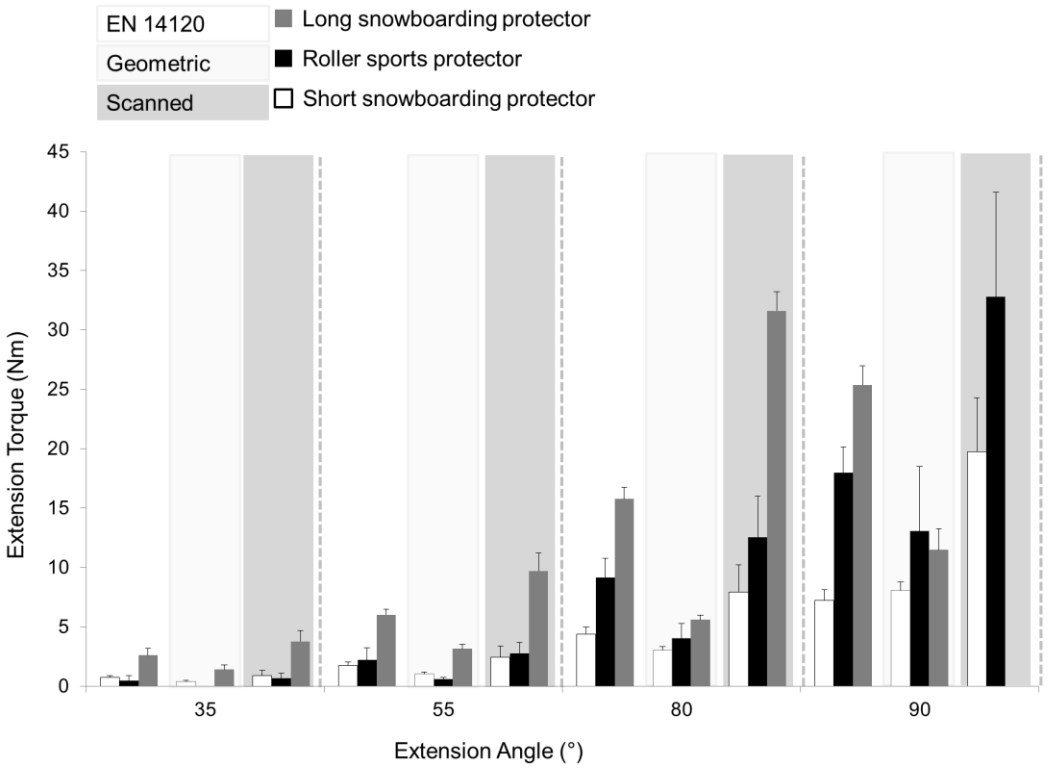

Figure 14.12: Comparison of extension torque at each angle for all protectors mounted on all three surrogates

14.3.3 Discussion

Surrogate design significantly influences the measured rotational stiffness of snowboarding wrist protectors in a quasi-static bending test. The Geometric and Scanned surrogates resulted in significantly different extension torque values for a given angle in all cases. The Geometric and EN 14120 surrogates resulted in significantly different extension torque values in 82% of measured cases. Whilst, the EN 14120 and Scanned surrogates only resulted in significantly different extension torques in 55% of measured instances. From a design perspective the EN 1420 and Scanned surrogates were considered to be the most different in terms of biofidelity, so it is surprising that the torque readings do not reflect this difference for 45% of tested conditions.

The Scanned surrogate required larger torques to displace the hand to each angle (Figure 14.11 b-d), which is likely due to the increased size of the forearm. The scanned surrogate had the largest volume of the three surrogates, with the biggest wrist and forearm circumferences (Table 14.4). The larger surrogate means the distance between

palmar and dorsal splints and the neutral axis has increased, in turn increasing the second moment of area, resulting in a higher rotational stiffness.

The coefficient of variation provides insight into the repeatability of the surrogate design. When considering the overall mean coefficient of variation, the Geometric and EN 14120 surrogates perform in a similar manner, 22% and 20% respectively, whilst the Scanned surrogate had increased variation, 30%. These results imply that the new Geometric surrogate is equivalent to the EN 14120 surrogate in terms of repeatability, whereas the Scanned surrogate was less repeatable. The Scanned surrogate is more representative of the human arm and therefore has a more complex and discontinuous shape, as details such as muscles and bones are captured. Given the rigid nature of the surrogate these anatomical features are likely to affect the interaction between the protector and surrogate influencing the variation between trials. The inclusion of a more pronounced thumb in the two new surrogates results in a visibly better fit between the surrogate and the protector but does not appear to improve repeatability.

Whilst the rotational stiffness ranking of the three protectors tended to be consistent across all three surrogates, the relative difference in protector performance varied. The smallest differences in protector rotational stiffness were measured when using the Geometric surrogate, whilst the scanned surrogate resulted in the greatest differences in protector rotational stiffness (Figure 14.12). The importance of these relative differences in protector rotational stiffness measurements is likely to be dependent on the application

Both the Geometric and Scanned surrogates offer improvements on the current gold standard EN 14120 surrogate, as their geometry better represents a human hand and wrist based on published anthropometric data. They also allow the testing of protectors integrated into gloves. The Geometric surrogate provided repeatable measurements; is based on readily available anthropometric data; can be communicated in an engineering drawing; can be scaled and updated as required with relative ease. Therefore, the geometric surrogate approach should lend itself well to test protocols in international standards.

The Scanned surrogate has increased realism and provides better differentiation between products. The scanned surrogate required participant recruitment to develop and is not easily communicated via an engineering drawing, thereby limiting its reproducibility. The main limitation of the scanned surrogate is the challenge of identifying participants with the desired wrist and hand size. The scanned surrogate will be used for the rest of this body of work as it is the most biofidelic design, enabling protectors to be tested in a user centred way, whilst simultaneously detecting differences between products.

Modifications to the test setup lead to improvements in product testing and data analysis. By selecting four angles of interest rather than fitting mathematical functions to all experimental data, it was possible to obtain a mean condition for each product, irrespective of whether the protector followed a common mathematical function. By setting the end of test based on displacement it was possible to measure end angles closer to 90° compared to the previous investigation in chapter 4. However, for the long snowboarding protector on the scanned surrogate maximum angles were restricted to 84°, as the limit of the load cell (500 N) was exceeded before the hand could be displaced to 90°.

The availability of load cells within the university is a practical limitation of this test setup, only 500N or 5000N were available. Both load cells facilitate measurements to 1/500th of force capacity, facilitating measurements every 1N for the 500N load cell and every 10N for the 5000N load cell (Instron, 2018). When using the higher rated load cell for lower load cases it has a lower sample fidelity, thus would mask differences at the lower torque ranges where much of the data was collected. Therefore, to maintain measurement fidelity the 500N load cell was used in this study.

Surrogate design significantly influences the measured rotational stiffness of snowboarding wrist protectors in a quasi-static bending test. Differences in protector performance with surrogate design have implications for the snowboarding wrist protector standard under development. This study has shown that surrogate design is an important consideration when comparing protector rotational stiffness results between laboratories, test houses and research studies. Threshold values in test standards should be linked to surrogates and should not be transferred across different designs.

14.4 Chapter Summary

Through the development of alternative surrogates, this chapter contributes to the third of the project's objectives: to develop and validate mechanical tests to characterise snowboarding wrist protectors. The newly developed surrogates, of increasing complexity enable the testing of both stand-alone protectors and those integrated into gloves, to detect differences between products in a repeatable manner.

This chapter has shown that the design of the surrogate significantly influences the measured rotational stiffness of wrist protectors, thus International standards should link pass thresholds to specific surrogate designs. Given the geometric surrogate is easy to communicate in an engineering drawing, can be scaled with relative ease and provides repeatable measurements it is recommended for use by the snowboard specific International Standard ISO/CD 20320. The scanned surrogate and modified test protocol will be used in the next chapter to compare the performance of 12 commercial wrist protectors, as it is the most representative design and offers increased differentiation of rotational stiffness for protector design.

15 Characterising wrist protector stiffness using a quasi-static test

15.1 Introduction

The quasi-static test setup and scanned surrogate developed in the previous chapters were used to characterise twelve commercially available products. The findings of that study are presented in this chapter.

15.2 Method

The experimental procedure and data analysis protocol outlined in chapter 5 was used, each protector was pulled back to a hyperextension angle of 90° or the maximum limit of the 500N load cell. Eight repeat trials were performed on each protector fitted on the scanned surrogate, resulting in a total of 96 trials. Torque and hand extension angle were compared at four angles: 35°, 55°, 80° and 90° using the interpolation technique specified in chapter 5 for each of the twelve protectors. The mean torque and standard deviation were calculated at each angle. The rotational stiffness was then calculated as the ratio of torque and hand angle, equivalent to the gradient of the line between each pair of sequential angles. Comparisons between products were made based on the torque and rotational stiffness at each angle. Two case studies were selected to explore the results in more detail and look at the ability of the developed test to distinguish differences in product performance across products utilising different design approaches.

15.2.1 Protectors

Twelve left hand wrist protectors that utilise different design approaches and provide a representative sample of what is commercially available were tested (Figure 15.1). Four of the products are integrated into gloves (G1-G4) whilst the rest are stand-alone protectors (P1-P8). One of the products is an EN 14120 approved roller sports protector (P8), all other products are marketed as snowboarding protectors. Table 15.1 outlines the design characteristics of the tested products, dimensions were measured using digital callipers (Mitutoyo CD-6”B). It was not possible to remove the splints without permanent damage, for most protectors, so measurements were taken through the external material. Manufacturers do not readily provide material information for protectors; therefore, material type was excluded from the product comparison.

Table 15.1: Characteristics of twelve tested products (all measurements in mm)

ID	Product	Construction	Length x Width at largest point	Palmar pad/plate			Palmar splint			Dorsal Splint		
				Length	Width	Thickness	Length	Width	Thickness	Length	Width	Thickness
P1	Dainese	1 Dorsal splint with sliding lock plate	190 x90	-	-	-	-	-	-	172 70	34-80 65	4 4
P2	Dakine	1 Palmar splint	170 x 95	-	-	-	140	35-70	7	-	-	-
P3	Arva	1 Palmar splint 1 Dorsal splint	245 x 80	-	-	-	230	50-70	3	220	50-80	3
P4	Reusch	Palmar pad 2 palmar splints 1 dorsal splint	200 x100	70	35-60	13	62	17	4	120	40-57	5
P5	Flexmeter	Palmar skid plate 1 palmar splint 1 dorsal splint	210 x 85	70	30-50	3	205	50-70	3	210	50-70	3
P6	Snowlife	Palmar pad 1 palmar splint 1 dorsal splint	190 x 76	50	45	17	152	35-45	4	155	45-56	4
P7	Burton	Palmar pad 3 palmar	160 x 72	50	43	12	70	9	5	160	10-20	5

ID	Product	Construction	Length x Width at largest point	Palmar pad/plate			Palmar splint			Dorsal Splint		
				Length	Width	Thickness	Length	Width	Thickness	Length	Width	Thickness
		splints 2 dorsal splint										
P8	Oxelo	Palmar skid plate 1 palmar splint 1 dorsal splint	175 x 85	70	40-55	3.8	155	30-55	4	135	30	5
G1	K-tech glove	Palmar pad 1 palmar splint 1 dorsal splint	300 x 125	10-60	10-60	3	130	35	4	120	40-45	2-9
G2	Obscure glove	Palmar pad 1 palmar splint	290 x 130	25-50	18-60	5	130	35	4	-	-	-
G3	Snowlife glove	Hybrid palmar pad/splint 1 dorsal splint	340 x 130	120	45	5	-	-	-	155	50	2
		3 splints in dorsal strap								95	18-25	6
G4	Flexmeter glove	Palmar pad 1 dorsal splint	335 x 120	20-70	15-50	6	-	-	-	210	50-68	6

Figure 15.1: Twelve tested products ordered from longest to shortest (G: protector integrated into gloves, P: stand-alone protectors)

15.3 Results

15.3.1 Protector comparison

In four cases it was not possible to obtain measurements to 90° as the load cell reached its measurement limit: Dainese (P1), K-tech (G2), Obscure (G2) and Snowlife (G3). Therefore, results are only presented up to an extension angle of 80° for all twelve products, to facilitate a comparison. Figure 15.2 shows the torque vs angle profiles for the twelve protectors, the rotational stiffness for each protector between each pair of angles is shown in Figure 15.3. At the lower angles, 35-55° all the protectors have a comparable rotational stiffness within a 0.25 Nm/° range. At the higher angles 55-80° there is a larger spread of rotational stiffness, with a range of 1.39 Nm/°.

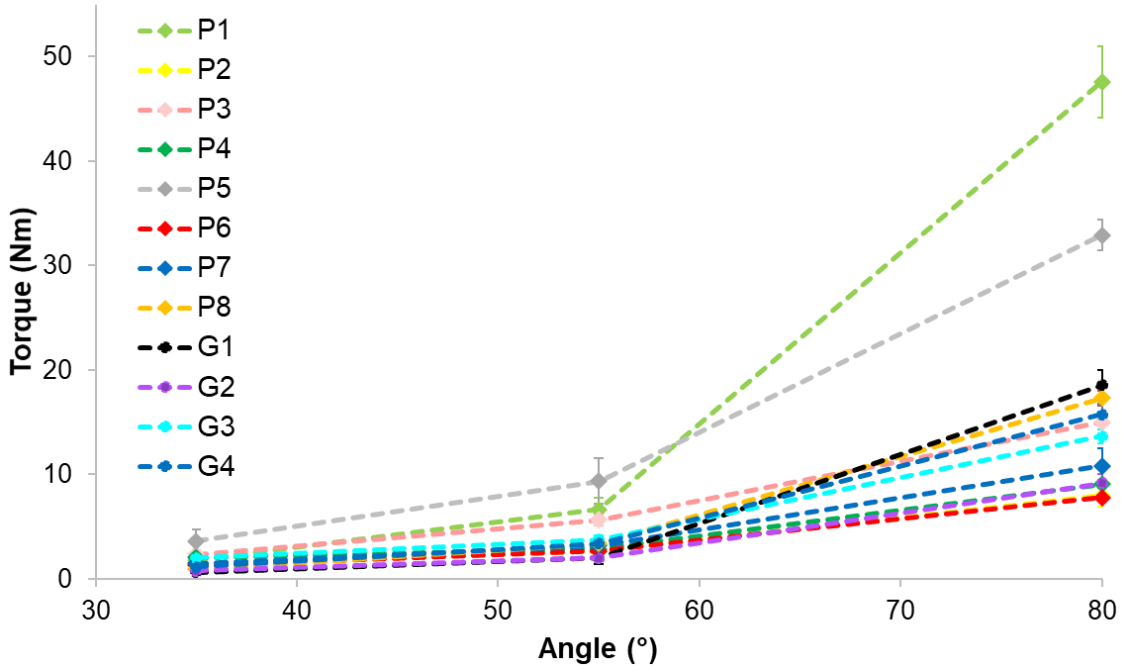

Figure 15.2: Torque hand angle profile for twelve protectors

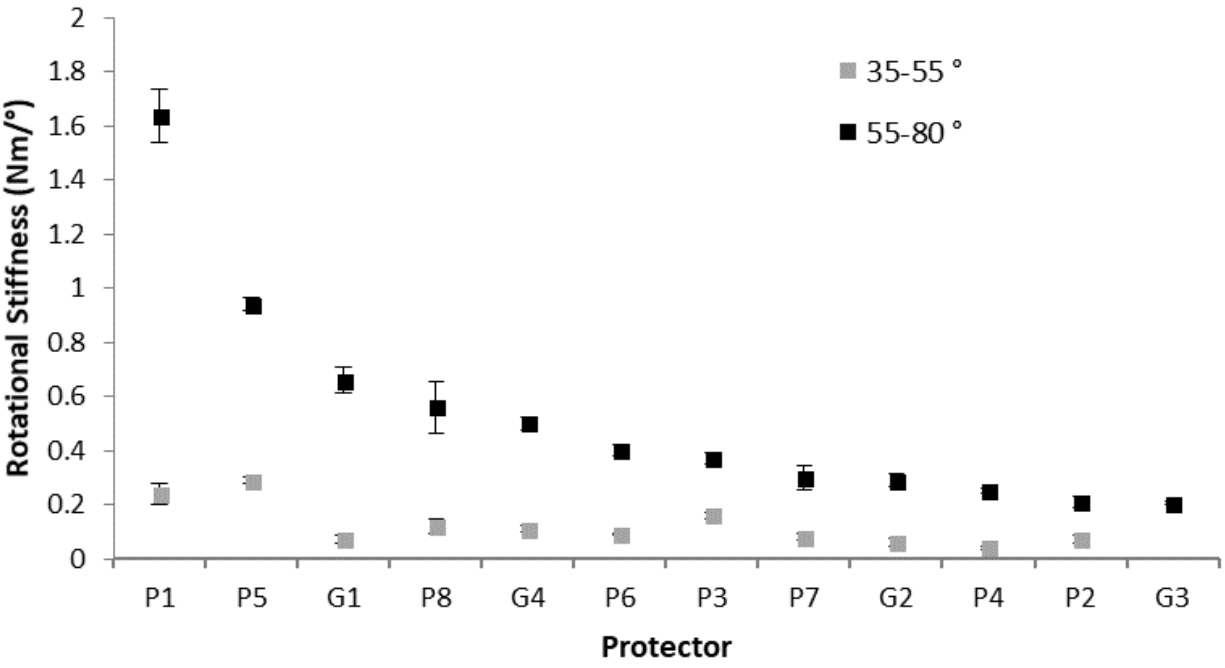

Figure 15.3: Rotational stiffness (mean and standard deviation) for twelve protectors between 35-55° and 55-80° ordered by highest stiffness at 55-80°

15.4 Case Studies

Two case studies were selected to explore the results in more detail and look at the effectiveness of the test in distinguishing differences between products. The Reusch (P4) and Burton (P7) stand-alone protectors, as these products have a similar design with similar dimensions; and the Snowlife glove (G3) and the Snowlife stand-alone protector (P6), which utilise different splint and pad designs despite being made by the same manufacturer.

15.4.1.1 Comparison between two stand-alone protectors with similar designs

The Reusch (P4) and Burton (P7) are stand-alone protectors which are similar in design, overall dimensions (Figure 15.4a-c) and perform similarly, Figure 15.4d. This is to be expected as both products have similar dorsal splint thicknesses; the fact that the test has been able to measure similar performances for similar products implies it is effective. The higher torque required to displace the Burton protector to 55° and 80° is likely due to the different shape and hence area of the protective elements.

c)

Thicknesses (mm)	Burton Protector (P7)	Reusch Protector (P4)
Palmar splint	5	4
Palmar pad	14	13
Dorsal splint	7	7

d)

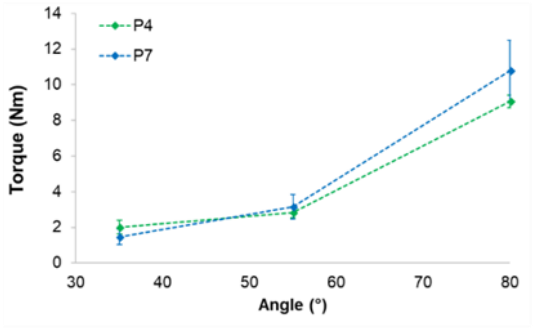

Figure 15.4: Comparison between a) Burton (P7) and b) Reusch (P4) protectors all measurements in mm c) thickness measurements d) Torque hand angle profile for P4 and P7

15.4.1.2 Comparison between glove and stand-alone protector from the same brand using different design approaches

The Snowlife glove (G3) and the stand-alone Snowlife protector (P6) utilise different protective design elements and as expected perform differently (Figure 15.5), demonstrating the effectiveness of the test. Both protectors have dorsal splints of similar dimensions; whilst the glove includes additional dorsal support from the strap. The Snowlife stand-alone protector includes a palmar splint whereas the glove does not. The palmar pad in the stand-alone protector is thicker than the palmar pad in the glove, but the glove is larger overall with more material. In this case the glove was stiffer than the protector at all three angles despite

not having a palmar splint. Differences in material may also play a part in the difference in product performance.

c)

Thicknesses (mm)	Snowlife Glove (G3)	Snowlife Protector (P6)
Palmar splint	5	20
Palmar pad	2	5
Dorsal splint	5	5

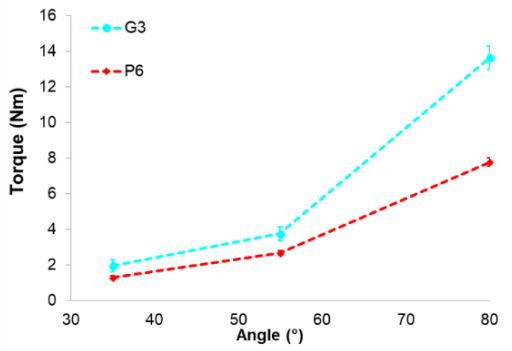

Figure 15.5: Comparison between a) Snowlife Glove (G3) and b) Snowlife protector (P6) all measurements in mm c) thickness measurements d) Torque hand angle profile for G3 and P6

15.5 Discussion

No difference in quasi-static performance between protective gloves and stand-alone protectors was observed during this study illustrated by the lack of clustering of results of both types (Figure 15.2). All the tested products follow a two-part loading curve with a steeper gradient at the later stages between 55-80°. At the lower angles the products perform similarly, within 3 Nm of each other at 35°. There is a larger spread between products at 55° and 80°. All products are within 7 Nm at 55°, whilst at 80° products are within 40 Nm of each other. When excluding the Dainese the remaining products are within 25 Nm of each other at 80°. When the flexmeter protector is also excluded, the 10 other protectors are within 11 Nm at 80°.

The Dainese protector (P1) required a torque 40% higher than any other tested design to reach 80° (Figure 15.2 and Figure 15.3). This difference in performance is likely due to the sliding lock plate used by the Dainese instead of a more traditional dorsal splint (Figure 15.6). Unlike other designs the Dainese plate engages with the splint body when the wrist is displaced resulting in the sudden ramp up of rotational stiffness at larger displacements. The fact that the Dainese protector which has the most unique design was found to be the stiffest product measured using the test and considered an outlier, demonstrates that the test setup can be used to identify differences in performance across products.

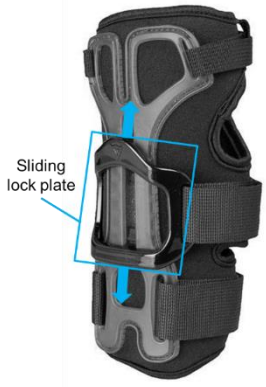

Figure 15.6: Dainese stand-alone protector with sliding lock plate

As mentioned previously the 500 N load cell was used to maintain measurement fidelity, however as four products exceeded the limit of the load cell it was only possible to compare all protectors up to 80°. For future studies it is recommended that a 1000N load cell is sourced to enable product comparisons up to 90°. Further testing with a greater number of

products could be beneficial to better quantify surrogate repeatability and further understanding of differences in stiffness between protectors.

The quasi-static test enables protectors of different design approaches to be compared and the influences of those approaches to be explored. Based on research to date it is difficult to relate protector stiffness to injury threshold. Therefore, studies using cadavers to investigate studying the relationship between hyper-extension, torque and injury threshold are recommended.

15.6 Chapter Summary

This chapter demonstrates that the quasi-static test and scanned surrogate developed in Chapter 4 and 5 can characterise the stiffness of snowboarding wrist protectors and effectively differentiate between products. This chapter partly addresses the fourth of the project's objectives: to compare the protective characteristics of a range of wrist protectors using the developed methods. This study has shown that protectors employing different design approaches perform differently in a quasi-static test, enabling the influence of protector design on performance to be explored.

A limitation of the test method presented here is the quasi-static application of load; whilst this facilitates an understanding of product stiffness related to hyperextension, it does not enable a full assessment of the product protective capacity. A complementary approach employing a dynamic test that facilitates the measurement of energy absorption and load transfer will be presented in the following chapter.

7 Development of Impact Test

7.1 Introduction

In chapter 3 the need for two tests to characterise snowboarding wrist protectors was identified. Having developed a quasi-static test in chapters 4-6, this chapter will present the development of the impact test. The aim of this chapter was to develop a mechanical impact test and protocol to replicate injurious snowboard falls and measure the associated forces and hyperextension angles, achieved through the following objectives:

- To develop an impact test using the boundary conditions and criteria outlined in chapter 3
- To determine the suitability of the experimental setup

7.2 Development of impact test

7.2.1 Concept Design

From the literature two approaches that are typically used to impact test protective equipment were identified. Moving a surrogate onto a rigid surface or moving a mass onto a surrogate fixed to a rigid surface. Based on these two approaches ideation sessions with input from the university's design engineer resulted in the development of seven concepts which could meet the criteria set out in chapter 3. Setups using a linear drop or angular pendulum (concepts a-e) can be driven by gravity making them preferential compared to the two concepts with horizontal positioning (concepts f and g).

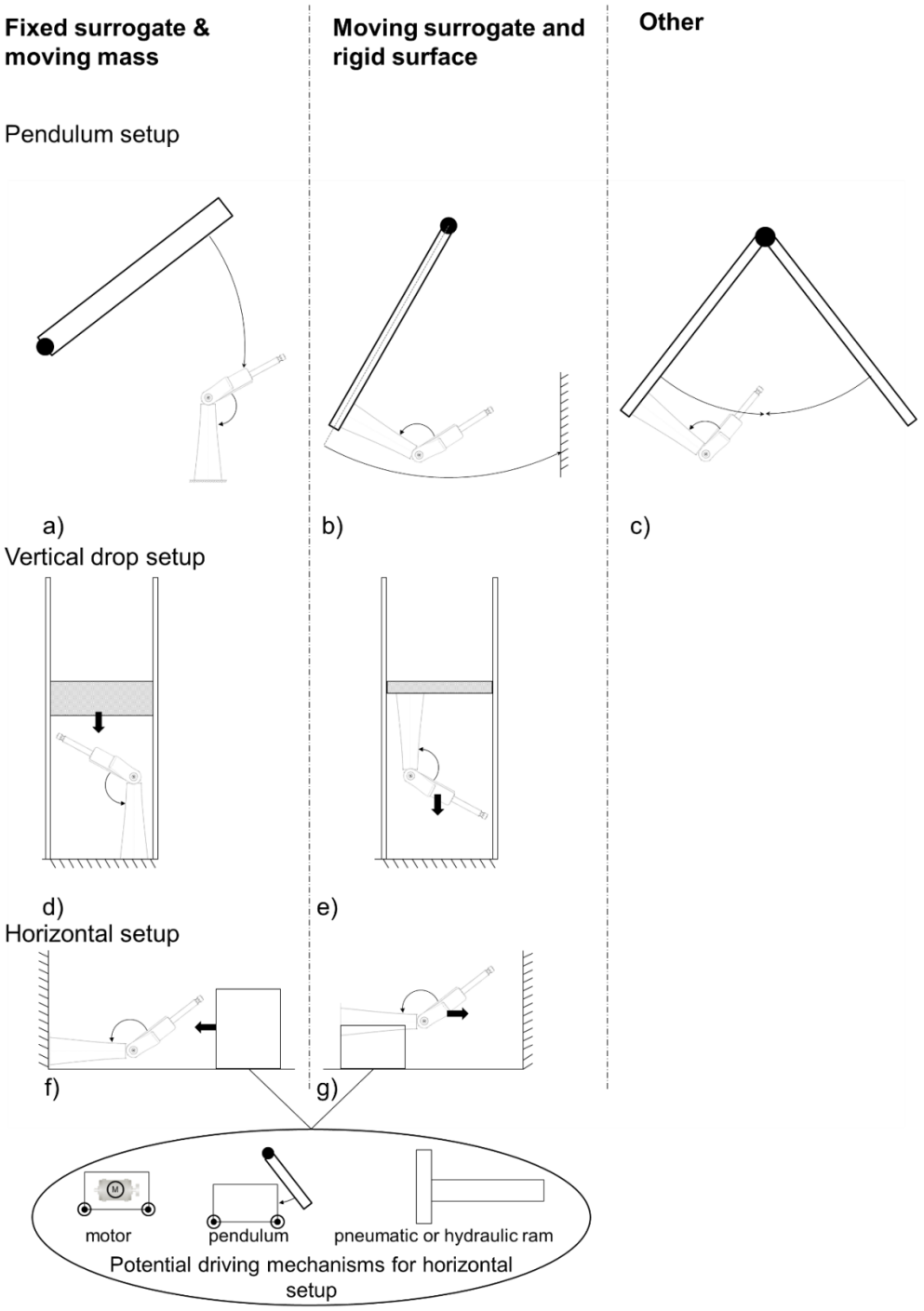

Figure 7.1: Concept design **a)** Moving pendulum and fixed surrogate **b)** Moving surrogate via a pendulum onto a rigid surface **c)** Double pendulum **d)** Linear drop onto a fixed surrogate **e)** Moving surrogate via a linear drop onto a rigid surface **f)** Horizontal setup with a fixed surrogate and a driven moving mass **g)** Horizontal setup with a driven surrogate into a rigid surface

7.2.2 Concept Selection

All the developed concepts meet the criteria outlined in the product design specification for an impact test in section 3.3. Therefore, in order to determine which concept should be taken forward to further development and manufacture a decision matrix was established. The criteria were informed by the product design specification, discussions with the design engineer responsible for the construction of the setup and conversations

with instrumentation suppliers. As can be seen in Table 7.1 these criteria are based on manufacturability, potential for instrumentation and usability. Each of the seven concepts is rated on a scale of 1-3 for its feasibility to meet the design criteria, where a score of 1 means it would poorly satisfy the criterion, and 3 means it fully satisfies the criterion.

Table 7.1: Concept selection matrix

Criteria	**Concepts**						
	Pendulum			**Vertical drop test**		**Horizontally mounted**	
	a	**b**	**c**	**d**	**e**	**f**	**g**
Easy to manufacture - Uses off the shelf components with short lead times where possible - Can be built within 12 months	3	3	2	2	2	2	2
Easy to operate	2	2	1	3	3	3	3
Wrist protectors can be easily mounted and removed from the surrogate	3	2	2	3	2	3	2
Easy to instrument - Uses instrumentation which are readily available with short lead times - Uses instrumentation which can be mounted to the surrogate or rig with minimum modification	3	3	1	3	3	2	2
Requires minimal maintenance during service life	3	1	1	1	1	2	2
Gravity Driven	3	3	3	3	3	1	1
Surrogate is fixed	3	1	1	3	1	3	1
Total	20	15	11	18	15	14	13

Concept a the moving pendulum applied to a fixed surrogate scored the highest based on the design criteria. Concept d the linear drop onto a fixed surrogate also scored well, however off-axis loads may be generated under higher masses when using a drop test, which could be problematic and cause damage to the bearings in the guide rails. Therefore, a bespoke impact pendulum setup with a fixed surrogate was further developed.

7.2.3 Detail Design

Based on the pendulum concept presented in the previous section a mechanical rig and surrogate was developed. The setup enables an impact to the palm of both an unprotected and protected wrist at different settings based on the boundary conditions of Greenwald et al. (1998). The following section outlines the design and development of the surrogate, rig and their associated subassemblies.

7.2.3.1 Surrogate development

A surrogate based on the scanned surrogate used in the quasi-static test was developed (Figure 7.2). The surrogate consists mainly of a central core, hand and 2-part forearm casing. The central core is bolted to a mild steel base plate which attaches to a three-axis dynamometer (Kistler, 9257A, Switzerland) connected to a charge amplifier (Fylde, FE-128-CA, UK) to facilitate force measurements. Wrist extension angle is measured by a potentiometer (Metalux POL 200, USA) mounted within the surrogate, which generates a voltage during angular movement.

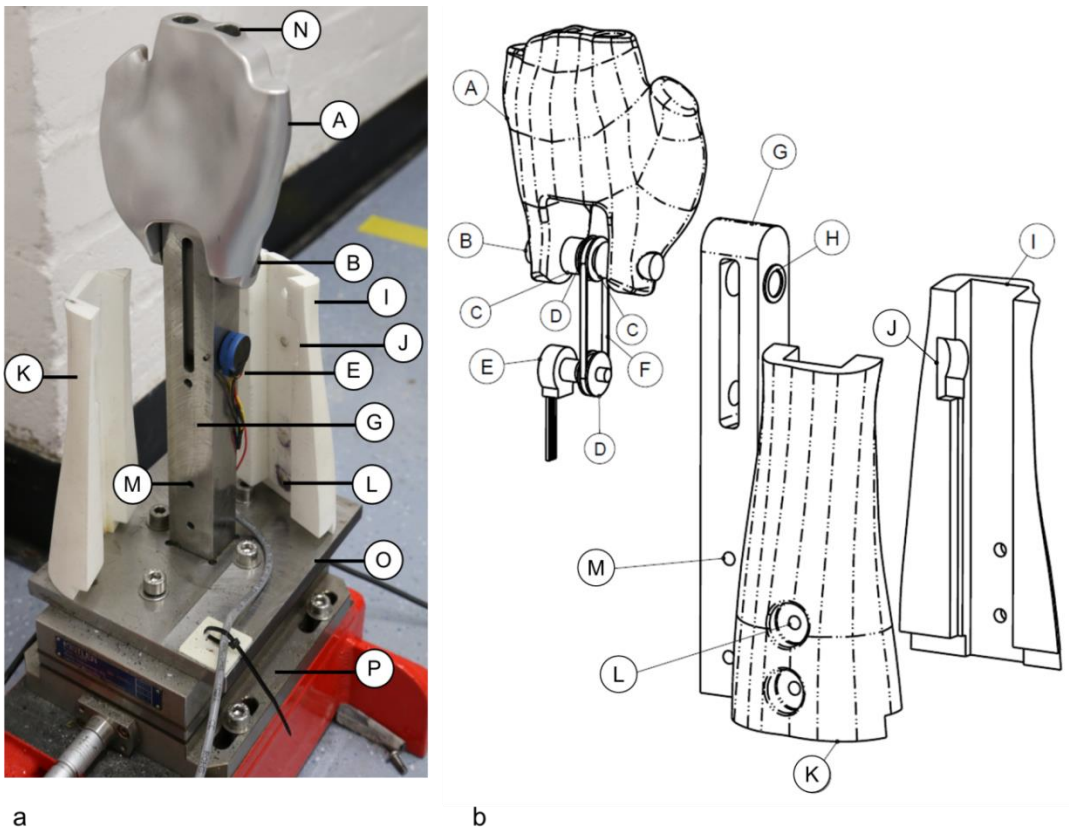

a b

A	Hand
B	Shaft
C	Bearing x2
D	Toothed timing pulley x2
E	Potentiometer
F	Toothed timing belt
G	Central metal core
H	Washer
I	Casing part 1
J	Slot in casing for potentiometer and wiring
K	Casing part 2
L	Fixing to bolt casing to central core
M	Hole to mount casing to central core
N	Finger slots
O	Base plate
P	Dynamometer

Figure 7.2 a) Surrogate with forearm casing unbolted to show internal components b) Exploded view of surrogate showing potentiometer setup

Modifications were made to the surrogate design used for the quasi-static test to make it suitable for impact testing; rig attachment, finger design, arm orientation, instrumentation and material. The surrogate is vertically mounted, unlike Greenwald et al. (1998) where the cadaver arm was orientated at 75° to the force plate. Vertically mounting the surrogate enables force measurements to be taken in the direction they are applied, limiting torques at the base of the surrogate.

It was hypothesised based on the Greenwald et al. (1998) force time trace, that the fingers provide little resistance during the impact. Flexing out of the way before the palm contacts the ground compressing the carpals and causing injury. As the fingers do little during an impact and the dorsal splints on commercial products don't extend beyond the knuckles, they were excluded. The scan used for the quasi-static surrogate was found to be inappropriate for the new surrogate. As the hand and forearm were not orientated centrally around the long axis, it was not possible to insert a metal core within the surrogate due to insufficient clearance between the edge of surrogate and central core (Figure 7.3a). This was overcome by rescanning the participant's forearm ensuring it was orientated centrally around the long axis (Figure 7.3b).

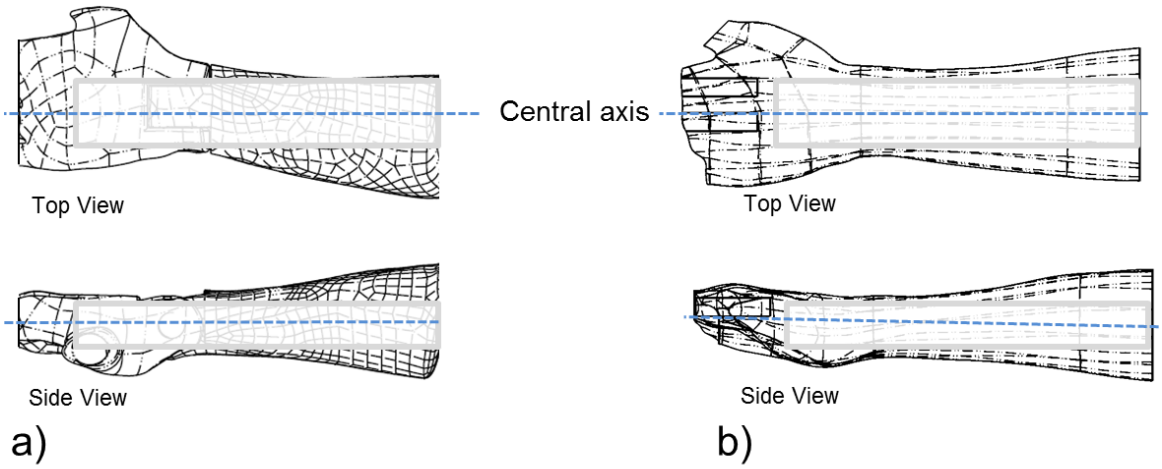

Figure 7.3: Surrogate shape comparison with superimposed metal core **a)** Quasi-static scanned surrogate shape **b)** New surrogate shape based on scan with altered orientation to ensure part is central to the long axis

The scan point cloud geometry was post processed and imported into CAD software as before. The fingers and thumb were removed, the forearm converted into a shell (variable wall thickness due to forearm shape 3-26mm) and a hinge joint added to the wrist using a top down modelling approach. Based on the forearm dimensions a central core (26 x 30 x 214 mm) was modelled as a separate part. Two holes (ø 12 x 60 mm)

were added to the hand to facilitate removable finger rods, to enable the surrogate to be used for quasi-static testing and aid in the wrist potentiometer calibration. The hand was CNC machined in aluminium (Protolabs, UK).

The position of the potentiometer was offset below the wrist joint in the forearm (Figure 7.2), due to the size of available potentiometers. As no potentiometers were found to be commercially available that would fit within the central core. The hand is mounted onto a silver steel shaft (ø12 x 60 mm, RS Pro, UK) in conjunction with two bearings. By locking the hand and a timing pulley to the shaft with two grub screws, the movement of the wrist shaft can be transferred 52.5 mm down the forearm, to a region wide enough to accommodate the potentiometer. A secondary timing pulley was mounted onto the potentiometer shaft and connected to the wrist joint via a toothed timing belt, to enable wrist angles to be measured. The core was milled from medium carbon steel to withstand multiple impacts and enclosed by a two-part non-load bearing forearm casing. The casing was made from polyamide using laser sintering (Materialise, UK), slots within the casing housed the potentiometer and wiring.

7.2.3.2 Rig development

The rig was designed in CAD (PTC Creo, USA) and manufactured at the University (Figure 7.4). The pendulum arm facilitates inbound velocities up to 5.2 m/s (assuming no friction) to replicate a range of fall heights based on the work of Section 3.2.2.4. The mass of the pendulum at the point of impact is 12.7 kg, and additional mass of up to 30 kg can be attached, if required to replicate different fall scenarios. The dynamometer and surrogate assembly can be bolted on to the base of the rig. The angular displacement of the pendulum arm is measured by a potentiometer (Bourns 6657, USA). This instrument is mounted to the pendulum pivot shaft enabling the release and rebound height of the pendulum arm to be determined. The potentiometer shaft is locked to the pendulum pivot shaft via a grub screw, and its body clamped onto the rig.

An impact head was mounted onto the tip of the pendulum arm to provide a larger surface for the interaction between the pendulum and the surrogate palm. The pendulum is raised using a ceiling mounted pulley system and released by a quick release pin (not pictured) to ensure it can be operated by one user. Most of the rig was welded from 80 x 40 mm steel box section with a 3 mm wall thickness (Hillsborough Steelstock, UK).

The pendulum arm is locked to a silver steel shaft (ø20 x 125 mm, RS Pro, UK) with a grub screw and aligned by fabricated bushings (Figure 7.2 & Figure 7.3). The shaft is mounted to the rig via pillow bearings (RS components, UK) attached to a fabricated bracket, which enables different arm heights to be set. The rig was powder coated before assembly. The rig is bolted to the floor using concrete fixings at four positions (0 m, 0.5 m, 1.15 m and 1.7 m).

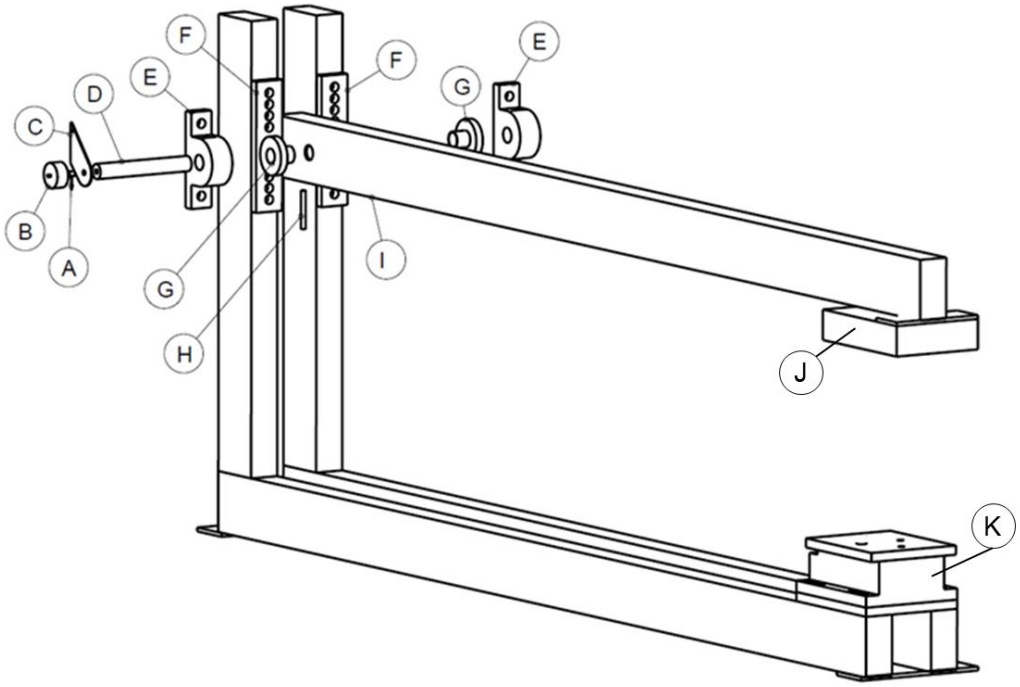

A	Grub screw to lock potentiometer to shaft
B	Potentiometer
C	Bracket to mount potentiometer body to stationary rig
D	Shaft
E	Pillow bearing x2
F	Fabricated bracket to mount pillow bearings x 2
G	Fabricated bushings x2
H	M6 bolt to lock shaft to pendulum
I	Pendulum
J	Impact head
K	Force plate

Figure 7.4: Exploded view of impact rig showing pendulum and bearing mount

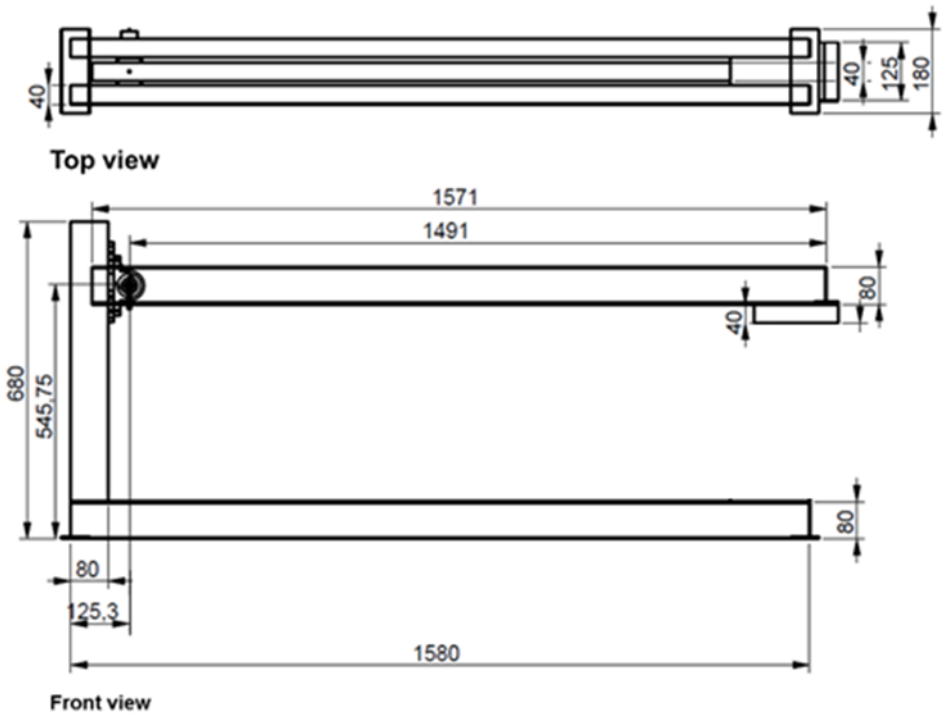

Figure 7.5: Dimensioned view of impact rig (all dimensions in mm)

7.2.3.3 Instrumentation

In addition to the three measurement sensors previously mentioned a high speed camera (Vision Research, Phantom Miro Lab 320, USA) was integrated into the system to enable the impact to be visualised. To enable the three measurement sensors and the high speed camera to collect and store synchronised data during an impact additional instrumentation was used. A data acquisition device (DAQ) (National instruments, USB-6211, USA) was used as an interface between the instrumentation and laptop to collect and store the voltages outputted by the measurement sensors. A stand-alone 24-volt power source (Powertraveller, powergorilla 24000MAH, UK) was used to drive both potentiometers, whilst the charge amplifier and high speed camera had their own power supplies.

To enable high speed camera footage to be synced with the potentiometers and dynamometer a BNC cable with a trigger button was connected to the DAQ. When the high-speed camera trigger was pressed the DAQ reads 0 volts for this channel, therefore, the last frame of the high-speed camera footage can be matched with the time step when the trigger channel reads 0 volts, enabling all data collected at the same frequency to be synced.

Instrument Calibration

Prior to mounting the dynamometer to the rig it was calibrated by removing masses while measuring voltage change. Nine loads (250-2,500 N) were measured to calibrate the z-axis. 2,500 N was selected as it was close to reported fracture threshold. Four loads (250-1000 N) were taken in the other two axes as lower forces were expected in these directions. For each load five repeat measurements were taken, and loads were increased at 250 N increments. A linear relationship between voltage and load was observed, enabling the calibration parameters for all three axes to be determined (Figure 7.6).

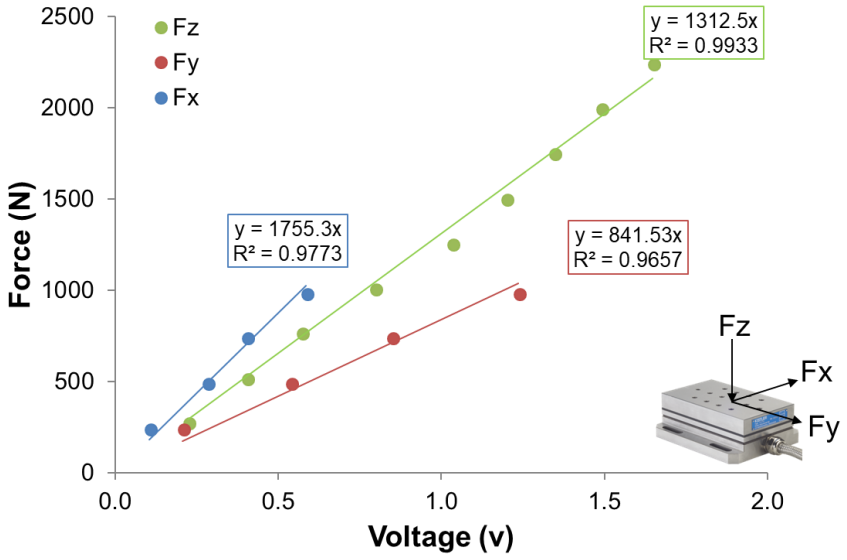

Figure 7.6: Force plate calibration factors

To calibrate the potentiometers the pendulum arm and surrogate hand were set at a series of angles for 2 s, the angle was measured with a digital inclinometer (MW570-01, Moore & Wright) and voltage readings taken at each point (Figure 7.7). The pendulum arm was held at ten instances across its range of motion and the inclinometer mounted on top of the pendulum arm by a magnet. The surrogate was held in fourteen positions; the inclinometer was mounted to the removable fingers of the surrogate using the load application clamp from the quasi-static setup. A linear relationship between voltage and angular position was observed, enabling the calibration parameters for both potentiometers to be determined (Figure 7.8). The absolute error of the measurement (the difference between the inclinometer value and the predicted value) was determined for both potentiometers across all measurements and the mean determined. Both potentiometers have a mean absolute error of 0.3°.

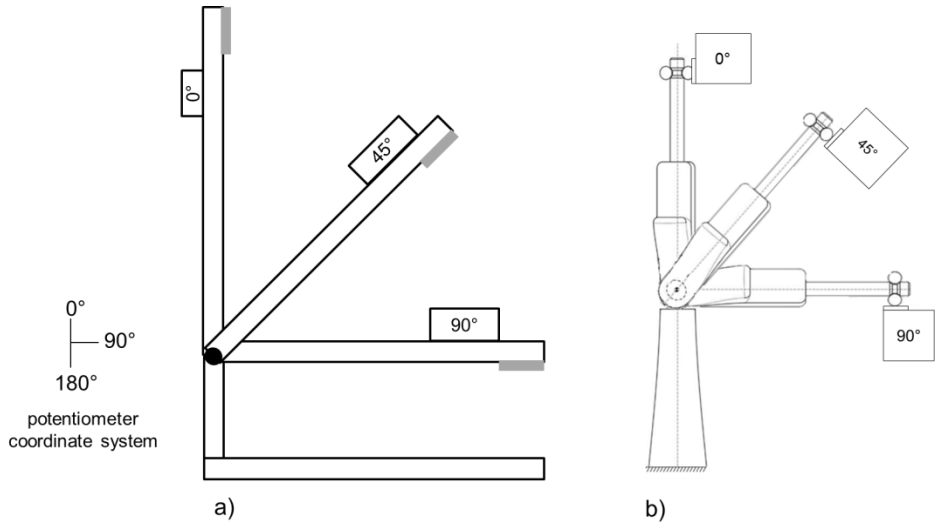

Figure 7.7: Potentiometer calibration (3 cases shown) a) Pendulum arm b) Wrist surrogate, not to scale

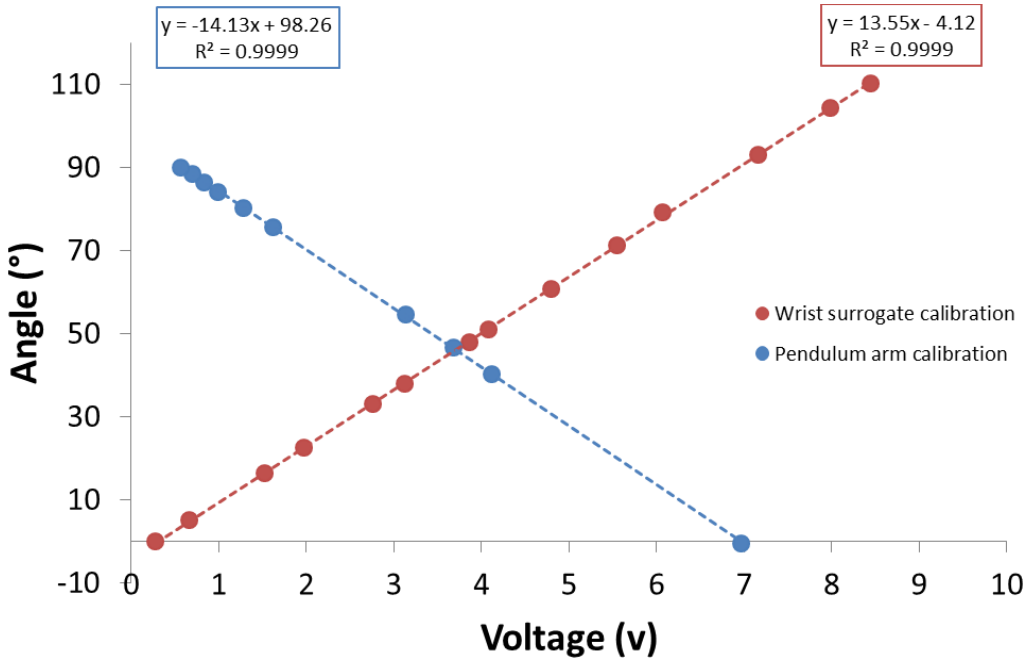

Figure 7.8: Potentiometer calibration factors

7.2.3.4 Impactor design

To alter the compliance of the system, material replicating the loading rate of Greenwald et al., (1998) was mounted to the impact head of the rig. Through mounting a range of different polymers of varying thicknesses, 100 mm of Neoprene shore hardness 50 (Boreflex UK) was identified as the best match (Figure 7.9). In addition to different grades of Neoprene, four foams were tested: Polyurethane (pur30fr, D3o pulse and Poron xrd 09750-65) and low-density polyethylene (LD33). The tested foams were found to be too compliant, whilst the commercial standard of Neoprene 65 was too stiff. Neoprene 50 is only available in 20 mm thickness, so five blocks were bonded together using an adhesive (Loctite 480). The Neoprene block was also bonded to a 1 mm

aluminium sheet which was bolted onto the rig, enabling blocks to be easily replaced (Figure 7.10). The Neoprene block had a mass of 2.6 kg, bringing the impactor mass to 15.3 kg.

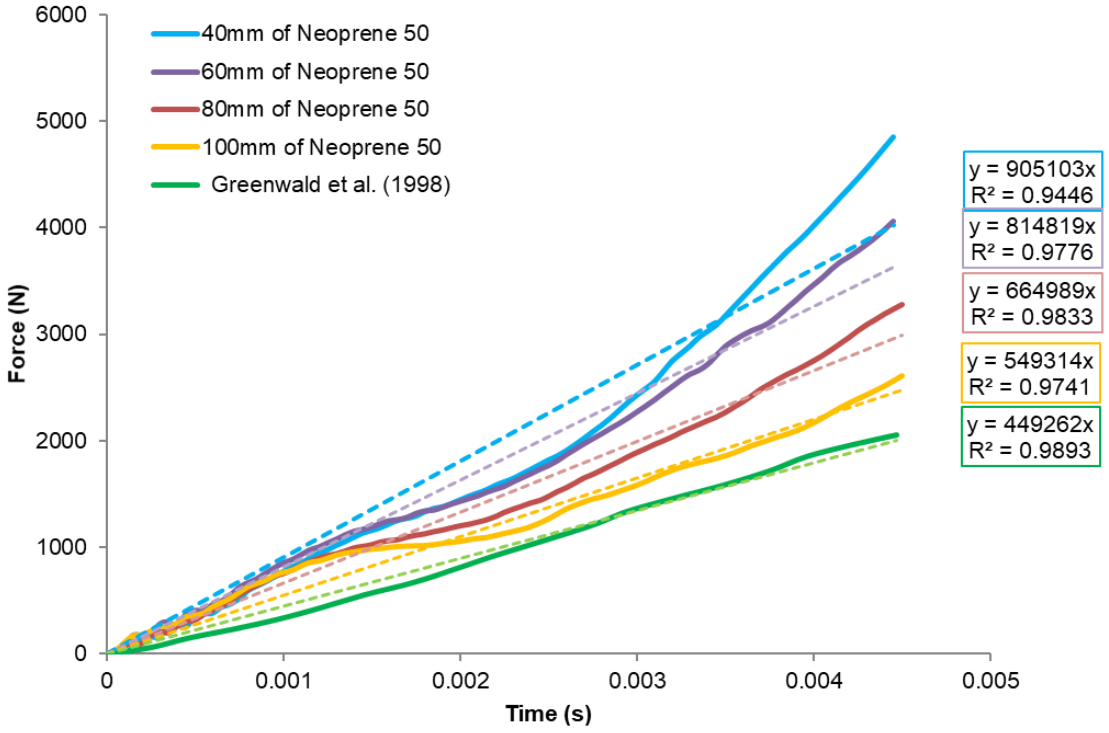

Figure 7.9: Loading rate comparison between different thicknesses of Neoprene and Greenwald case over 0.0045 second window of interest

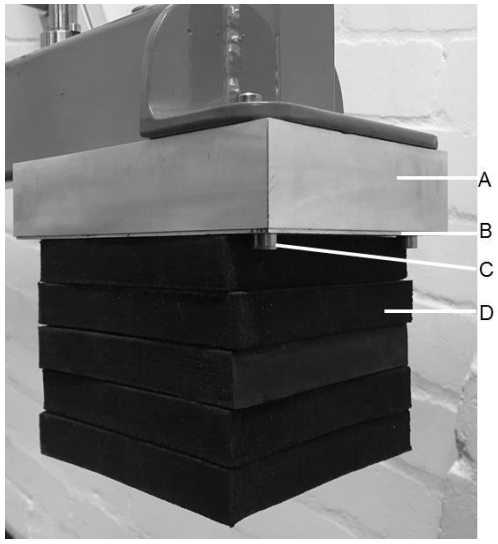

Figure 7.10: Impactor setup. A-Aluminium block, B-1mm Aluminium mounting sheet,C-M5 bolts, D-5x20mm Neoprene 50 sheets

Fatigue testing of impactor

Multiple impacts were conducted to determine whether the Neoprene block could withstand multiple impacts and monitor the repeatability of the experimental setup. An untested block was preconditioned at 18° for 24 hours. Shore hardness measurements were taken at 16 locations on the block (four repeats per location) using a durometer tester (Checkline AD100, USA), prior to impact (Figure 7.11). The Neoprene block was bolted onto the pendulum arm and impacted 50 times, from a 0.4 m drop height with an impact energy of 60 J onto the bare surrogate core. Force measurements were taken in 3-axis for these 50 impacts. All the instrumentation was sampled simultaneously at 20,000 Hz. The block was then removed, and hardness measurements taken at the 16 locations.

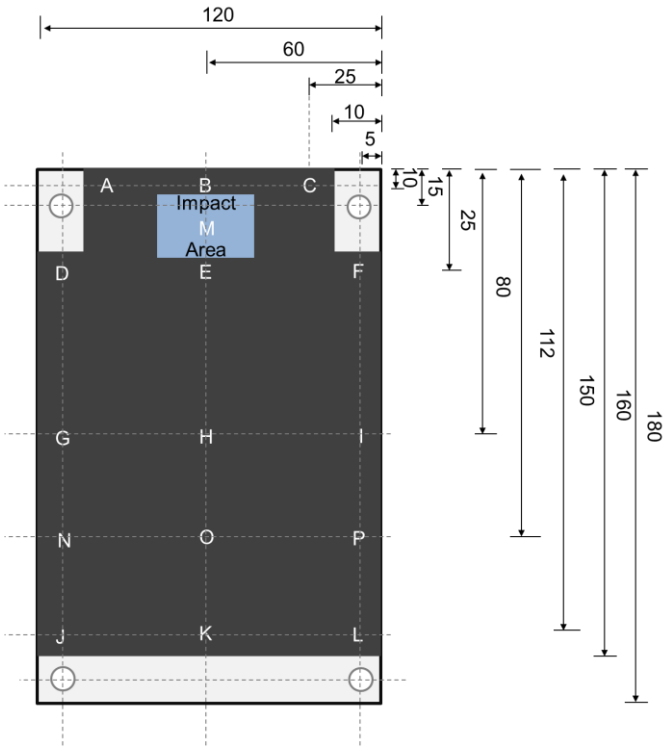

Figure 7.11: Annotated Neoprene block showing hardness measurement locations

Of these 50 impacts, force measurements were collected for 49 impacts on the same block; one was missed due to technical difficulties. Figure 7.12shows that the force time traces for repeat impacts are very similar with the exception of the first impact which had a lower peak force in the vertical direction and a different shape force trace in the y-axis. Table 7.2 presents the descriptive statistics for all 49 measured trials and all trials excluding the first one. Variation between repeat trials is less when the first trial is

excluded. Based on this data the first impact can be described as a conditioning trial, after which the Neoprene block appears to become more stable.

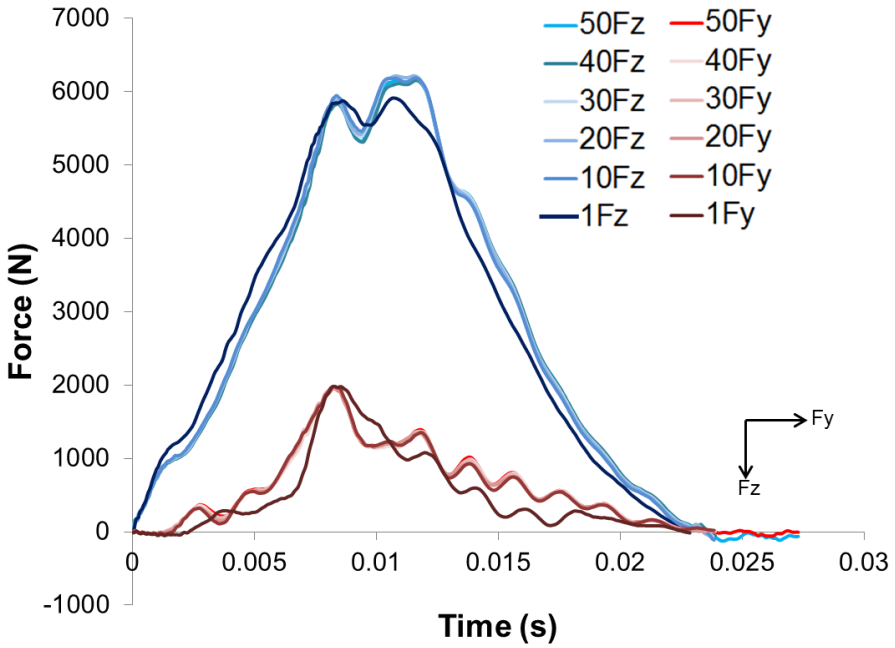

Figure 7.12: Fz and Fy force time trace for 6 repeat conditions showing the similarity in the force traces except for the first impact

Figure 7.13 shows there is a general trend that peak force in both z and y decreases as the number of impacts increases. The percentage degradation of the Neoprene block, resulting from multiple impacts was calculated as a ratio of the three lowest force values to the three highest three force values. The degradation in the block, resulting from multiple impacts is presented in Table 7.2.

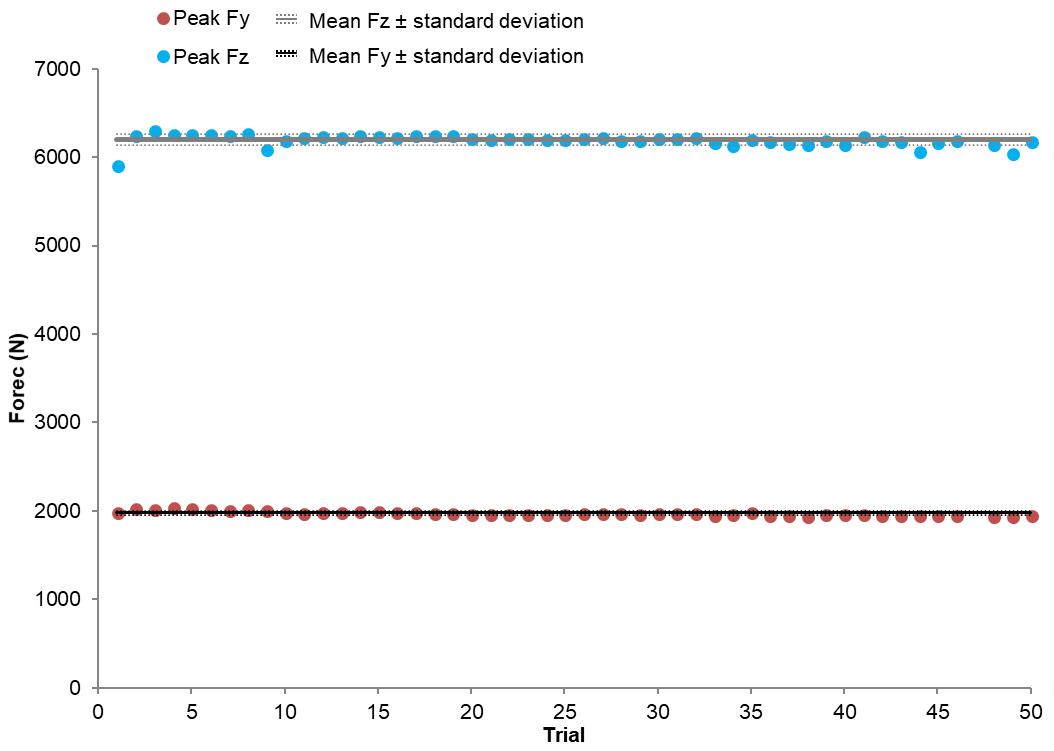

Figure 7.13: Variation in peak Fz and Fy

Table 7.2: Descriptive statistics for impacts

	All 49 trials		Excluding first trial	
	Peak Fz (N)	**Peak Fy (N)**	**Peak Fz (N)**	**Peak Fy (N)**
Mean ± SD	6201 ± 66	1978 ± 25	6207 ± 51	1987 ± 25
CV (%)	1.06	1.27	0.82	1.28
Range	391	107	263	107
Degradation (%)	4.4	4.6	3.4	4.6

Prior to impact testing the mean hardness of the Neoprene block across all 16 locations was 59 ± 1.6 shore. After 50 impacts the mean hardness of the Neoprene block across all 16 locations had decreased to 58 ± 1.6 shore. When comparing hardness at individual locations the greatest reduction in hardness (7.5%) was seen at the point of impact; position M (Figure 7.14). Smaller differences (2-4%) were seen at the positions neighbouring the point of impact. It is not clear why a difference was seen at position J as this is at the opposite edge of the block from the impact.

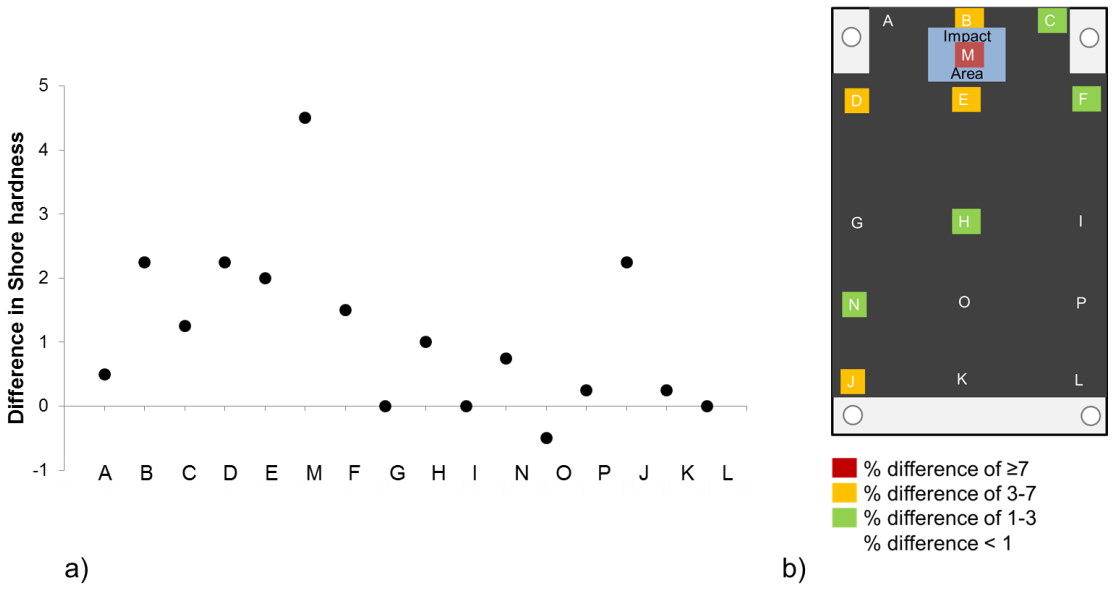

Figure 7.14: a) Difference in mean hardness between pre and post 50 impacts **b)** Heat map showing position of largest differences in hardness pre and post 50 impacts

The Neoprene block is susceptible to degradation from multiple impacts. It has been shown that the block requires one impact to condition it; the block is then stable for repeated impacts to within 5% of peak force for the following 49 impacts. If more than 50 impacts are to be conducted it is advisable to extend degradation testing to a greater number of impacts. Future testing protocols should include bare hand impacts in-between protected impacts to monitor degradation.

7.2.4 Overview of Impact test setup

The complete test setup can be seen in Figure 7.15.

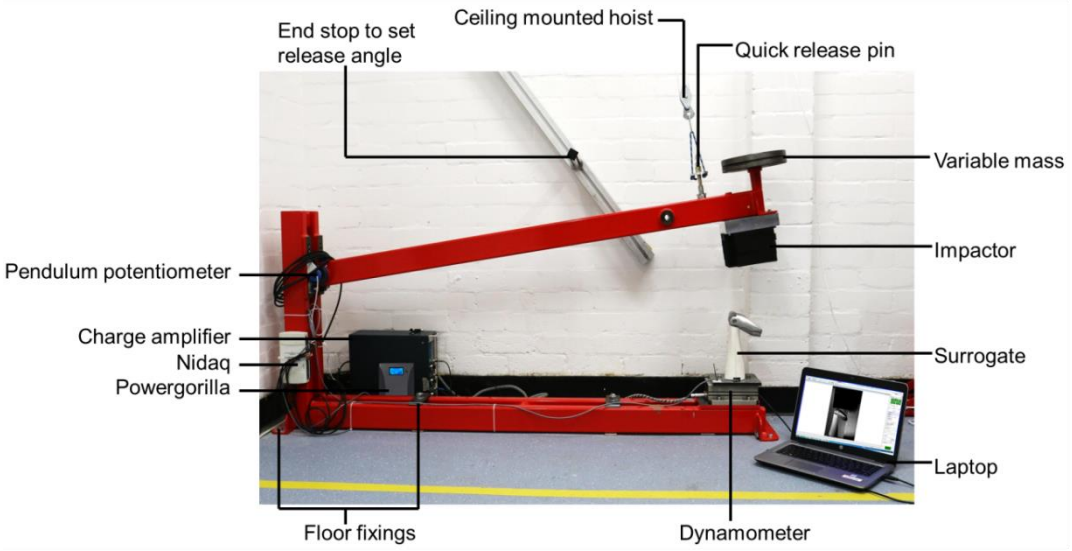

Figure 7.15: Impact test

7.3 Experimental validation of impact test

To determine the suitability of the test setup and identify areas for improvement, pilot tests were carried out. Initial tests were conducted to compare the forces measured in developed test setup with the forces measured by Greenwald et al (1998). Further tests were conducted to check that the developed setup was suitable for measuring the performance of wrist protectors. This section discusses the findings of the pilot tests and provides an overview of a bare hand impact to demonstrate the capability of the developed system.

7.3.1 Pilot testing: bare hand condition

7.3.1.1 Setup

As the test was designed to replicate the test case of Greenwald et al. (1998), the hand was positioned out of the way at maximum extension (Figure 7.16), enabling the impactor to strike the core (equivalent to the palm). Impacting the core directly meant all loads were transmitted to the dynamometer, without overloading the silver steel rod used for the wrist hinge. Repeat impacts using the same boundary parameters as Greenwald et al., (1998) were conducted 23 kg dropped from 0.4 m with an impact energy of 90 J onto the bare surrogate core. Figure 7.17 shows the test setup, high-speed footage synchronised with the dynamometer and potentiometers via a post trigger was captured to better understand the impact. The DAQ recorded all 6 channels at 20,000 Hz: force in x-axis (Fx), force in y-axis (Fy), veritcal force in z-axis (Fz), pendulum potentiometer, surrogate potentiometer, HSV trigger.

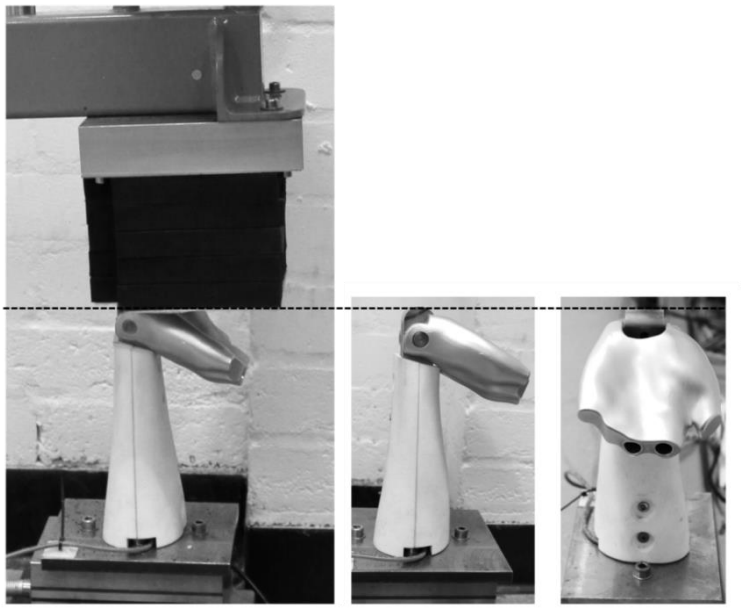

Figure 7.16: Bare hand condition with central core protruding above hand

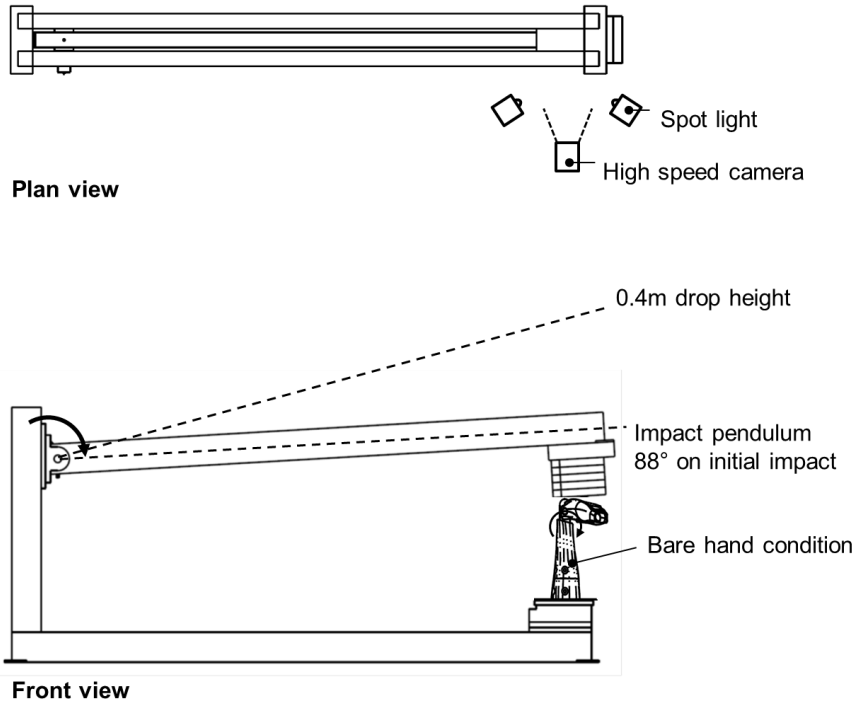

Figure 7.17: Test setup schematic

7.3.1.2 Findings

When compared to the fracture force presented by Greenwald et al. (1998) when impacting a cadaver, the newly developed impact test resulted in a mean measured peak Fz force of 10.2 kN, 3.6 times larger than the fracture force presented by Greenwald et al. (1998) (Figure 7.18). It was expected that the peak force would be higher than the fracture force obtained by Greenwald et al. (1998), as the frangible bone fractured in the Greenwald case removing energy from the system. As no peak force is presented by Greenwald et al. (1998) it is difficult to compare the two setups and determine what the equivalent force for a non-fracture scenario would have been by Greenwald et al. (1998). Human structures provide a complex response to impact scenarios. Whilst there is no muscle activation when a cadaver is impact tested the combination of soft tissue, frangible bones and skin means the system is not rigid.

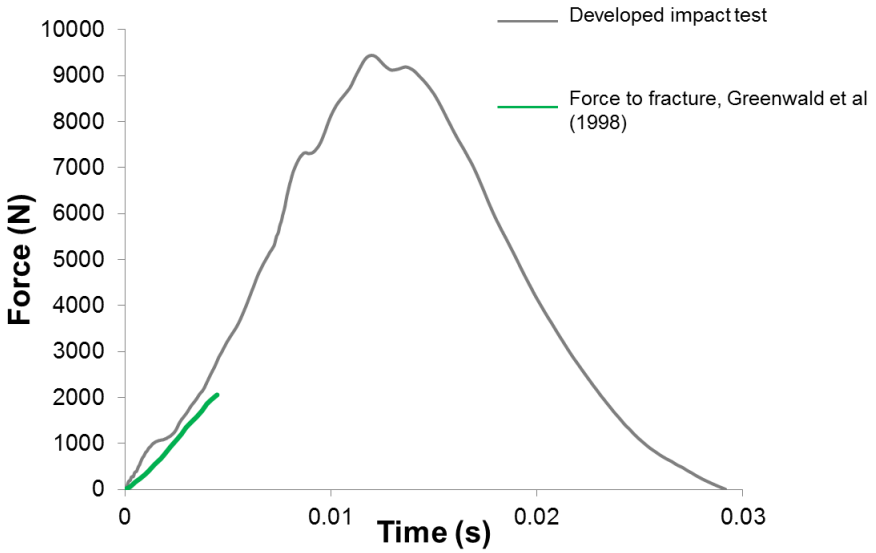

Figure 7.18: Force trace comparison between developed impact test and Greenwald et al (1998) with an inbound energy of 90 J v=2.8m/s, m=23kg

7.3.2 Pilot testing: protected condition

To monitor the interaction between the wrist protector and impactor, pilot tests with the surrogate wearing a protector were conducted. In the protected condition the hand is held at a neutral angle by the wrist protector. In this case, the impactor strikes the hand, extending it before hitting the palm and transferring any remaining force down the forearm. High levels of friction were observed between: the Neoprene block and surrogate on initial contact; and the Neoprene block and wrist protector once the hand had extended. The interactions between the impactor and protector caused the Neoprene to grip the protector and drag the protector, altering its position on the surrogate.

7.3.3 Modifications to the test setup

Based on learnings from these tests a number of modifications to the setup were necessary.

7.3.3.1 Altering the boundary conditions to lower the peak force

As the peak force of the setup for the bare hand case replicating the loading case of Greenwald et al. (1998), is much greater than fracture force, modifications to the boundary conditions were necessary to lower the peak force to a more appropriate level. A lower peak force could be achieved by altering the compliance of the system or lowering the inbound energy through a lower velocity or mass. Decreasing the stiffness of the pendulum or surrogate would have implications for durability and repeatability of the test method, therefore lowering the inbound energy is preferable.

The inbound velocity of 2.8 m/s used in the pilot study is a reasonable approximation for a fall (Hwang and Kim, 2004; Maurel *et al.*, 2013; Thoraval *et al.*, 2013), whereas mass values used by other authors are lower than the 23 kg (33% of male body mass) used by Greenwald et al. (1998) (Schmitt *et al.*, 2012). Due to the mass of the pendulum arm, the lowest mass possible is 15.3 kg, 66% of the mass used by Greenwald et al. (1998). 15.3 kg is equivalent to 20% of 50th percentile male body mass (Alvin R Tilley and Henry Dreyfuss Associates, 2002). A mass of 15.3 kg dropped from the same height as Greenwald et al. (1998) (0.4 m) equates to a 60J inbound energy.

To monitor the influence altering the mass of the pendulum had on the peak force of the system as well as the deformation of the Neoprene, and hence the loading rate of the system, the same inbound energy (60 J) was tested using two different boundary conditions (Table 7.3).

Table 7.3: Overview of pilot test conditions

Test	Inbound Energy (J)	Mass (kg)	Inbound velocity (m/s)
Pilot test 1	90	23.0	2.8
Pilot test 2	60	15.3	2.8
Pilot test 3	60	23.0	2.3

From Figure 7.19 it can be seen that the peak force is lowered to 6.3 kN (225% of fracture force), for a lower impact energy (60 J). The deformation of the Neoprene was found to depend on the rate at which loads were applied, shown by the difference in

gradient for impacts with a lower inbound velocity (Figure 7.19, grey and blue lines vs red). Based on the findings of the pilot tests the mass on the end of the pendulum was reduced to lower the inbound energy and hence peak force, whilst the velocity was kept constant, thus not altering the compliance of the system.

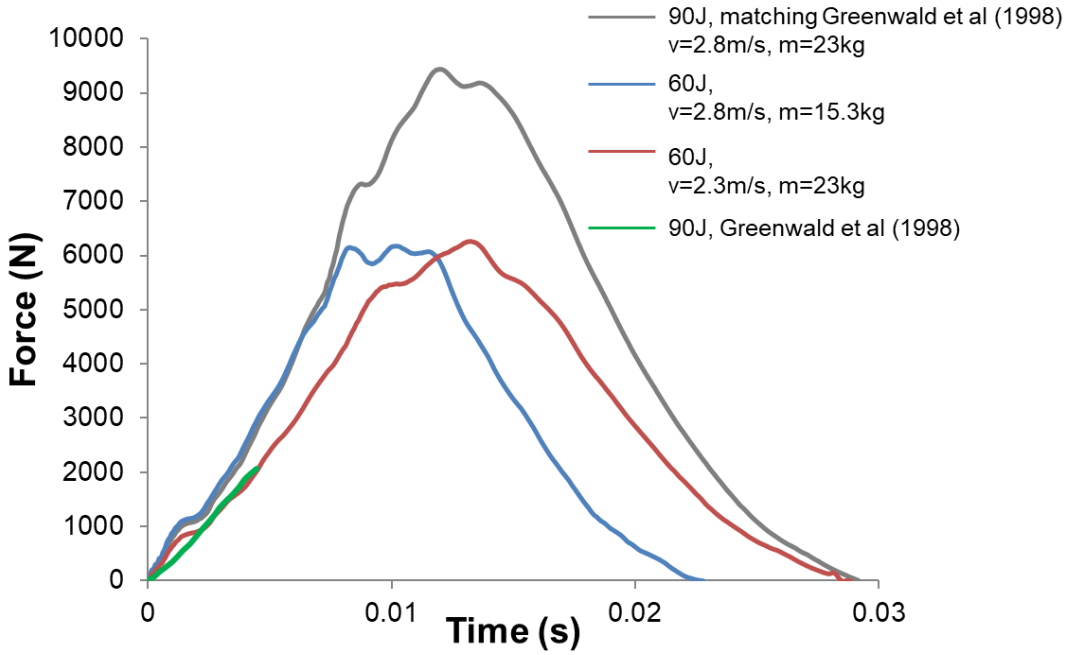

Figure 7.19: Force time trace comparison for different mass and velocity conditions

7.3.3.2 Altering the interaction between impactor and wrist protectors

To lower the coefficient of friction and prevent the impactor gripping the protector in the protected case, a 1 mm thick polypropylene sheet (15 grams) (Direct plastics, UK) was attached to the Neoprene block with double sided tape. The addition of the plastic sheet did not alter the loading behaviour of the system (Figure 7.20 & Figure 7.21). The polypropylene sheet was only used for protected cases to reduce friction as direct contact with the core damaged the polypropylene.

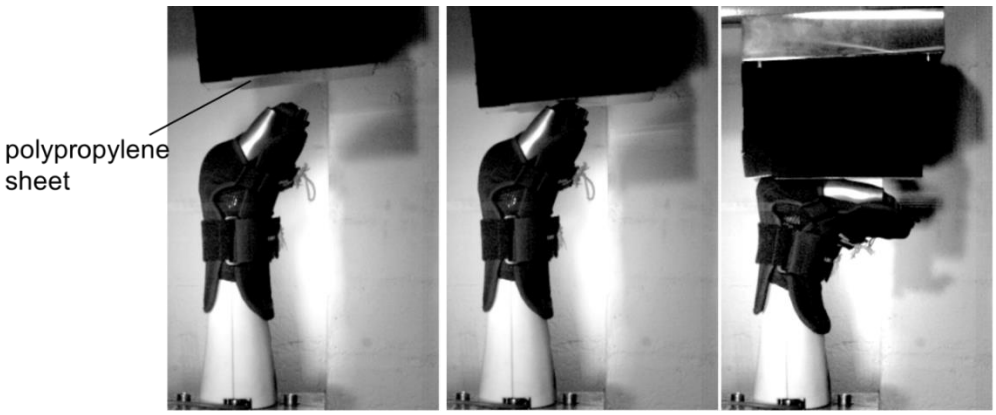

Event	Pre-impact	Start of impact	Impactor in contact with palm
Time (s)	-0.0096	0.000	0.0304

Figure 7.20: Overview of impact for surrogate wearing protector

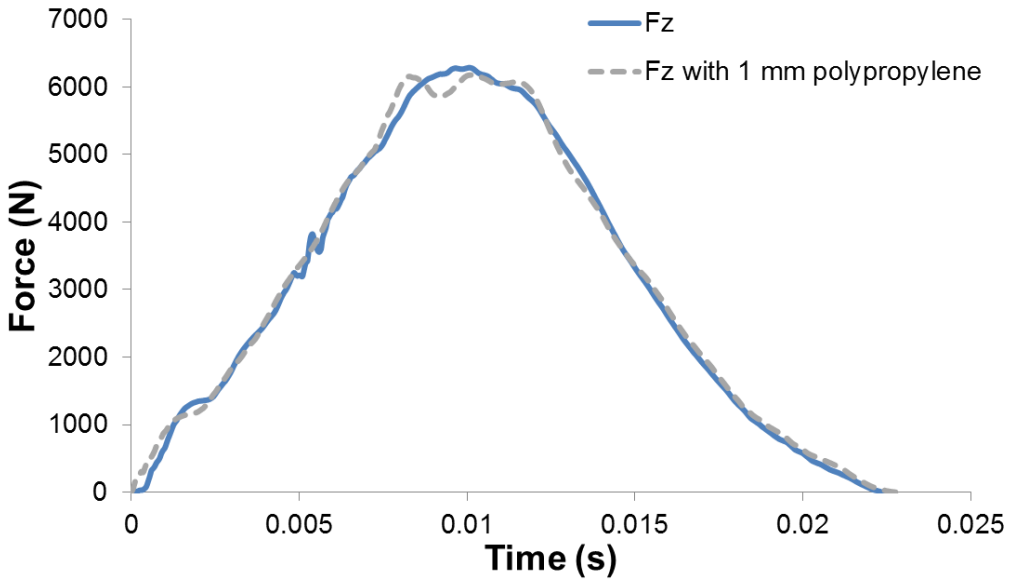

Figure 7.21: Comparison in force time trace between bare Neoprene and Neoprene covered by 1mm polypropylene sheet

7.3.4 Overview of impact

The following section provides an overview of the impact onto the bare surrogate based on pilot tests that were conducted after modifications were made to the boundary conditions. Figure 7.22shows the typical force time trace for an impact onto the unprotected surrogate, and corresponding high-speed images. At a pendulum arm angle of 88° (relative to vertical) the Neoprene block initiates impact with the metal core of the surrogate (b). The Neoprene partially compresses decelerating the pendulum arm, at 0 m/s the pendulum rebounds away from the surrogate (d). In a rigid surrogate system, the force in the x-axis should be 0 N as it is constrained in this direction. However, as can be seen from the x-axis force trace in Figure 7.22 there is movement of the rig and surrogate, this movement was confirmed from the high-speed footage. As the force

measurements in the x-axis are negligible compared to the y and z axis they were excluded from all further analysis.

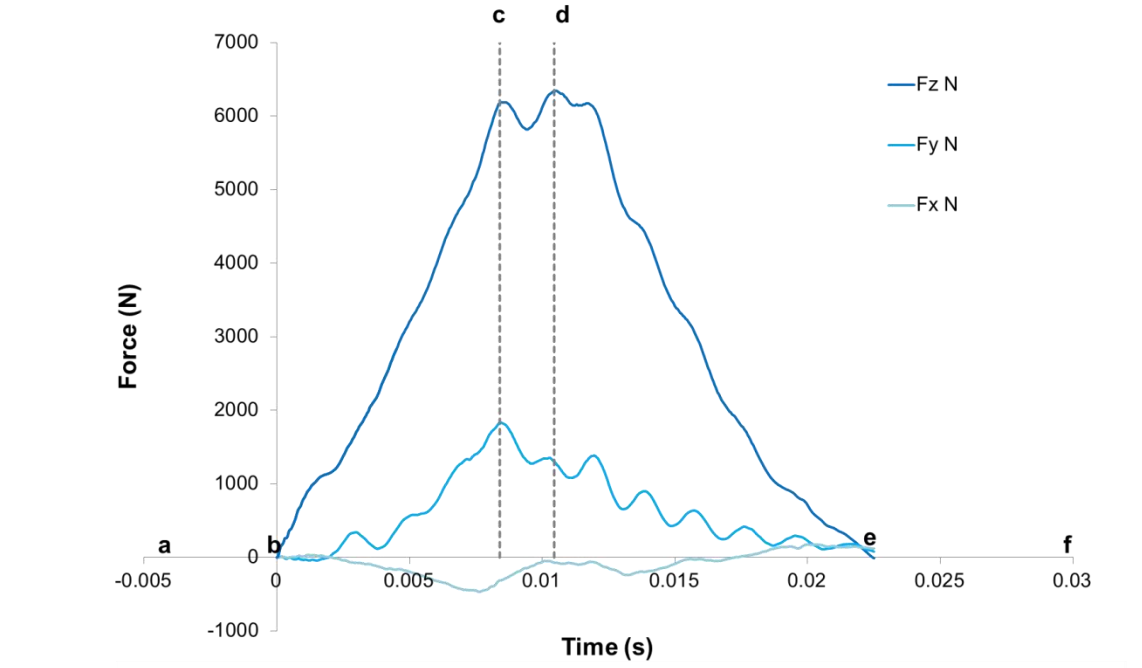

Event	a. Pre- impact	b. Start of impact	c. Peak Fy force	d. Peak Fz force	e. End of impact	f. Post impact
Time	-0.00475	0.00000	0.00840	0.01045	0.02250	0.03130

Figure 7.22: Typical force time curve for an impact onto the surrogate core and corresponding high-speed video frame

7.4 Chapter Summary

This chapter addressed objective three, through the development of a mechanical impact test to replicate injurious snowboard falls and measure the associated forces and hyperextension angles. The developed setup uses a mechanical surrogate and impact pendulum coupled with boundary conditions from a published cadaver study (Greenwald *et al.*, 1998). A 100 mm thick block of Neoprene 50 provides compliance in the system to approximate the loading rate of Greenwald et al. (1998). The mechanical setup based on Greenwald et al. (1998) resulted in a peak force 360% of fracture force for a bare hand impact directly onto the surrogate core. To reduce the peak force to 6.3 kN (225% of fracture force), mass was removed from the rig reducing

it to 15.3 kg with an inbound energy of 60 J. The developed setup is repeatable to within 5% of the peak force in the z and y axis, enabling at least 49 impacts after a brake in trial to be conducted with one Neoprene block. The developed setup facilitates a comparison of products in a repeatable way. In the next chapter, the rig will be used to compare the performance of twelve commercial wrist protectors.

16 Characterising wrist protectors using an impact test

16.1 Introduction

Chapter 7 describes the development of an impact test method to characterise the protective performance of snowboarding wrist protectors. Therefore, the aim of this chapter is to characterise twelve commercially available snowboarding wrist protectors using the developed impact test to determine if it can differentiate between protectors.

16.2 Method

The same twelve protectors tested using the quasi-static test and presented in chapter 6 were tested using the developed impact test. Prior to testing the Neoprene block was precondition at 18°C for 24 hours. All testing was completed within 9 hours at a temperature of 18±1°C. All protectors were strapped to a consistent tightness, with a 2 kg mass using the method described in chapter 5. All protectors underwent two preconditioning impacts on a different Neoprene block from testing. Before protectors were impacted, one drop was conducted to condition the Neoprene. A further three bare hand trials were conducted to establish an unprotected condition peak force baseline.

Each protector was impacted three times with the same Neoprene block, the testing order was randomised for each repeat (Table 16.1). In-between each testing bout three bare hand trials were conducted to monitor Neoprene degradation and check that the instrumentation had not been damaged by checking that bare hand results were as expected. After the third bout of impact testing a further three bare hand trials were conducted, resulting in 49 impacts overall. The surrogate wearing the protector was manually set to a start angle of ~30°, prior to each impact to ensure the inbound velocity was consistent across products (Figure 16.1). The fingers on protective gloves were pinned back using dressmaker pins, so as not to interfere with the impact. High speed footage was collected for each impact whilst the DAQ recorded all 6 channels at 20,000 Hz: Fx, Fy, Fz, pendulum potentiometer, surrogate potentiometer, HSV trigger.

Table 16.1: Randomised testing order for each protector

Impact test bout 1 - protector order	**Impact test bout 2 - protector order**	**Impact test bout 3 - protector order**
Dainese (P1)	Snowlife glove	Flexmeter
K-tech glove (G1)	Dainese	Dakine
Obscure glove (G2)	Burton	Flexmeter glove
Snowlife glove (G3)	Snowlife	Oxelo
Dakine (P2)	Arva	Arva
Flexmeter glove (G4)	Reusch	Reusch
Arva (P3)	Oxelo	Snowlife glove
Reusch (P4)	Flexmeter glove	K-tech glove
Flexmeter (P5)	Flexmeter	Obscure glove
Snowlife (P6)	Obscure	Dainese
Burton (P7)	K-tech glove	Snowlife
Oxelo (P8)	Dakine	Burton

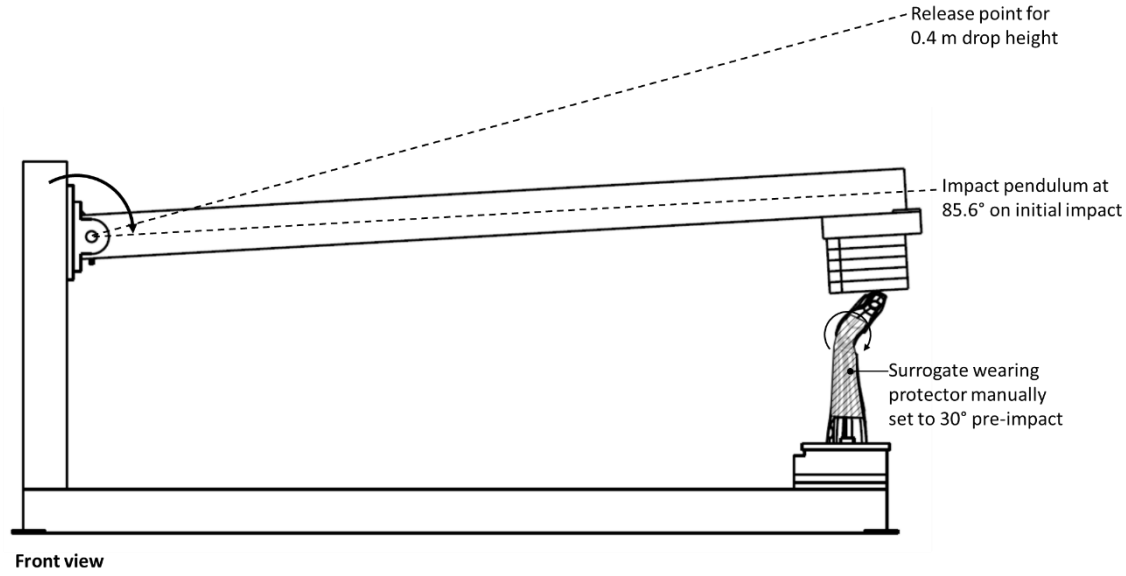

Figure 16.1: Test setup schematic

16.2.1 Data analysis

All data was loaded into spreadsheets (Microsoft Excel 2010, USA) for post processing and analysis. Force and angular displacement data was converted from voltage into SI units using pre-determined calibration factors. The force offset was removed by determining the average force during the 0.5 seconds (10,000 data points) prior to impact and subtracting it from the raw value. The resultant YZ force was calculated using vector summation based on the y and z components. A moving average filter with a window size of 31 selected empirically was used to remove unwanted noise from the pendulum position data.

To determine the start of trial, start of impact, end of impact and end of trial, numerous steps were conducted (Figure 16.2). The start of trial was defined as the point at which the pendulum started to rotate, when pendulum position > mean pendulum position prior to release +10 SD. After the trial had started different approaches were used to determine the start of impact depending on whether it was a protected or bare hand condition. For protected conditions, the start of the impact was determined based on the wrist surrogate position, wrist angle > mean wrist angle prior to impact + 10 SD. For unprotected cases Fz was used rather than wrist rotation, as the hand is already hyperextended in these situations. The start of impact for bare hand conditions was the point at which Fz > Mean Fz prior to impact + 10 SD. The end of the impact was defined as the first instance at which the force Fz < 0 N after the peak force reading. After impact the pendulum bounces away from the surrogate, there are several rebound impacts before the pendulum finally comes to rest on top of the surrogate. Therefore, the end of the trial is defined as the highest point the pendulum rebounds to after the first impact, all other rebound impacts are ignored.

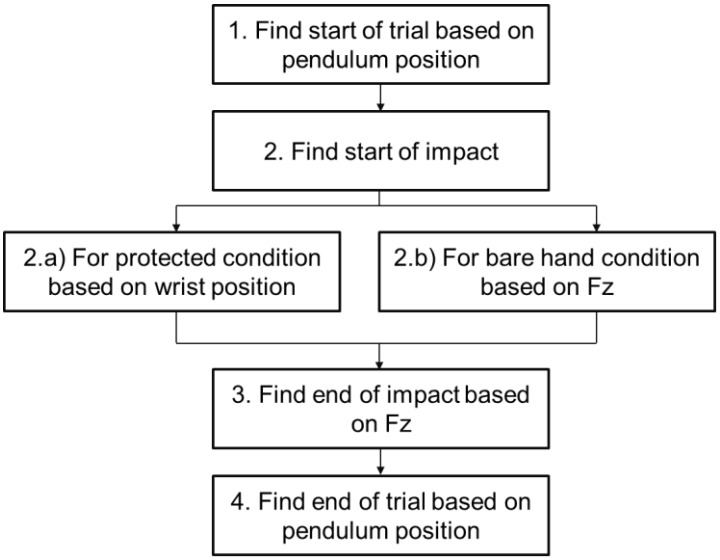

Figure 16.2: Steps required to identify key points within test trial

Peak impact force of the resultant YZ and the corresponding time to peak were subsequently identified and recorded. To determine percentage energy absorbed by the protector, the ratio of impactor drop height and rebound height was used, assuming frictional forces are negligible (equation 1).

$$percentage\ energy\ absorbed = \frac{rebound\ height}{start\ height} x100. \quad (1)$$

For the bare hand case there is 45% energy loss in the system, this energy loss is likely due to energy being lost through friction between the impactor and the surrogate, Neoprene compression, heat and movement in the rig and surrogate. Since energy losses occur in the system during the bare hand case, energy absorbed for all products was calculated relative to the bare hand case, by subtracting 45% from the value determined using equation 1.

Comparisons between protectors were made based on peak vertical force, time to peak force, energy absorption and surrogate angle. Correlations were used to determine if relationships between three protective characteristics exist. To monitor protector degradation over repeat impacts the peak vertical force for all three impacts was studied for each protector.

Correlations were also used to determine if relationships between the protective characteristics: peak vertical force, time to peak force, energy absorption exist. Spearman's correlation coefficient was used to determine the strength of relationship between the protective characteristics. The data was analysed with SPSS statistical software for analysis (IBM SPSS Statistics for Windows, USA). The significance level was set at $p<0.05$ for all correlation outputs. The magnitudes of the correlations were interpreted using Cohen's thresholds where:<0.1, is trivial; 0.1–0.3 is small; 0.3–0.5 is moderate; and>0.5 is large (Cohen, 1988).

Like chapter 6 two cases studies were conducted to monitor whether the test detected differences between products utilising different design approaches. The same products as chapter 6 were used, Reusch (P4) and Burton (P7); Snowlife glove (G3) and the Snowlife stand-alone protector (P6).

16.3 Overview of impact

To better understand the impact scenario the following section will provide an overview of the impact before discussing the results of the twelve tested protectors. Figure 16.3 shows a typical overview of the collected data for the Flexmeter protector, this plot is typical of all the tested products. The excess data is shown both prior to the pendulum release (point 1) and after the impact of interest (points 5 to 8). Two rebound impacts

occur (points 6 and 7) after the incident of interest before the pendulum comes to rest on top of the surrogate (point 8).

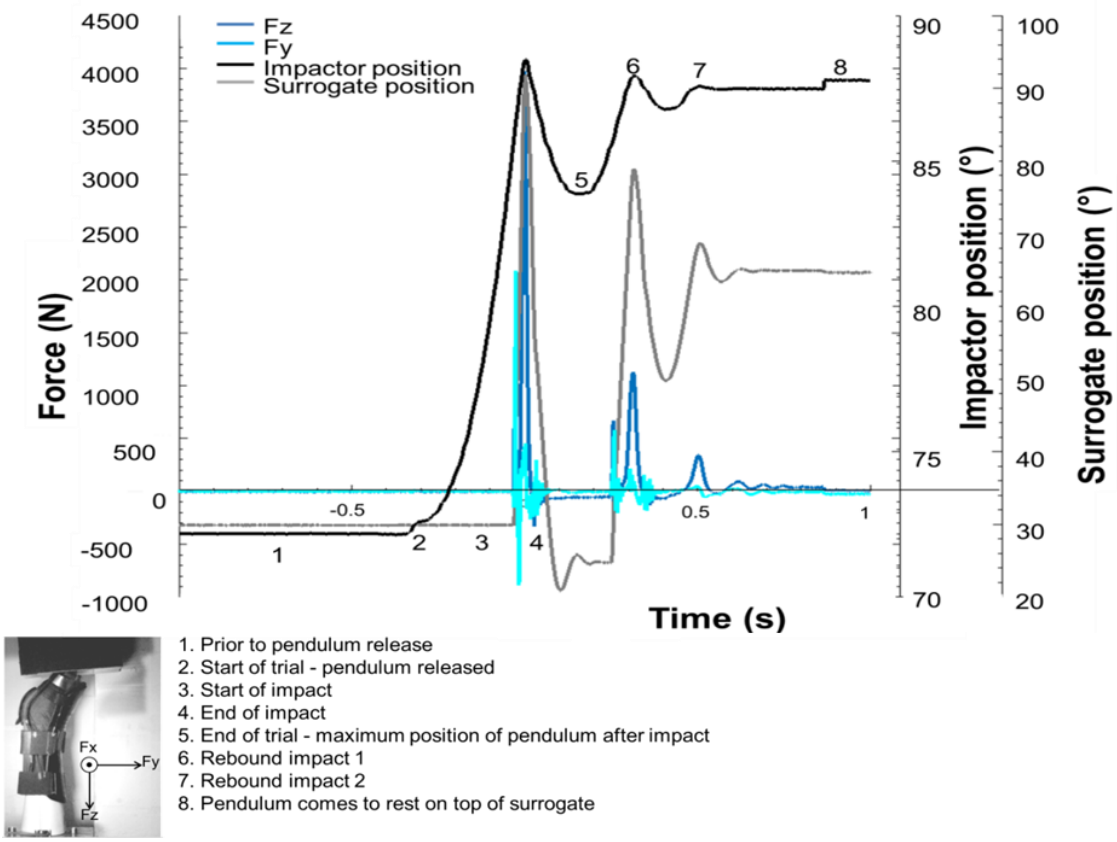

Figure 16.3: Overview of collected data with peak force aligned to 0 seconds for Flexmeter protector

Figure 16.4 shows the data clipped to the impact event with respect to time and surrogate position. From looking at the measurement data in conjunction with the high-speed video footage it is possible to identify key events during the impact (Figure 16.4). Initially there is a spike in the force in the z axis (b) when the impactor meets the surrogate, the force then becomes dominate in the (positive) y-axis (c) as the hand starts to rotate. The direction of the force in the y-axis changes (d-h), as the hand continues to rotate backwards at a relatively constant rate and the force is consistently increasing in the z-axis.

The surrogate hand then rotates backwards beyond 88.2° (e); the point at which the central core is protruding above the palm of the hand, so all remaining force is directed straight down the arm. As the impactor starts to decelerate a peak force in the z-axis occurs (f) just before the surrogate hand (g) reaches its maximum displacement. The impactor comes to rest at its maximum displacement (i) before rebounding away from the surrogate, enabling the hand to spring back towards vertical. The force in the z-axis returns to zero (j) once the impactor is no longer in contact with the surrogate.

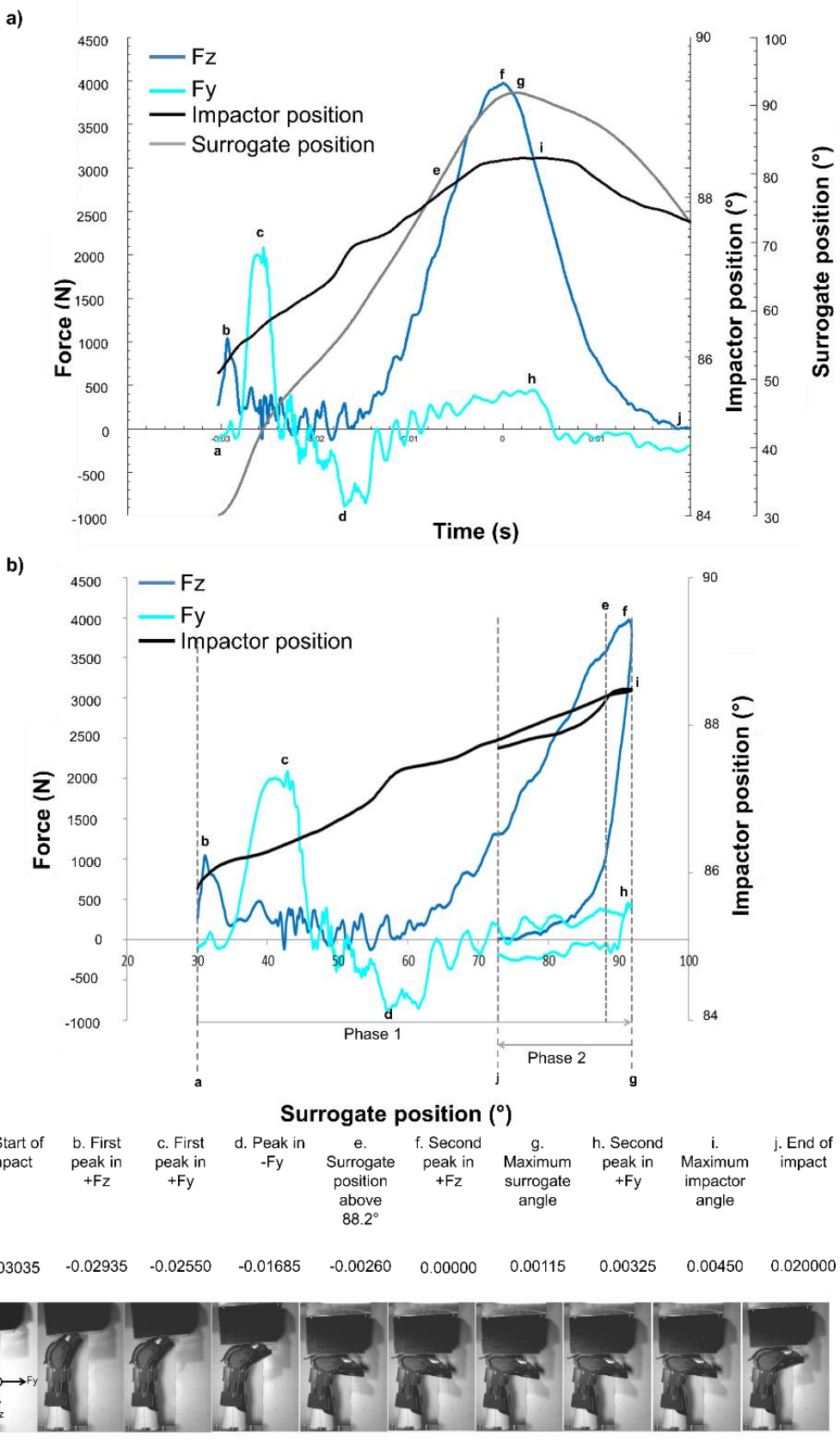

Phase 1: From start of impact to peak force
Phase 2: From peak force to end of impact

Figure 16.4: Overview of impact case for Flexmeter protector with corresponding high-speed video footage for key events a) with respect to time b) with respect to surrogate hand position

Figure 16.5 shows differences between the unprotected surrogate and a sample protected case with the Flexmeter stand-alone protector. The peak force in the z-axis is lower with an elongated time to peak. For 83% of tested protectors the peak force in the y-axis was higher than for the bare hand condition. At the point of impact, the resultant YZ force is almost vertical (1° from vertical) for the barehand case, whereas in the protected case it is acting 64° from vertical in the negative y direction as shown below.

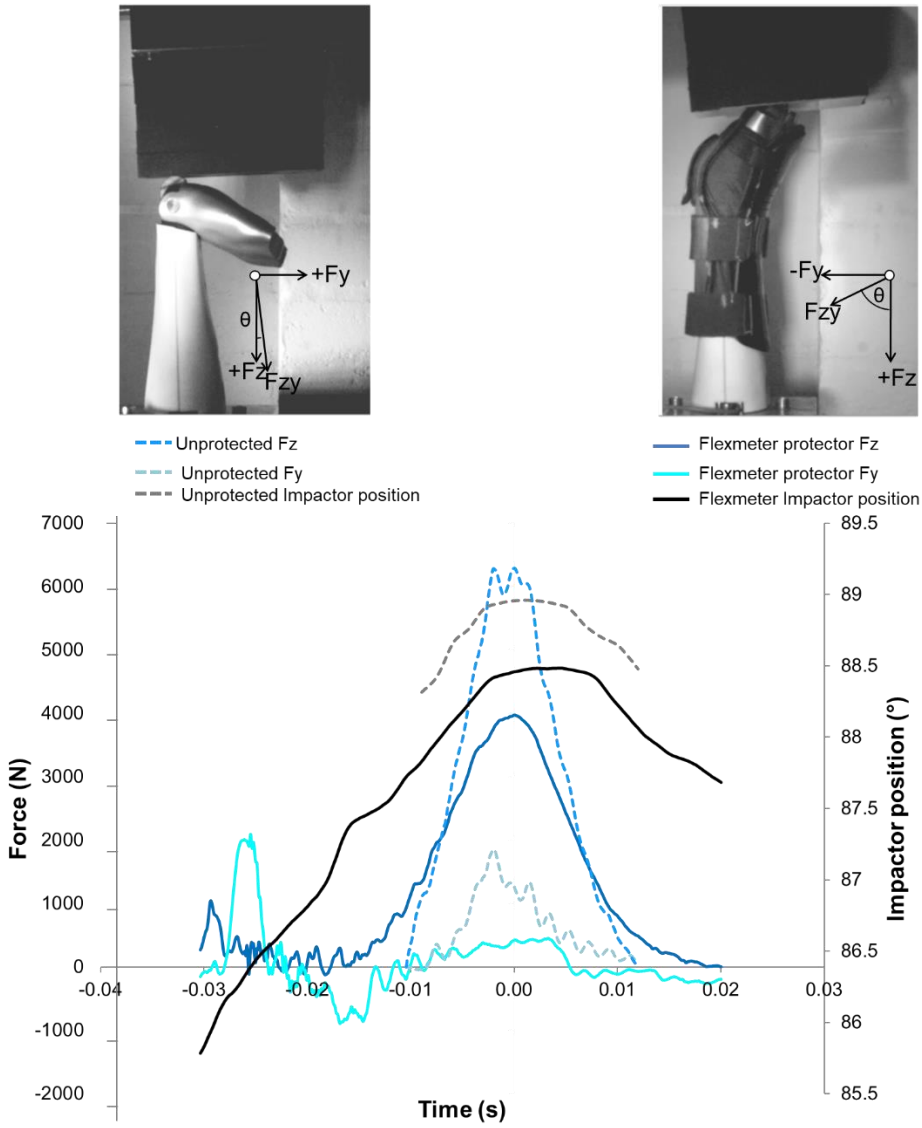

Figure 16.5: Comparison between unprotected and protected case aligned at peak Fz at 0 seconds, resultant YZ angle θ = 1° for unprotected case and resultant angle θ = 64° for protected case

From the high-speed footage, movement of the surrogate arm can be seen in the lateral direction (y-axis) for both protected and unprotected cases. For all protected cases the force direction fluctuates in the y-axis. Based on known dimensions the lateral surrogate displacement was determined using the high-speed footage for two representative cases. This lateral movement can be seen in Figure 16.6 for the unprotected condition, the

movement can be seen based on the position of the surrogate joint centre relative to the central axis. For the unprotected condition the maximum surrogate displacement in the -y direction was 2.88 mm (Figure 16.6b) and 0.96 mm in the + y direction (Figure 16.6c). For the Burton protector a maximum displacement of 1.92 mm was measured in the -y direction and 4.80 mm in the + y direction (not pictured).

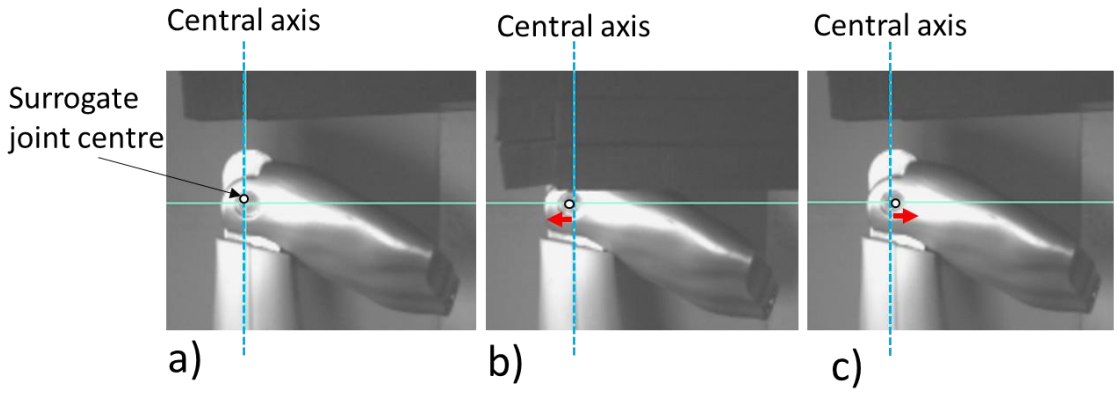

Figure 16.6: Surrogate movement in y-direction based on digitised high-speed footage relative to the central axis a) central position at the start of trial b) lateral movement of -2.88mm from the central axis during the impact c) lateral movement of +0.96mm from the central axis post impact

16.4 Results

16.4.1 Protector comparison

16.4.1.1 Impact Attenuation

A comparison for all twelve tested protectors based on peak vertical force and time to peak force for the first impact is shown in Figure 16.7. All twelve protectors lowered the peak force by 1.5 kN or more and elongated the time to peak by at least 21 ms compared to the bare hand surrogate; however none of them lowered the force below the 2802 N fracture force (Greenwald *et al.*, 1998). The implication here is that none of the guards would have prevented a wrist fracture for the chosen representative loading condition.

From Figure 16.7 it can be seen that there is a general trend that products resulting in a lower peak force have a longer time to peak force, with the exception of two clear outliers the Dainese protector (P1) and the Obscure glove (G2). When considering all tested products there is no significant correlation between peak Fz force and time to peak (Spearman's $\rho = 0.03$, $p=0.92$). Whereas when P1 and G2 are excluded there is a

moderate not statistically significant correlation between peak Fz force and time to peak (Spearman's ρ = -0.5, p=0.15).

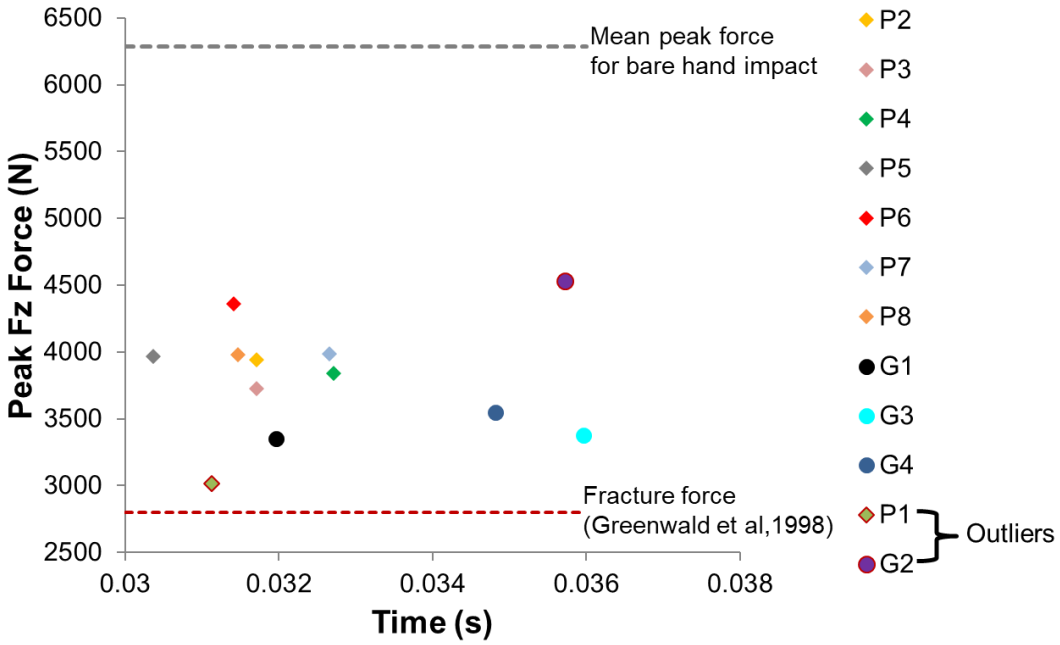

Figure 16.7: Protector comparison based on time to peak Fz force and peak Fz force, diamond markers indicate stand-alone protectors and circles indicate protective gloves, outliers P1 and G2 shown by red border.

The dorsal lock plate on the Dainese protector snapped during impact (Figure 16.8), with the energy absorbed during the product's deformation likely to be the cause of the Dainese having the lowest peak force of all tested protectors over a shorter time frame. When comparing the force time trace for four tested protective gloves, the Obscure has a longer initial ramp in for force in the z axis than the other 3 gloves (Figure 16.9).

Figure 16.8: Damaged Dainese protector

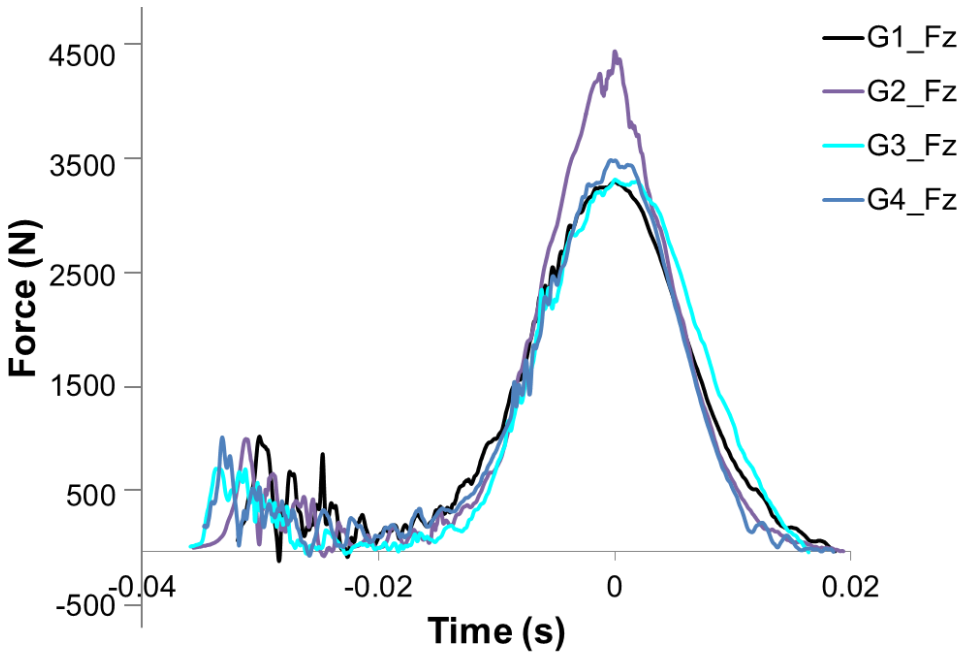

Figure 16.9: Fz force time trace comparison for tested protective gloves

16.4.1.2 Energy Absorption

For protected cases the energy absorbed ranges between 17-37% relative to the bare hand case. Figure 16.10 shows the relationship between peak Fz and energy absorption. A strong statistically significant correlation exists between peak force and percentage energy absorbed (Spearman's $\rho = -0.72$, $p=0.01$). As more energy has been absorbed by the protector in lowering the peak force, the impactor does not rebound as high.

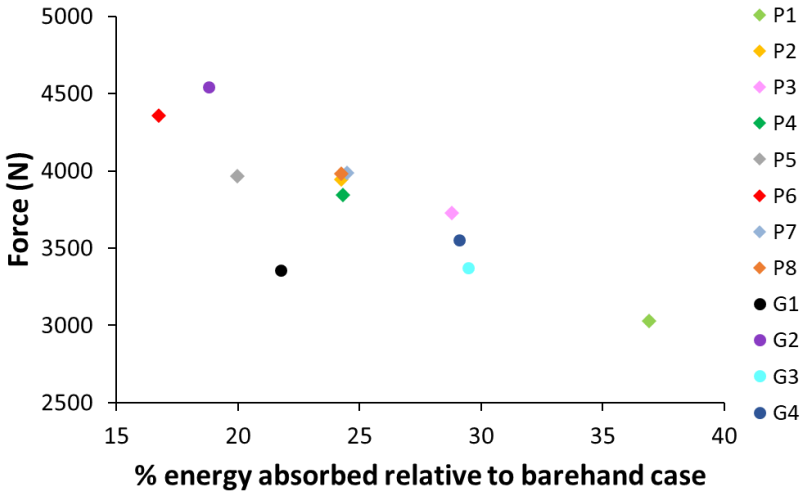

Figure 16.10: Protector comparison showing relationship between peak force and energy absorbed

16.4.1.3 Protector degradation

The vertical peak force over all three impacts per protector provides insight on protector degradation. If products were degrading, the peak force would increase with each impact. For 72% of the tested protectors the transmitted vertical force was lowest for the first impact (Figure 16.11). Whilst the peak vertical force was highest during the third impact for 64% of tested protectors: P2, P4, P6, P7, P8, G3, G4. The largest difference is seen for P2 (Dakine protector), in this case the peak Fz force increases by 22% between the first two impacts and the third impact.

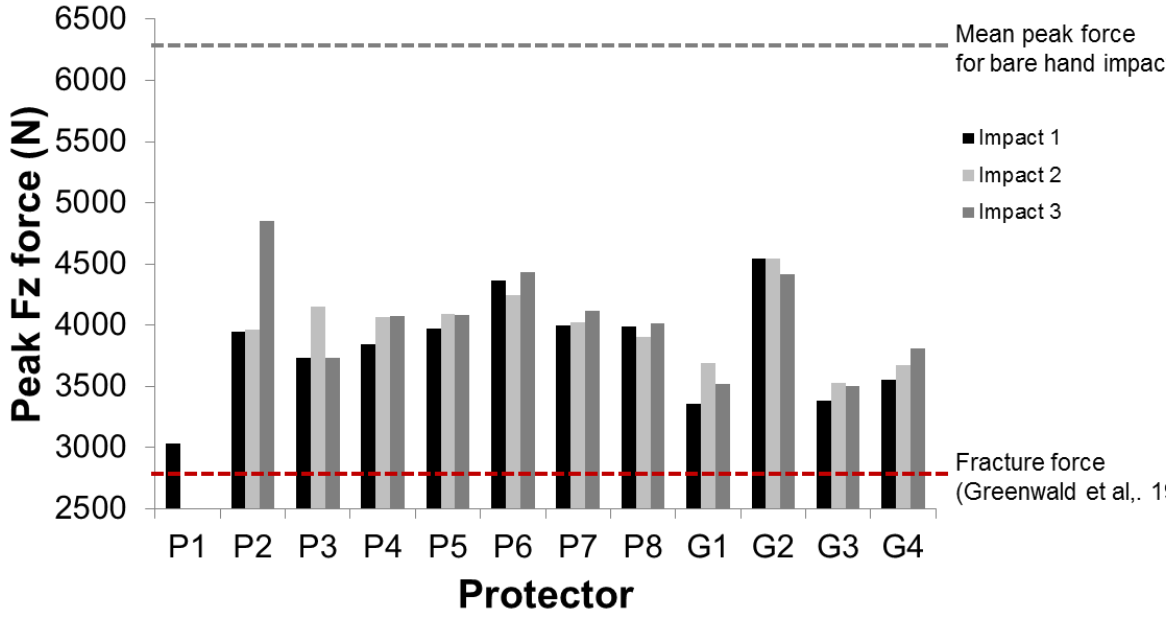

Figure 16.11: Peak Fz force for multiple impacts for each protector

16.5 Case studies

16.5.1.1 Comparison between two stand-alone protectors with similar designs

The Reusch (P4) and Burton (P7) are stand-alone protectors, similar in both design and overall dimensions (Figure 16.12). As can be seen from Figure 16.13 both protectors result in a similar vertical peak force (3995 N and 3847 N for the Burton and Reusch, respectively with a similar time to peak vertical force (difference = 0.05 ms). In this case the test has performed as expected with products of similar designs resulting in a similar performance. How the products reduce the peak Fz force appears to be different, Figure 16.13b shows there is a difference in force with respect to surrogate displacement between the protectors. The Burton protector has a two-part loading curve; it requires a relatively low force to displace the surrogate until ~85°, whereas after this

point the force increases exponentially. However, the rate of force required to displace the surrogate when wearing the Reusch protector is quasi-linear from ~65°. The first peak in +Fy is 347 N higher for the Burton protector, whilst the surrogate displaces 4° more when wearing the Reusch protector. Whilst the test is able to distinguish such differences, further research is required to understand the design mechanism behind the difference.

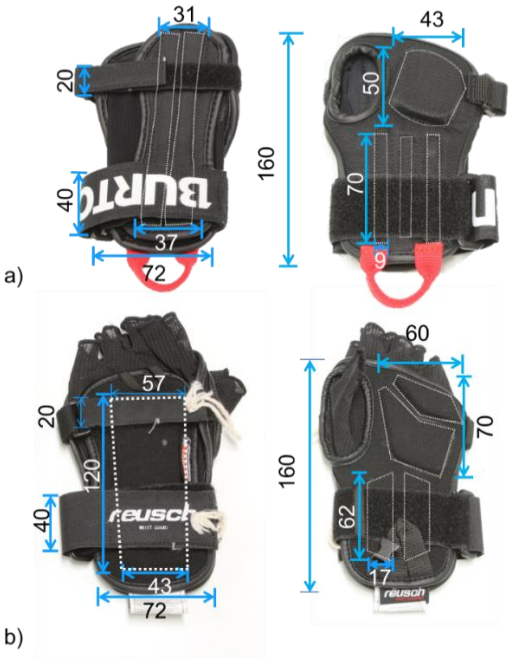

c)

Thicknesses (mm)	Burton Protector (P7)	Reusch Protector (P4)
Palmar splint	5	4
Palmar pad	14	13
Dorsal splint	7	7

Figure 16.12: Comparison between a) Burton (P7) and b) Reusch (P4) protectors all measurements in mm c) thickness measurements

Table 16.2: Comparison between Burton (P7) and Reusch (P4) protectors

	Peak Force (N)		Time to peak force (ms)		Maximum surrogate angle (°)
	Fz	Fy	Fz	Fy	
Burton (P7)	3995	2207	32.35	5.25	97
Reusch (P4)	3847	1860	32.70	4.35	101

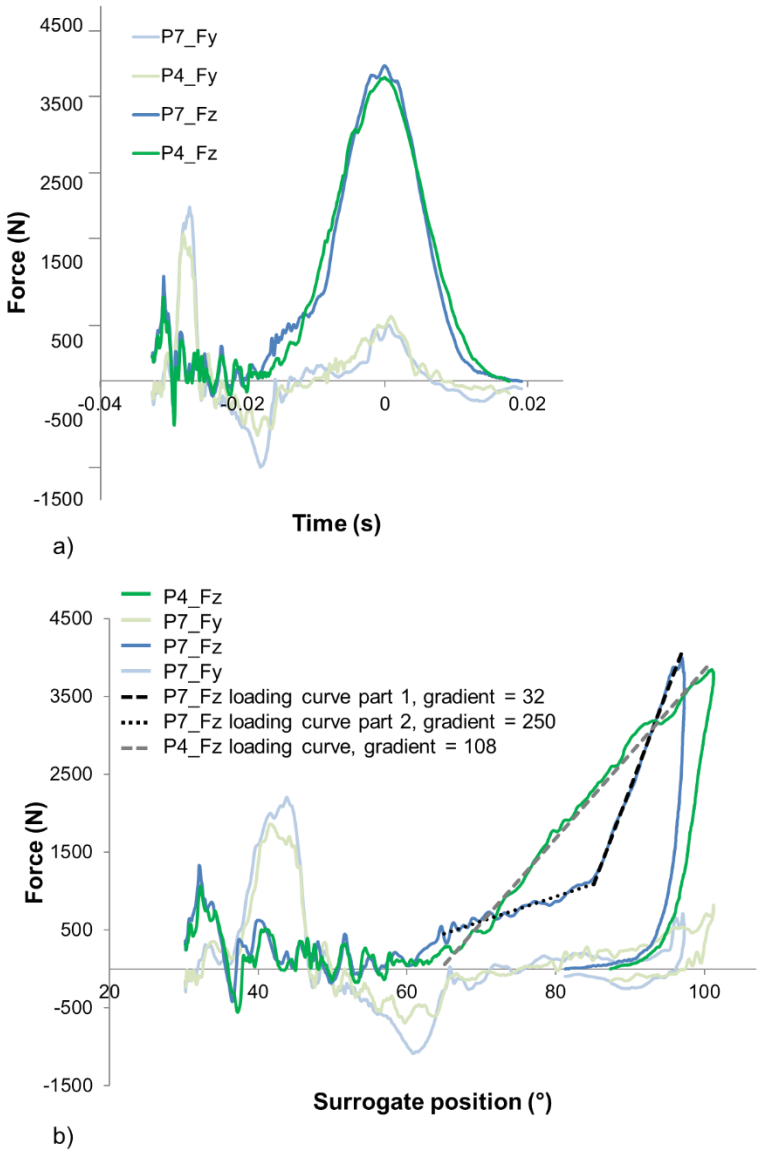

Figure 16.13: Comparison between Burton (P7) and Reusch (P4) protectors a) force over time peak force aligned at 0s for impact test b) force with respect to surrogate position for impact test

16.5.1.2 Comparison between glove and stand-alone protector from the same brand using different design approaches

Despite being made by the same manufacturer the Snowlife glove (G3) and the Snowlife stand-alone protector (P6) (Figure 16.14) utilise different design elements and the test has detected that the products perform differently. Both protectors have dorsal splints of similar dimensions; whilst the glove includes additional dorsal support from the strap. The Snowlife stand-alone protector includes a palmar splint whereas the glove does not. The palmar pad in the stand-alone protector is thicker than the glove, but the glove is larger overall with more material.

c)

Thicknesses (mm)	Snowlife Glove (G3)	Snowlife Protector (P6)
Palmar splint		5
Palmar pad	5	20
Dorsal splint	2	5
Dorsal strap	5	

Figure 16.14: Comparison between a) Snowlife Glove (G3) and b) Snowlife protector (P6) all measurements in mm c) thickness measurements

Palmar pads have typically been associated with reducing the impact force (Maurel *et al.*, 2013), however in spite of the stand-alone protector having a thicker palmar pad the glove results in a lower peak Fz force and has a longer time to peak (3381 N over 35.95 ms vs 4364 N over 30.14 ms for the glove and stand-alone, respectively) (Figure 16.15a and Table 8.3). Figure 16.15b shows there is a difference in force surrogate

displacement gradient between the protectors. The stand-alone Snowlife protector requires a larger force to displace the surrogate between 60-90° in contrast to the Snowlife glove which has a less steep gradient and a larger maximum surrogate angle. Whilst a portion of the difference between peak Fz force and time to peak is likely attributed to the additional material in the glove, given the magnitude of the difference (983 N) other design attributes such as dorsal splint thickness and material are also likely to play a role.

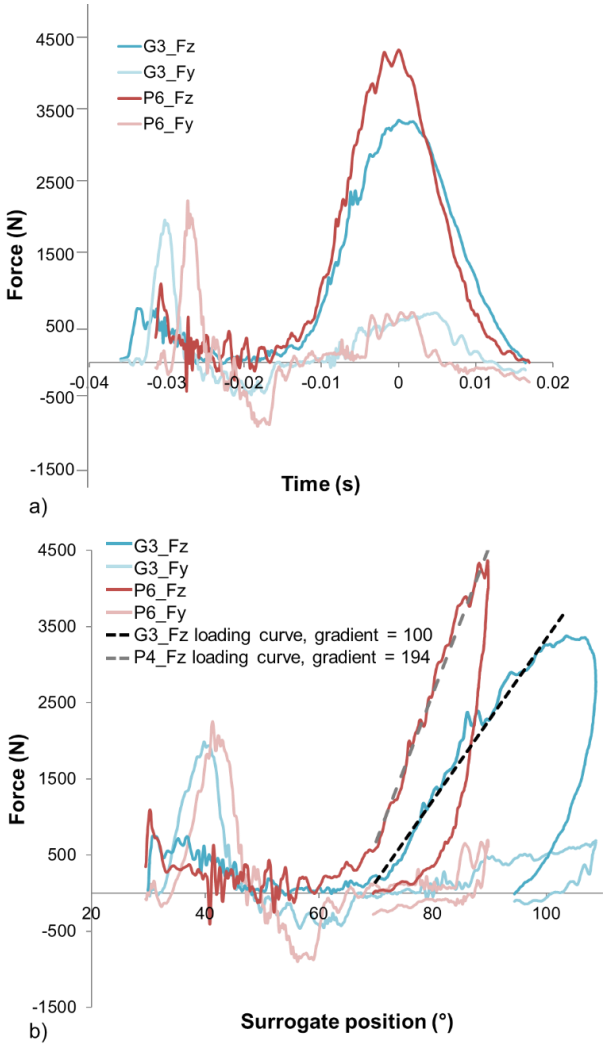

Figure 16.15: Comparison betweem Snowlife glove (G3) and Snowlife protector (P6) a) force over time peak force aligned at 0s for impact test b) force with respect to surrogate position for impact test

Table 16.3: Comparison between Snowlifeglove (G3) and stand-alone Snowlife protector (P6)

	Peak Force (N)		Time to peak force (ms)		Maximum surrogate angle (°)
	Fz	Fy	Fz	Fy	
Snowlife glove (G3)	3381	1987	35.95	5.70	109
Snowlife protector (P6)	4364	2258	30.14	4.15	90

16.6 Discussion

Through testing twelve different protectors using the impact setup it has been shown that the setup is able to i) distinguish differences between the bare hand case and unprotected conditions, ii) distinguish differences in protective characteristics between different wrist protector designs.

Differences in force distribution were noted when comparing the bare hand case to protected cases. A lower peak force was observed in the z-axis for all tested protectors, whereas a higher peak force was observed in the y-axis for the majority of protected cases. This difference in Fy is due to differences in test setup. In the bare hand condition, the hand is already at maximum extension when impacted, whereas in the protected condition the wrist protector provides a level of resistance to the impactor resulting in a higher force in the y-axis. For all protected cases the force direction was found to fluctuate in the y-axis due to lateral movement of the surrogate. This lateral movement is likely the result of a torque applied to the surrogate during the interaction between the impactor and surrogate; as the pendulum contacts the top of the surrogate at an angle before continuing its rotational trajectory.

Despite the limitations of the setup, such as the high stiffness of the system and lateral movement of the surrogate during impact, the setup can differentiate between products. All twelve products lowered the transferred peak Fz force by 28-52% whilst elongating the time to peak vertical force, however none of the products lowered the force below the 2802 N fracture force reported by Greenwald et al. (1998). This is a similar finding to previous studies, in which protectors were shown to reduce the force but still result in fractures (Greenwald et al. 1998; McGrady, Hoepfner et al. 2001; Giacobetti et al. 1997). The finding that protectors do not lower the peak force below reported fracture loads may explain why wrist injuries still occur even when wearing a protector (Cheng

et al., 1995; Idzikowski, Janes and Abbott, 2000). It is probable that under different loading conditions products could lower the force below fracture threshold, so for lower energy falls at a lower speed or involving a lower mass, or a lower system stiffness these products may prevent injury. Future studies are suggested to determine the effect of impact energy on peak force and to identify the inbound energy at which protectors no longer reduce the transmitted force below fracture force.

Two outliers were observed when studying the spread of the data in Figure 16.7, the Dainese stand-alone protector and the Obscure glove. The Dainese protector resulted in the lowest vertical force over the second shortest time to peak of all tested products (3029 N over 32.2 ms). Whereas, the Obscure glove elongates the time to peak force, but still results in the highest peak force of the twelve products (4655 N over 38.5 ms). The low peak force measured for the Dainese is likely a result of the products dorsal splint lock plate snapping during impact (Figure 16.8). It could be argued that the product played its part by acting in a similar way as helmets or car crumple zones, which are only designed for one impact. Although multiple models of this protector would need to be tested to confirm whether the protector damaging under load is a characteristic of the product, or a random occurrence based on how the lock plate was positioned relative to the surrogate.

It is not clear why despite having the second longest time to peak the Obscure glove has the highest peak force. The Obscure is the only glove that does not include a dorsal splint which may explain the higher peak force, but the reasons for the longer time to peak are less clear. From the force trace a longer initial ramp in for force in the z axis can be seen for the Obscure glove compared to the other tested gloves (Figure 16.9). This increased time to generate force in Fz, could be due to the interaction between the impactor and surface of the gloves. The texture of the Obscure glove appears to be smoother than the other three gloves, so it is possible the impactor is causing the glove to slide during the impact elongating the time to peak, but this is not clear from the current high-speed footage.

Based on the tested products it appears that protective gloves provide more effective impact attenuation than stand-alone protectors, by elongating the time to peak force (Figure 16.7). The protective gloves tend to result in a lower peak in the vertical axis (G1, G3, and G4) and a longer time to peak than the stand-alone protectors (P2, P3, P5,

P6 and P8). It is not clear if this difference in behaviour between gloves and stand-alone protectors is unique to the test setup due to the interaction between the glove and the impactor, or if gloves do in fact provide superior protective performance. The elongated time to peak by gloves, may be due to them having more material and a textured surface on and around the palm enhancing grip, this could be gripping on the polypropylene surface of the impactor and elongating the time to peak. The pinned back fingers may also be bunching up around the impact point elongating the impact.

A difference in protective performance between stand-alone protectors and protectors integrated into gloves was not observed in a previous study Schmitt, Michel, & Staudigl, (2012), however their test setup used a linear drop test onto the palm and the EN 14120 bending test so the test setup is not directly comparable. To confirm whether this difference in behaviour between stand-alone protectors and protective gloves is meaningful additional testing is necessary. Future work testing a larger range of protective gloves as well as testing stand-alone protectors in conjunction with a glove is recommended.

For the bare hand case there is a 45% energy loss in the system, this energy loss is likely due to friction between the impactor and the surrogate, Neoprene compression, heat and movement in the rig and surrogate. Relative to the bare hand case 17-37% of the inbound energy was absorbed by the protectors (Figure 16.10). This energy is absorbed in various ways: tensile failure of textiles, compression of palmar padding, bending of splints and displacement of hand. With the exception of the Dainese protector, no visual damage was seen to the tested protectors with repeated impacts. However, the increase in peak vertical force with each impact suggests that changes may have occurred in the material properties (Figure 16.11). This finding suggests that snowboarders should replace their wrist protectors after a bad fall regardless of whether there is visual damage to the product, a similar informal rule exists about bike helmets (Wells, 2016).

The developed impact test method enables for comparison of protectors with different design approaches. This was done using case studies comparing two different products; it was found that products with similar dimensions (P4 and P7) performed comparable in terms of peak vertical force and time to peak vertical force. However, they exhibited different impact dynamics in terms of surrogate displacement. When comparing a stand-alone protector and the protective glove using different design elements (G3 and P6)

different results were measured. Future work should use the developed test and consider factors such as material; splint and palmar pad dimensions; splint and palmar pad construction and strapping design to understand the influence of protector design on performance. Systematically changing one variable at a time, would allow for a thorough analysis of the effects of protector design on performance, to inform the design of future products. Existing products could be adapted, and protective elements systematically modified to test a range of dimensions and materials. Testing could be done mechanically using the developed test set-ups presented here or through finite element analysis. Previous research has sought to use neural networks to understand the influence of football design parameters on traction performance (Bob Kirk, Matt Carré, Stephen Haake, 2006), providing a sufficient mechanical data is collected this approach could support the design of optimised wrist protection.

16.7 Chapter Summary

This chapter demonstrates that the impact test developed in Chapter 7 can characterise the protective performance of snowboarding wrist protectors and effectively differentiate between products. This chapter addresses the fourth of the project's objectives: to compare the protective characteristics of a range of wrist protectors using the developed methods. The test setup has been shown to detect differences in force transfer, energy absorption and wrist extension angle energy absorption between commercially available products. The results show that protectors absorb and dissipate inbound energy during the impact to lower the transferred Fz force. However, none of the tested products effectively lower the force below fracture threshold. Future research is recommended to: i) investigate protective performance under different inbound parameters, ii) explore the differences between stand-alone protectors and those integrated into gloves and iii) identify the influence of protector design on performance to optimise product design to enhance safety.

9 Discussion and Future work

Chapters 3-8 have presented the development and validation of two new test methods to evaluate the protective characteristics of snowboarding wrist protectors. This chapter compares the results from the two test setups, discusses the limitations of the developed test setups and highlights potential areas for future work.

9.1 Comparison in measured performance between quasi-static test and impact test

To determine whether a relationship between the protective characteristics: peak Fz force and time to peak measured using the impact test and protector stiffness measured using the quasi-static test exists correlation coefficients were used. Given that, in Chapter 6 it was found that there is a difference in rotational stiffness between 35-55° and 55-80°, both groups were looked at independently. Spearman's correlation coefficient was determined for all twelve protectors and for eleven protectors excluding the Dainese (P1), which was found to be an outlier using both setups. As previously the significance level was set at $p>0.05$ for all correlation outputs. With magnitudes of the correlations interpreted using Cohen's thresholds where:<0.1, is trivial; 0.1–0.3 is small; 0.3–0.5 is moderate; and>0.5 is large (Cohen, 1988).

From Table 9.1 it can be seen that none of the correlations reached statistical significance. The lack of statistical significance despite moderate and large correlations is likely due to the low sample size and the non-normally distributed variables. When the outlier P1 was removed from the analysis the strength of the correlation decreased in every case. From Figure 9.1a and c it can be seen that products with a higher quasi-static stiffness result in a lower peak force. This correlation was found to be stronger when considering the rotational stiffness closer to hyperextension angles, 55-80° (spearman's $\rho = -0.5$ for all products, spearman's $\rho = -0.45$ excluding P1) than at the lower angles between 35-55, (spearman's $\rho = -0.31$ for all products, spearman's $\rho = -0.16$ excluding P1).

Figure 9.1b and d show that products with a higher quasi-static stiffness resulted in shorter time to peak. Stronger correlations were observed between time to peak and rotational stiffness at the lower angles. When all protectors were considered, a large negative correlation was observed between quasi-static rotational stiffness at 35-55° and

time to peak force (spearman's $\rho = -0.51$). Whereas a small correlation was observed at the higher angles (spearman's $\rho = -0.30$). When the outlier P1 was excluded from the analysis the strength of these correlations dropped for both angle ranges, between 35-55° spearman's $\rho = -0.36$ and between 55-80° spearman's $\rho = -0.10$.

Given there are relationships, albeit non-significant between quasi-static rotational stiffness and peak Fz force and time to peak force measured in the impact test, it can be concluded that the quasi-static test is a suitable starting point to compare and characterise snowboarding protectors. The quasi-static test facilitates a comparative ranking between products; however as the relationship between torque, extension angle and injury threshold is unknown the outputs from this test setup are limited. Whereas, the impact test enables products to be categorised based on their ability to reduce peak force which can be directly linked to published fracture thresholds from cadaver studies.

All testing was conducted at room temperature, however, given the cold environment associated with snowboarding it is recommended that in the future testing is carried out in a climate chamber or that the surrogate and wrist protectors are precondition at -25 °C ± 2 °C for at least 4 hours in line with the testing procedure used for ski helmets (European Committee for Standardization, 2007). The instrumented surrogate used in the impact test enabled the wrist extension angle to be measured throughout impact. It is recommended that this surrogate is mounted to quasi-static rig, by synchronising the potentiometer with the Instron output it would be possible to measure extension angle with respect to torque and eliminate the need to take manual start and end angle measurements using the inclinometer.

Table 9.1:Inferential statistics: correlation test results and significance values between two test setups

Protective characteristic		**Protectors**	**Spearman correlation coefficient**	**Significance (p value)**
Quasi-static Rotational stiffness	**Impact test**			
Between 35-55°	Peak Fz force	All	-0.31	0.33
		Excluding P1	-0.16	0.63
Between 35-55°	Time to peak Fz	All	**-0.51**	0.09
		Excluding P1	-0.36	0.28
Between 55-80°	Peak Fz force	All	**-0.55**	0.06
		Excluding P1	-0.42	0.21
Between 55-80°	Time to peak Fz	All	-0.30	0.34
		Excluding P1	-0.10	0.78

bold indicates a large correlation

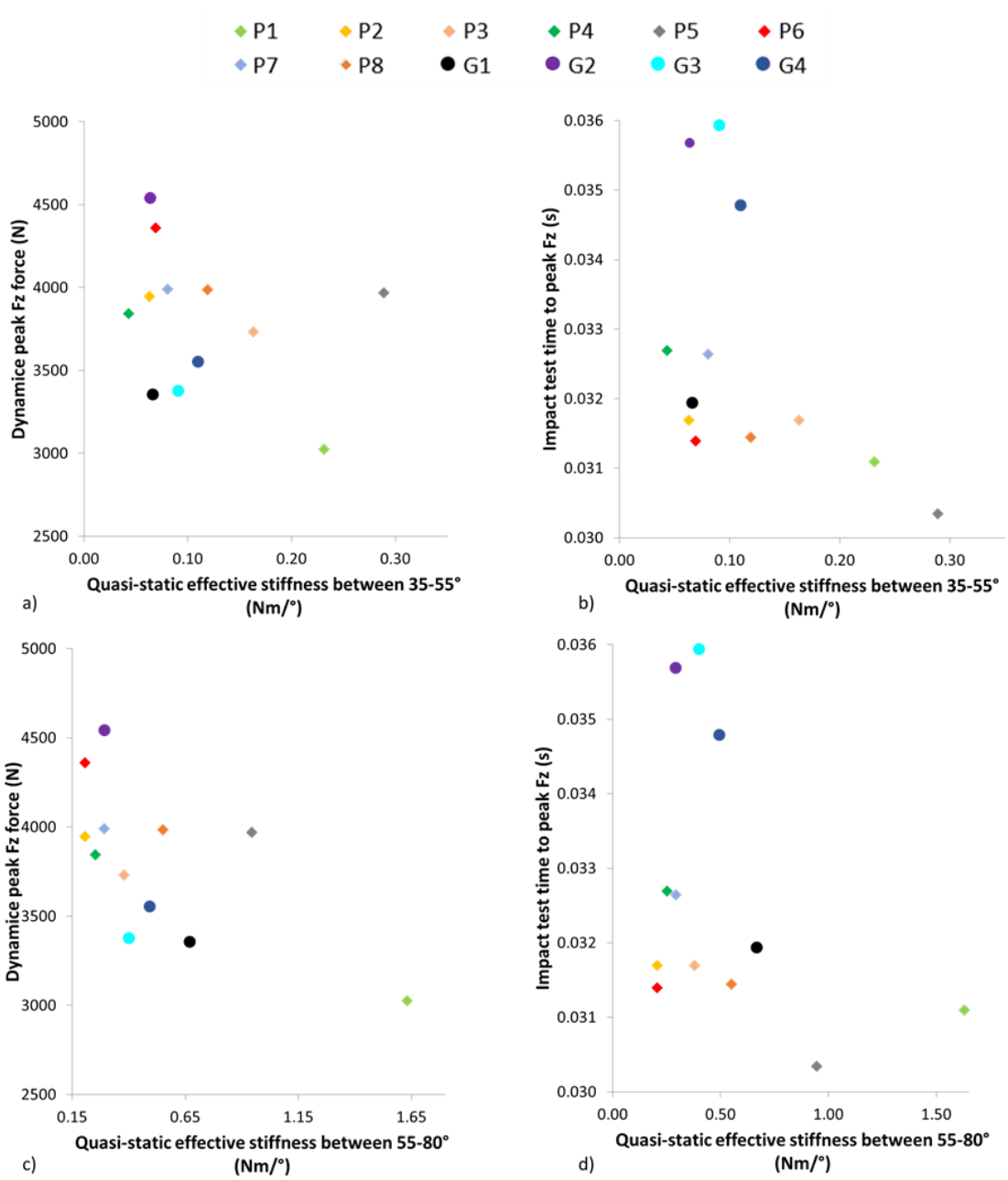

Figure 9.1: Comparison between two test setups, a) Impact test peak Fz vs Quasi-static stiffness between 35-55° b) Impact test time to peak Fz vs Quasi-static stiffness between 35-55° c) Impact test peak Fz vs Quasi-static stiffness between 55-80° d) Impact test time to peak Fz vs Quasi-static stiffness between 55-80°.

9.2 Limitations of Developed Tests

Several limitations have been identified in each chapter of this programme of research, there are three that warrant the most consideration: instrumentation, test parameters and surrogate biofidelity. A practical limitation of the quasi-static test was the availability of suitable load cells. To facilitate hyper-extension angles up to 90° whilst maintaining measurement fidelity, it is recommended that a 1000 N load cell is used in future studies. This project has shown that product differences can be detected, however it was limited

by the underpinning research on injury mechanics. The fall scenario surrounding a wrist fracture is poorly understood with a wide range of fracture forces (1104-3896 N), effective masses (2.5-45.5 kg) and inbound velocities (1.6-3.5 kg) being reported in literature. Therefore the impact test was developed to replicate a single study by Greenwald et al. (1998),

To facilitate the development of a repeatable mechanical test setup several simplifications were made to the surrogate, compromising its biofidelity. A low friction hinged was used to achieve a single degree of freedom replicating wrist flexion and extension. However, previous studies have shown the nature of the sustained injury is related to ulnar-radial deviation and not only hyperextension (Frykman, 1967; Mayfield, JK., Johnson, RP., & Kilcoyne, 1980). For both tests a rigid surrogate was used, whilst efforts were made to alter the compliance of the system for the dynamic test through the addition of Neoprene, the loading rate was 20% higher than the cadaver setup reported by Greenwald et al. (1998). The scanned surrogate is based on one participant who was deemed closest to 50^{th} percentile measurements from a sample of twenty forearms. However, the selected participant had measurements closer to the 80th percentile for forearm circumference, the degree to which this surrogate is representative of the wider population is limited.

9.3 Future work

Several recommendations for future research have been identified in each chapter of this programme of research. The five key areas based on the limitations stated throughout are summarised in the following section.

9.3.1 Surrogate Design

Future research should focus on increasing the biofidelity of the surrogate. Through the addition of further degrees of freedom; a more advanced hinge accounting for the influence of muscles and tendons in the joint and the use of skin and tissue simulants, a more representative surrogate could be developed. This would alter the stiffness of the surrogate and allow energy absorption through the soft tissue, making it a closer representation to the forearm used in cadaver testing (T. Payne *et al.*, 2015). As previously mentioned, incorporating a thin layer of compliant material, as a basic representation of skin could enhance protector fit and limit unwanted movement during both test setups to improve repeatability.

The development of additional scanned surrogates based on different sized participants identified from larger samples sizes is recommended. This would enable products designed for other members of the snowboarding population, children, youth and women to be tested. A scanned surrogate based on another 50^{th} percentile male (equivalent to hand size 8/9) is recommended, to enable a sensitivity analysis on the influence of hand and forearm dimensions within one protector size to be evaluated. Additional instrumentation in the surrogate, such as the inclusion of force or pressure sensors could be beneficial to monitor the interaction between protector and surrogate throughout testing to quantify fit and map areas of high pressure. Similar to the approach used by Ankrah and Mills, (2003) to monitor the pressure distribution of shin guards under impact.

9.3.2 Test Setup

Whilst the impact setup enables wrist protectors to be tested in injurious scenarios, it is recommended that future iterations consider modifications to alter the system stiffness and pendulum mass. System stiffness can be altered by modifying the compliance of the surrogate or the impactor. In this study Neoprene was added to the impactor, however this required preconditioning and hardness was found to decrease with multiple impacts, an alternative approach could be the use of a leaf spring, similar to that employed by Laing and Robinovitch, (2008) in their hip impact pendulum setup. To enable products to be tested with lower impact energies for the same inbound velocity, the pendulum arm could be replaced with something lighter by modifying the material (e.g. aluminium) or dimensions. Future work should also consider the surrogate mounting and the angle of impact to reduce unwanted surrogate movement during impact.

All the products tested with the impact test failed to lower the peak force below fracture threshold, although it is probable that under different loading conditions products could lower the force below fracture threshold. So it is likely for lower energy falls at a lower speed or involving lower mass or lower system stiffness these products may prevent injury. Future studies with modified boundary conditions are suggested to identify the limit of products protective capabilities, i.e. the inbound energy at which protectors no longer reduce the transmitted force below fracture force.

9.3.3 Injury monitoring and promotion of injury prevention strategies

A standardised monitoring process across ski resorts is recommended to provide consistent data regarding injury site, type and causation (Finch and Staines, 2017). Snowboarders presenting to medical centres with wrist injuries should be surveyed as to whether wrist protection was worn, and if so the model of wrist protector should be documented. This would enable a database of injuries and associated equipment to be established, facilitating potential trends between injury type, fall scenario and protector design to be established similar to the work of (Wadsworth, Binet and Rowlands, 2012). Through improved documentation of injury rates, it should be possible to track the efficacy of wrist protectors, once the new standard has been introduced.

9.3.4 Test Parameters

The versatile nature of the rig means that as knowledge advances different boundary conditions can be tested, therefore it is recommended that further work is conducted both on the slope and in the laboratory. Slope based studies are beneficial to better understand the circumstances surrounding a fall and the body position, so that lab-based biomechanics studies can measure the relevant boundary conditions. Further studies using cadaver forearms is also recommended. Given that the majority of work with full forearms, including that of Greenwald *et al.*, (1998) used in this project was conducted over 20 years ago, the use of new technologies recording at high sampling frequencies could support a deeper understanding. Similar to the work of Gilchrist, Guy and Cripton, (2013) who used digital image correlation to measure strain and enhance understanding of femur fracture mechanics.

9.3.5 Product Design

Using the two test setups presented further research is recommended to: explore the differences between stand-alone protectors and those integrated into gloves; to investigate protective performance under different inbound energies; and identify the optimal approach to wrist protector design to support manufacturers. Based on differences observed between protective gloves and stand-alone protectors in chapter 8, further testing is recommended to determine whether protective gloves alter the impact and elongate the time to peak force or if this phenomena is due to the test setup. Stand-alone protectors should be tested individually and in conjunction with a glove. All twelve products failed to lower the peak force below the reported fracture threshold. It

is recommended, therefore, to test the products under lower impact energies, to identify under which boundary condition the products are effective.

To better understand the influence of design parameters future tests should involve characterising protectors based on material type and construction as well as dimensions. Systematically changing one variable at a time, would allow for a thorough analysis of the effects of protector design on performance, to inform the design of future products. Existing products could be adapted, and protective elements systematically modified to test a range of dimensions and materials. A similar approach was taken by Toon, (2008) to investigate the effects of longitudinal bending stiffness on sprint spike design through varying the thickness of each sole at 0.5 mm increments. Testing could be done mechanically using the developed test setups presented here or through finite element analysis (Schmitt, Spierings and Derler, 2004).

This project has presented a new impact test in which snowboarding wrist protectors can be tested as a unit, enabling the protective capacity of splints and palmar pads to be tested simultaneously. It is recommended that future testing is conducted on the same models of protector with the same input parameters, using a linear drop test to test the palmar pad in isolation similar to the approach presented in the EN 14120 standard. Such a comparison would enable an assessment to be made on the role of the palmar pad and be able to further inform the development of international standards. Falls resulting in wrist fractures are also a common occurrence amongst the elderly population (DeGoede, Ashton-Miller and Schultz, 2003), using the impact test the inbound parameters could be modified to replicate different fall scenarios and test different types of wrist protector.

9.4 Chapter Summary

In this chapter, the results between the two test setups have been compared. The quasi-static setup is a suitable starting point to compare and characterise products. However, as the relationships between torque, extension angle and injury threshold are unknown the outputs from the quasi-static test are limited. It is, therefore, recommended that the impact test is used to monitor the protective characteristics of wrist protectors. The limitations of the developed test setups have been discussed and potential areas for future work introduced to support the design and development of better wrist protectors.

10 Conclusion

10.1 Introduction

The aim of this body of work was to develop new methods to evaluate the protective characteristics of snowboarding wrist protectors. The research was motivated by a call for the development of a standard to stipulate minimum performance standards snowboarding wrist protectors should meet (Michel *et al.*, 2013), in an attempt to mitigate the number of snowboarding fall induced wrist injuries. This chapter summarises the findings in relation to each objective, which have culminated in the development of two new test methods.

10.2 Summary of findings

10.2.1 To investigate current practices in protective equipment testing and determine performance criteria to evaluate snowboarding wrist protectors

From a review of the literature in chapter 2, the need for a representative test method and surrogate to evaluate the performance of a range of different snowboarding wrist protectors has been established. Fall-related wrist injuries are the most common injury in snowboarders affecting various demographics. Given the frequency of such injuries, especially amongst beginners and adolescents, a need for prevention based on an understanding of injury mechanisms and causation was established. Previous studies have shown that wrist protectors are an effective method in reducing wrist injuries, yet injuries still occur. From a review of protective mechanisms, three criteria wrist protectors should meet to be an effective preventative measure were identified:

- Attenuate peak impact force below published fracture thresholds
- Store, absorb and transfer impact energy safely away from the wrist joint without putting other regions at risk
- Stabilise the wrist and limit hyperextension

Through an examination of the current best practices in the field of mechanical testing and surrogate design, the limitations of current approaches were identified and the need for a representative test method and surrogate to evaluate the performance of a range of

different snowboarding wrist protectors was established. Different test setups and mechanical surrogates were identified that have been used to evaluate the performance of snowboarding wrist protectors. To date these tests have been limited to measuring the behaviour of either the palmar pad or splint in isolation. No appropriate surrogate exists to facilitate the testing of wrist protectors integrated into gloves whilst simultaneously measuring the wrist extension angle during a dynamic impact in a repeatable way.

10.2.2 To identify boundary conditions, the mechanical test should replicate to characterise snowboarding wrist protectors

The literature review informed the selection of boundary parameters in chapter 3 to ensure the developed mechanical tests characterise wrist protectors in conditions equivalent to an injurious snowboarding fall. Based on the observations of Greenwald, Simpson and Michel, 2013 who measured wrist extension angles of 76.8 ± 15.8° (mean ± standard deviation) in non-injurious snowboarding falls, the quasi-static test was specified to facilitate a wide range of torques and wrist extension angles up to 90°. Boundary parameters for the dynamic test were selected based on a study conducted by Greenwald *et al.* 1998 in which a cadaver forearm was fractured under conditions equivalent to a backwards fall in snowboarding. Given that the dynamic test involved a stiff impact rig and surrogate to allow the repeatable testing of wrist protectors under injurious loads, it was necessary to build a level of compliance equivalent to the human body into the system. The level of compliance was determined from the loading rate based on the gradient of the force time curve presented by Greenwald and colleagues. The system was specified to replicate a loading rate of 449262 N/s over 0.0045 s. In the case of velocity and mass parameters, the system was to enable a range of different fall scenarios to be tested facilitating a maximum inbound velocity of 5m/s and inbound masses up to 23kg.

10.2.3 To develop and validate mechanical tests to characterise snowboarding wrist protectors

Two new mechanical tests were developed and validated: a quasi-static test to measure the rotational stiffness of protectors; and an impact test replicating injurious snowboard falls to measure peak vertical force, energy absorption and wrist extension angle.

The quasi-static test presented in chapters 4 and 5 facilitates the measurement of wrist extension angles over a range of torques. Experimental tests validated that the method

can distinguish differences in rotational stiffness between wrist protector designs. Preliminary results showed that differences in protector performance exist between products. The results were found to be dependent on how tightly the protectors were strapped to the surrogate. Therefore, strapping tightness was accounted for in the rest of the body of work.

Alternative surrogates were developed to enable both stand-alone protectors and those integrated into gloves to be tested. The design of surrogates was found to significantly influence the measured rotational stiffness of wrist protectors. The scanned surrogate was the most representative surrogate and offered increased differentiation of rotational stiffness compared to the geometric surrogate. Therefore, the scanned surrogate was used for all further testing in the project.

An impact test presented in chapter 7 was developed to characterise product performance under boundary conditions representative of an injurious fall. The impact test uses an instrumented mechanical surrogate and impact pendulum coupled with boundary conditions from a published cadaver study (Greenwald *et al.*, 1998).

10.2.4 To compare the protective characteristics of a range of wrist protectors using the developed methods

The two test setups developed during this project were used to characterise the protective performance of twelve snowboarding wrist protectors (chapter 6 and 8). Differences in quasi-static rotational stiffness; peak vertical force, time to peak and energy absorption during impact were observed between products. However, none of the tested products effectively lower the force below fracture threshold. This PhD project showed that protectors employing different design approaches perform differently in mechanical tests, enabling initial explorations on the influence of protector design on performance. The developed test setups enable manufacturers to quantify the performance of different designs for the first time.

When comparing the performance of products tested using both developed setups, non-significant correlations were observed between quasi-static rotational stiffness and peak vertical force and time to peak force. Whilst the quasi-static test facilitates comparisons between wrist protectors, the impact test is recommended for monitoring the ability of

products to limit peak force below published fracture thresholds. These two test setups have supported the development of a snowboard specific international standard and aid manufacturers in the design and development of future products.

10.3 Contributions to knowledge

The two test methods and accompanying surrogates developed during the PhD project and presented in the thesis are an original contribution to knowledge, as no methods measuring these variables currently exist. The impact test provides the capacity to evaluate snowboard wrist protectors based on displaced angle and force transmission, a relationship no other study to date has considered.

Through working with the International Standards Committee as an expert member of the British Institute of Standards, the quasi-static test and surrogates developed as part of this body of work have influenced a draft ISO standard - ISO/TC 94/SC 13/WG 11, testing snowboarding wrist protectors. When this standard is published it will prompt a change in practice as manufacturers have the option to have their products certified to this standard. The test setup acts as a tool for manufacturers, providing them with a repeatable and representative way to test new design concepts and optimise product design to maximise consumer safety.

11 References

AA (2013) *Crash Test Dummies: Meet the Family*. Available at: http://www.theaa.com/motoring_advice/euroncap/dummies.html (Accessed: 19 October 2015).

Adams, C. *et al.* (2016) 'Development of a Method for Measuring Quasi-static Stiffness of Snowboard Wrist Protectors', *Procedia Engineering*, 147, pp. 378–383. doi: 10.1016/j.proeng.2016.06.320.

Adams, C. *et al.* (2018) 'Effect of surrogate design on the measured stiffness of Snowboarding wrist protectors', *Sports Engineering*. Springer London, 1. doi: 10.1007/s12283-018-0266-1.

Allen, B., Curless, B. and Popović, Z. (2003) 'The space of human body shapes: reconstruction and parameterization from range scans', *ACM Transactions on Graphics*, 22(3), pp. 587–594. doi: 10.1145/882262.882311.

Ankrah, S. and Mills, N. J. (2003) 'Performance of football shin guards for direct stud impacts', *Sports Engineering*, 6(4), pp. 207–219. doi: 10.1007/BF02844024.

Bahr, R. & Krosshaug, T. (2005) 'Understanding injury mechanisms: a key component of preventing injuries in sport.', *British Journal of Sports Medicine*, 39(6), pp. 324–329.

Bartlett, R. and Bussey, M. (2013) *Sports Biomechanics: Reducing Injury and Improving Performance, Book*. Routledge.

Bianchi, G. *et al.* (2012) 'The Use of Wrist Guards by Snowboarders in Switzerland', in R. J. Johnson, J. E. Shealy, R. M. Greenwald, and I. S. Scher, E. (ed.) *Skiing Trauma and Safety*, pp. 38–53. doi: 10.1520/STP104585.

Bob Kirk, Matt Carré, Stephen Haake, G. M. (2006) 'Modelling Traction of Studded Footwear on Sports Surfaces using Neural Networks', *The Engineering of Sport 6*, pp. 403–408.

Boone, D. C. and Azen, S. P. (1979) 'Normal range of motion of joints in male subjects', *Journal of Bone and Joint Surgery - Series A*, 61(5), pp. 756–759. Available at: http://www.scopus.com/inward/record.url?eid=2-s2.0-0018777891&partnerID=tZOtx3y1.

Brown, J. H. and Deluca, S. A. (1992) 'Growth plate injuries: Salter-Harris classification', *Am Fam Physician*, 46, pp. 1180–1184.

Burkhart, T. A. (2012) *Biomechanics of the Upper Extremity in Response to Dynamic Impact Loading Indicative of a Forward Fall: An Experimental and Numerical*

Investigation.

Burkhart, T. a., Andrews, D. M. and Dunning, C. E. (2012) 'Failure characteristics of the isolated distal radius in response to dynamic impact loading', *Journal of Orthopaedic Research*, 30(6), pp. 885–892. doi: 10.1002/jor.22009.

Burkhart, T. A., Andrews, D. M. and Dunning, C. E. (2013) 'Multivariate injury risk criteria and injury probability scores for fractures to the distal radius', *Journal of Biomechanics*. Elsevier, 46(5), pp. 973–978. doi: 10.1016/j.jbiomech.2012.12.003.

Burkhart, T. a and Andrews, D. M. (2010) 'The effectiveness of wrist guards for reducing wrist and elbow accelerations resulting from simulated forward falls.', *Journal of applied biomechanics*, 26(3), pp. 281–9. Available at: http://www.ncbi.nlm.nih.gov/pubmed/20841619.

Burkhart, T. a, Dunning, C. E. and Andrews, D. M. (2012) 'Predicting distal radius bone strains and injury in response to impacts using multi-axial accelerometers.', *Journal of biomechanical engineering*, 134(10), p. 101007. doi: 10.1115/1.4007631.

Burton (2015) *Burton Impact Wrist Guard*. Available at: http://www.burton.com/default/burton-impact-wrist-guard/W16-103471.html?dwvar_W16-103471_variationColor=10347101002&cgid=mens-snowboard-helmets-protection (Accessed: 15 October 2015).

Chen, Y. R. *et al.* (2014) 'Contact areas of the scaphoid and lunate with the distal radius in neutral and extension: correlation of falling strategies and distal radial anatomy.', *The Journal of hand surgery, European volume*, 39(4), pp. 379–83. doi: 10.1177/1753193413507810.

Cheng, S. L. *et al.* (1995) '"Splint-top" fracture of the forearm: a description of an in-line skating injury associated with the use of protective wrist splints.', *The Journal of trauma*, pp. 1194–7. Available at: http://www.ncbi.nlm.nih.gov/pubmed/7500422.

Chiu, J. and Robinovitch, S. N. (1998) 'Prediction of upper extremity impact forces during falls on the outstretched hand.', *Journal of biomechanics*, 31(12), pp. 1169–76. Available at: http://www.ncbi.nlm.nih.gov/pubmed/9882050.

Choi, W. J. and Robinovitch, S. N. (2011) 'Pressure distribution over the palm region during forward falls on the outstretched hands.', *Journal of biomechanics*. Elsevier, 44(3), pp. 532–9. doi: 10.1016/j.jbiomech.2010.09.011.

Choppin, S. and Allen, T. (2012) 'Special issue on predictive modelling in sport', *Proceedings of the Institution of Mechanical Engineers, Part P: Journal of Sports Engineering and Technology*, 226(2), pp. 75–76. doi: 10.1177/1754337112443933.

Chou, P. *et al.* (2001) 'Effect of elbow flexion on upper extremity impact forces during

a fall', *Clinical Biomechanics*, 16, pp. 888–894.

Chow, T. K., Corbett, S. W. and Farstad, D. J. (1996) 'Spectrum of injuries from snowboarding', *Journal of Trauma - Injury, Infection and Critical Care*, 41(2), pp. 321–325. Available at: http://www.scopus.com/inward/record.url?eid=2-s2.0-0029742052&partnerID=tZOtx3y1.

Cohen, J. (1988) *Statistical power analysis for the behavioural sciences*. 2nd edn. Hillsdale, NJ: Lawrence Erlbaum Associates.

Costa-Scorse, B. A. *et al.* (2017) 'New Zealand Snow Sports Injury Trends Over Five Winter Seasons 2010--2014', in Scher, I. S., Greenwald, R. M., and Petrone, N. (eds) *Snow Sports Trauma and Safety: Conference Proceedings of the International Society for Skiing Safety: 21st Volume*. Cham: Springer International Publishing, pp. 17–28. doi: 10.1007/978-3-319-52755-0_2.

Davidson, T. M. and Laliotis, A. T. (1996) 'Snowboarding injuries a four-year study with comparison with alpine ski injuries', *Western Journal of Medicine*, 164(3), pp. 231–237. Available at: http://www.scopus.com/inward/record.url?eid=2-s2.0-0029876184&partnerID=tZOtx3y1.

Deady, L. H. and Salonen, D. (2010) 'Skiing and snowboarding injuries: a review with a focus on mechanism of injury.', *Radiologic clinics of North America*, 48(6), pp. 1113–24. doi: 10.1016/j.rcl.2010.07.005.

Decathlon (2015) *WED'ZE DEFENSE WRIST-P*. Available at: https://www.decathlon.co.uk/defense-wrist-p-id_8286542.html (Accessed: 15 October 2015).

DeGoede, K. . and Ashton-Miller, J. . (2002) 'Fall arrest strategy affects peak hand impact force in a forward fall', *Journal of Biomechanics*, 35(6), pp. 843–848. doi: 10.1016/S0021-9290(02)00011-8.

DeGoede, K. M. *et al.* (2002) 'Biomechanical Factors Affecting the Peak Hand Reaction Force During the Bimanual Arrest of a Moving Mass', *Journal of Biomechanical Engineering*, 124, p. 107. doi: 10.1115/1.1427702.

DeGoede, K. M., Ashton-Miller, J. A. and Schultz, A. B. (2003) 'Fall-related upper body injuries in the older adult: a review of the biomechanical issues', *Journal of Biomechanics*, 36(7), pp. 1043–1053. doi: 10.1016/S0021-9290(03)00034-4.

Dickson, T. J. and Terwiel, F. A. (2011) 'Snowboarding injuries in Australia: investigating risk factors in wrist fractures to enhance injury prevention strategies.', *Wilderness & environmental medicine*, 22(3), pp. 228–35. doi: 10.1016/j.wem.2011.04.002.

Duma, S. M. *et al.* (2003) 'Upper extremity interaction with a deploying side airbag: A characterization of elbow joint loading', *Accident Analysis and Prevention*, 35(3), pp. 417–425. doi: 10.1016/S0001-4575(02)00020-9.

Ekeland, A., Rødven, A. and Heir, S. (2017) 'Injury Trends in Recreational Skiers and Boarders in the 16-Year Period 1996-2012', in Scher, I. S., Greenwald, R. M., and Petrone, N. (eds) *Snow Sports Trauma and Safety: Conference Proceedings of the International Society for Skiing Safety: 21st Volume*. Cham: Springer International Publishing, pp. 3–16. doi: 10.1007/978-3-319-52755-0_1.

Englander, F., Hodson, T. . and Terregrossa, R. A. (1996) 'Economic dimensions of slip and fall injuries', *Journal of Forensic Sciences*, 41, pp. 733–746.

European Committee for Standardization (2003a) 'BS EN 420:2003 +A1:2009 Protective gloves — General requirements and test methods'.

European Committee for Standardization (2003b) 'EN 14120:2003 Protective clothing — Wrist , palm , knee and elbow protectors for users of roller sports equipment — Requirements and test methods'.

European Committee for Standardization (2006) 'BS EN 511:2006 Protective gloves against cold'.

European Committee for Standardization (2007) 'BS EN 1077:2007 Helmets for alpine skiers and snowboarders'.

European Committee for Standardization (2010) 'BS EN 14404:2004 + A1:2010 Personal protective equipment — Knee protectors for work in the kneeling position'.

Field, A. (2009) *Discovering statistics using SPSS*. London: SAGE.

Finch, C. F. and Staines, C. (2017) 'Guidance for sports injury surveillance: the 20-year influence of the Australian Sports Injury Data Dictionary', *Injury Prevention*, p. injuryprev-2017-042580. doi: 10.1136/injuryprev-2017-042580.

Flørenes, T. W. *et al.* (2012) 'Injuries among World Cup ski and snowboard athletes.', *Scandinavian journal of medicine & science in sports*, 22(1), pp. 58–66. doi: 10.1111/j.1600-0838.2010.01147.x.

Frykman, G. (1967) 'Fracture of the Distal Radius Including Sequelae-Shoulder-Handfinger Syndrome, Disturbance in the Distal Radio-Ulnar Joint and Impairment of Nerve Function. A clinical and experimental study', *Acta Orthop. Scand.*, 108, pp. 1–153.

Giacobetti, F. *et al.* (1997) 'Biomechanical analysis of the effectiveness of in-line skating wrist guards for preventing wrist fractures.', *The American journal of sports medicine*, 25(2), pp. 223–225. Available at:

http://www.ncbi.nlm.nih.gov/pubmed/9474417.

Gilchrist, S., Guy, P. and Cripton, P. a (2013) 'Development of an inertia-driven model of sideways fall for detailed study of femur fracture mechanics', *Journal of biomechanical engineering*, 135(12), p. 121001. doi: 10.1115/1.4025390.

Gislason, M. . and Nash, D. (2012) 'Finite element modelling of a multi bone joint: The human wrist', in *Element Analysis - New Trends and Developments*. Croatia: InTech, pp. 77–98.

Gíslason, M. K., Stansfield, B. and Nash, D. H. (2010) 'Finite element model creation and stability considerations of complex biological articulation: The human wrist joint', *Medical Engineering and Physics*, 32(5), pp. 523–531. doi: 10.1016/j.medengphy.2010.02.015.

Greenwald, R. M. *et al.* (1998) 'Dynamic Impact Response of Human Cadaveric Forearms Using a Wrist Brace', *The American journal of sports medicine*, 26(6), pp. 2–7.

Greenwald, R. M., Simpson, F. H. and Michel, F. I. (2013) 'Wrist biomechanics during snowboard falls', *Proceedings of the Institution of Mechanical Engineers, Part P: Journal of Sports Engineering and Technology*, 227(4), pp. 244–254. doi: 10.1177/1754337113482706.

Gruber, K. *et al.* (1998) 'A comparative study of impact dynamics: wobbling mass model versus rigid body models', *Journal of Biomechanics*, 31, pp. 439–444.

Grund, T., Senner, V. and Grube, K. (2007) 'Development of a test device for testing soccer boots under gamerelevant highrisk loading conditions', *Sports Engineering*, 10(1), pp. 55–63. doi: 10.1007/BF02844202.

Hagel, B. (2005) 'Skiing and snowboarding injuries.', *Medicine and sport science*, 48, pp. 74–119. doi: 10.1159/000084284.

Hagel, B., Pless, I. B. and Goulet, C. (2005) 'The effect of wrist guard use on upper-extremity injuries in snowboarders.', *American journal of epidemiology*, 162(2), pp. 149–56. doi: 10.1093/aje/kwi181.

Harken (2017) *Micro upright pulley*. Available at: http://www.harken.co.uk/productdetail.aspx?id=7259&taxid=4102 (Accessed: 24 June 2017).

Helelä, T. (1969) 'Age-dependent variations of the cortical thickness of the clavicle', *Annals of Clinical Research*, 1(2), pp. 140–3.

Hsiao, E. T. and Robinovitch, S. N. (1998) 'Common protective movements govern unexpected falls from standing height', *Journal of Biomechanics*, 31(1), pp. 1–9. doi:

10.1016/S0021-9290(97)00114-0.

Hwang, I.-K. *et al.* (2006) 'Biomechanical efficiency of wrist guards as a shock isolator.', *Journal of biomechanical engineering*, 128(2), pp. 229–34. doi: 10.1115/1.2165695.

Hwang, I. K. and Kim, K. J. (2004) 'Shock-absorbing effects of various padding conditions in improving efficacy of wrist guards', *Journal of Sports Science and Medicine*, 3(1), pp. 23–29. Available at: http://www.scopus.com/inward/record.url?eid=2-s2.0-23844510276&partnerID=tZOtx3y1.

Idzikowski, J. R., Janes, P. C. and Abbott, P. J. (2000) 'Upper Extremity Snowboarding Injuries: Ten-Year Results from the Colorado Snowboard Injury Survey', *Am. J. Sports Med.*, 28(6), pp. 825–832. Available at: http://ajs.sagepub.com.lcproxy.shu.ac.uk/content/28/6/825.short (Accessed: 19 September 2014).

Institut fuer Arbeitsschutz der Deutschen (2015) *Knee protection*. Available at: http://www.dguv.de/medien/ifa/en/pub/ada/pdf_en/aifa0191e.pdf.

Instron (2017) *Flexure Fixture*. Available at: Flexure Fixture (Accessed: 24 June 2017).

Instron (2018) *2519 Series S-beam Static Load Cells*. Available at: http://www.instron.co.uk/en-gb/products/testing-accessories/load-cells/static/2519-series-s-beam (Accessed: 21 July 2018).

International Organization for Standardization (2011) *ISO / IEC Directives Part 2 Rules for the structure and drafting of International Standards*.

International Organization for Standardization (2016a) *ISO/CD 20320 Protective clothing for use in Snowboarding -- Wrist Protectors -- Requirements and test methods*. Available at: https://www.iso.org/standard/67665.html (Accessed: 7 May 2017).

International Organization for Standardization (2016b) 'ISO 10256 Protective equipment for use in ice hockey'.

International Organization for Standardization (2018) *13.340 - Protective equipment*. Available at: https://www.iso.org/ics/13.340/x/ (Accessed: 2 July 2017).

Kijima, Y. and Viegas, S. F. (2009) 'Wrist Anatomy and Biomechanics', *Journal of Hand Surgery*. Elsevier Inc., 34(8), pp. 1555–1563. doi: 10.1016/j.jhsa.2009.07.019.

Kim, K.-J. *et al.* (2006) 'Shock attenuation of various protective devices for prevention of fall-related injuries of the forearm/hand complex.', *The American journal of sports medicine*, 34(4), pp. 637–43. doi: 10.1177/0363546505281800.

Kim, K.-J. and Ashton-Miller, J. A. (2003) 'Biomechanics of fall arrest using the upper

extremity: age differences', *Clinical Biomechanics*, 18(4), pp. 311–318. doi: 10.1016/S0268-0033(03)00005-6.

Kim, S. *et al.* (2012) 'Snowboarding injuries: trends over time and comparisons with alpine skiing injuries.', *The American journal of sports medicine*, 40(4), pp. 770–6. doi: 10.1177/0363546511433279.

Kim, S. and Lee, S. K. (2011) 'Snowboard Wrist Guards–Use, Efficacy, and Design', *Bulletin of the NYU Hospital for Joint Diseases 2011;69(2):149-57*, 69(2), pp. 149–157.

Knox, C. L. and Comstock, R. D. (2006) 'Video analysis of falls experienced by paediatric iceskaters and roller/inline skaters.', *British journal of sports medicine*, 40(3), pp. 268–71. doi: 10.1136/bjsm.2005.022855.

Krosshaug, T. *et al.* (2005) 'Research approaches to describe the mechanisms of injuries in sport: Limitations and possibilities', *British Journal of Sports Medicine*, 39(6), pp. 330–339. doi: 10.1136/bjsm.2005.018358.

Kuhn, E. N. *et al.* (2017) 'Youth helmet design in sports with repetitive low- and medium-energy impacts: a systematic review', *Sports Engineering*. Springer London, 20(1), pp. 29–40. doi: 10.1007/s12283-016-0215-9.

Laing, A. C. *et al.* (2011) 'The effects of pad geometry and material properties on the biomechanical effectiveness of 26 commercially available hip protectors', *Journal of Biomechanics*. Elsevier, 44(15), pp. 2627–2635. doi: 10.1016/j.jbiomech.2011.08.016.

Laing, A. C. and Robinovitch, S. N. (2008) 'The force attenuation provided by hip protectors depends on impact velocity, pelvic size, and soft tissue stiffness', *J Biomech Eng*, 130(6), p. 61005. doi: 10.1115/1.2979867.

Langran, M. and Selvaraj, S. (2002) 'Increased injury risk among first-day skiers, snowboarders, and skiboarders.', *The American journal of sports medicine*, 32(1), pp. 96–103. doi: 10.1177/0095399703258684.

Langran, M. and Selvaraj, S. (2004) 'Increased Injury Risk Among First-Day Skiers, Snowboarders, and Skiboarders', *American Journal of Sports Medicine*, 32(1), pp. 96–103. doi: 10.1177/0095399703258684.

Lehner, S. *et al.* (2014) 'Wrist Injuries in Snowboarding – Simulation of a Worst Case Scenario of Snowboard Falls', *Procedia Engineering*. Elsevier Ltd, 72, pp. 255–260. doi: 10.1016/j.proeng.2014.06.037.

Levy, D. *et al.* (2015) 'A design rationale for safer terrain park jumps that limit equivalent fall height', *Sports Engineering*. Springer London, 18(4), pp. 227–239. doi: 10.1007/s12283-015-0182-6.

Lewis, L. M. *et al.* (1997) 'Do wrist guards protect against fractures?', *Annals of*

emergency medicine, 29(6), pp. 766–9. Available at: http://www.ncbi.nlm.nih.gov/pubmed/9174522.

Lieberman, D. E. *et al.* (2010) 'Foot strike patterns and collision forces in habitually barefoot versus shod runners', *Nature*. Nature Publishing Group, 463(7280), pp. 531–535. doi: 10.1038/nature08723.

Lilienfeldt, A. (1908) 'Über die Erzeugung der typischen Verletzungen der Handwurtzelknochen und des Radiusbruches auf direktem Wege an der Leiche und ihre Entstehungsart, erläutert durch den Mechanismus der Handgelenkbewegungen.', *Ztschr Orthop Chir*, 20, pp. 437–454.

Lo, J. *et al.* (2003) 'On reducing hand impact force in forward falls: results of a brief intervention in young males', *Clinical Biomechanics*, 18(8), pp. 730–736. doi: 10.1016/S0268-0033(03)00124-4.

Lubahn, J. *et al.* (2005) 'Adequacy of laboratory simulation of in-line skater falls.', *The Journal of hand surgery*, 30(2), pp. 283–8. doi: 10.1016/j.jhsa.2004.11.016.

Machold, W. *et al.* (2000) 'Risk of injury through snowboarding', *Journal of Trauma - Injury, Infection and Critical Care*, 48(6), pp. 1109–1114. Available at: http://www.scopus.com/inward/record.url?eid=2-s2.0-0033944919&partnerID=tZOtx3y1.

Machold, W., Kwasny, O. and Eisenhardt, P. (2005) 'Reduction of severe wrist injuries in snowboarding by an optimized wrist protection device: A prospective randomized trial', *J Trauma*, 52(3), pp. 517–520. Available at: http://www.scopus.com/inward/record.url?eid=2-s2.0-0942276723&partnerID=tZOtx3y1.

Majors, B. J. and Wayne, J. S. (2011) 'Development and validation of a computational model for investigation of wrist biomechanics', *Annals of Biomedical Engineering*, 39(11), pp. 2807–2815. doi: 10.1007/s10439-011-0361-y.

Mao, H., Cai, Y. and Yang, K. H. (2014) 'Numerical study of 10-year-old child forearm injury', 1(3), pp. 143–158.

Marshall, S. W. *et al.* (2002) 'An ecologic study of protective equipment and injury in two contact sports', *International journal of epidemiology*, 31, pp. 587–592. doi: 10.1093/ije/31.3.587.

Materialise (2017) *Laser Sintering Material Properties*. Available at: http://www.materialise.com/en/manufacturing/materials/pa-12-sls (Accessed: 18 April 2018).

Matsumoto, K. *et al.* (2004) 'Wrist Fractures From Snowboarding', *Clinical Journal of*

Sport Medicine, 14(2), pp. 64–71. doi: 10.1097/00042752-200403000-00003.

Maurel, M. L. *et al.* (2013) 'Biomechanical study of the efficacy of a new design of wrist guard.', *Clinical biomechanics (Bristol, Avon)*. Elsevier B.V., 28(5), pp. 509–13. doi: 10.1016/j.clinbiomech.2013.02.005.

Mayfield, JK., Johnson, RP., & Kilcoyne, R. (1980) 'Carpal dislocations: pathomechanics and progressive perilunar instability.', *The journal of hand surgery*, 5(3), pp. 226–241.

McGrady, Linda Hoepfner, P., Young, C. and Raasch, W. (2001) 'Biomechanical effect of in-line skating wrist guards on the prevention of wrist fracture', *KSME International Journal*, 15(7), pp. 1072–1076. Available at: http://www.scopus.com/inward/record.url?eid=2-s2.0-0035402659&partnerID=tZOtx3y1.

McIntosh, a. S. (2012) 'Biomechanical considerations in the design of equipment to prevent sports injury', *Proceedings of the Institution of Mechanical Engineers, Part P: Journal of Sports Engineering and Technology*, 226(3–4), pp. 193–199. doi: 10.1177/1754337111431024.

McNeil, J. A., Hubbard, M. and Swedberg, A. D. (2012) 'Designing tomorrow's snow park jump', *Sports Engineering*, 15(1), pp. 1–20. doi: 10.1007/s12283-012-0083-x.

Medlej, J. (2014) *Human Anatomy Fundamentals: Flexibility and Joint Limitations*.

Merkle, A. C. *et al.* (2013) 'Biomechanics and injury mitigation systems program: An overview of human models for assessing injury risk in blast, ballistic, and transportation impact scenarios', *Johns Hopkins APL Technical Digest (Applied Physics Laboratory)*, 31(4), pp. 286–295.

Michaud, P.-A., Renaud, A. and Narring, F. (2001) 'Sports activities related to injuries? A survey among 9-19 year olds in Switzerland.', *Injury prevention : journal of the International Society for Child and Adolescent Injury Prevention*, 7, pp. 41–45. doi: 10.1136/ip.7.1.41.

Michel, F. I. *et al.* (2013) 'White Paper: functionality and efficacy of wrist protectors in snowboarding—towards a harmonized international standard', *Sports Engineering*, 16(4), pp. 197–210. doi: 10.1007/s12283-013-0113-3.

Moore, M. S. *et al.* (1997) 'The effect of a wrist brace on injury patterns in experimentally produced distal radial fractures in a cadaveric model.', *The American journal of sports medicine*, 25(3), pp. 394–401. Available at: http://www.ncbi.nlm.nih.gov/pubmed/9167823.

NatureWorksLLC (2018) *PLA Material Information*. Available at:

http://www.faberdashery.co.uk/wp-content/uploads/2011/08/4043D-PLA-Material-info.pdf (Accessed: 18 April 2018).

Norman, R. (1983) 'Biomechanical evaluations of sports equipment', *Exercise & Sport Sciences Review*, 11, pp. 232–274. Available at: http://ovidsp.tx.ovid.com/sp-3.17.0a/ovidweb.cgi?WebLinkFrameset=1&S=ABJKFPHONIDDBNOFNCJKDFMCNPANAA00&returnUrl=ovidweb.cgi%3FMain%2BSearch%2BPage%3D1%26S%3DABJKFPHONIDDBNOFNCJKDFMCNPANAA00&directlink=http%3A%2F%2Fgraphics.tx.ovid.com%2Fovftpdfs%2FFPDDNCM.

O'Neill, D, F. (2003) 'Wrist injuries in guarded versus unguarded first time snowboarders', in *Clinical Orthopaedics and Related Research*, pp. 91–95. Available at: http://www.scopus.com/inward/record.url?eid=2-s2.0-0037388671&partnerID=tZOtx3y1.

O'Neill, D. F. (2003) 'Wrist Injuries in Guarded Versus Unguarded Firsth Time Snowboarders', *Clinical Orthopaedics and Related Research*, 409, pp. 91–95.

Odenwald, S. (2006) 'Test methods in the development of sports equipment', in *The Engineering of Sport 6*, pp. 301–306.

Ogawa, H. *et al.* (2010) 'Skill level-specific differences in snowboarding-related injuries.', *The American journal of sports medicine*, 38, pp. 532–537. doi: 10.1177/0363546509348763.

Palmer, A. *et al.* (1985) 'Functional wrist motion: a biomechanical study', *The Journal of hand surgery*, 10(1), pp. 39–46. Available at: http://www.sciencedirect.com/science/article/pii/S036350238580246X (Accessed: 16 March 2015).

Panjabi, M., White, A. and Southwick, W. (1973) 'Mechanical Properties of Bone of as a Function of Rate of Deformation', *The Journal of bone and joint surgery.*, 55–A(2), pp. 322–330.

Parkkari, J., Kujala, U. M. and Kannus, P. (2001) 'Is it possible to prevent sports injuries? Review of controlled clinical trials and recommendations for future work.', *Sports medicine (Auckland, N.Z.)*, 31(14), pp. 985–995. doi: 311403 [pii].

Parsons, J. (2014) *Sports Medicine Handbook*. National Collegiate Athletic Association. doi: 10.1136/bmj.319.7224.1582.

Payne, T. *et al.* (2015) 'Development of a synthetic human thigh impact surrogate for sports personal protective equipment testing', *Proceedings of the Institution of Mechanical Engineers, Part P: Journal of Sports Engineering and Technology*, 230(1), pp. 1–12. doi: 10.1177/1754337115582294.

Payne, T. *et al.* (2015a) 'Development of novel synthetic muscle tissues for sports impact surrogates', *J Mech Behav Biomed Mater*, 41, pp. 357–374. doi: 10.1016/j.jmbbm.2014.08.011.

Payne, T. *et al.* (2015b) 'The evaluation of new multi-material human soft tissue simulants for sports impact surrogates', *Journal of the mechanical behavior of biomedical materials*, 41, pp. 336–56. doi: 10.1016/j.jmbbm.2014.09.018.

Payne, T., Mitchell, S. and Bibb, R. (2013) 'Design of human surrogates for the study of biomechanical injury a review', *Critical Reviews in Biomedical Engineering*, 41(1), pp. 51–89.

Peebles, L. and Norris, B. (1998) *Adultdata: The Handbook of Adult Anthropometric and Strength Measurements. Data for Design Safety*.

Pheasant, S. (2001) *Bodyspace: Anthropometry, ergonomics and the design of work (2nd ed.)*. Taylor & Francis.

Porrino, J. (2015) *Distal Radial Fracture Imaging*. Available at: http://emedicine.medscape.com/article/398406-overview (Accessed: 25 October 2014).

Pugh, S. (1991) *Total Design*. Pearson Education.

Ratkowsky, D. A. (1983) *Nonlinear regression modelling*. Marcel Dekker.

Rexroth, B. (2017) *40x40 Aluminium struts*. Available at: http://www13.boschrexroth-us.com/Framing_Shop/Product/View_Product.aspx?partnumber=3842529339 (Accessed: 24 June 2017).

Robinovitch, S. N. and Chiu, J. (1998) 'Surface stiffness affects impact force during a fall on the outstretched hand', *Journal of Orthopaedic Research*, 16(3), pp. 309–313. doi: 10.1002/jor.1100160306.

Rønning, R. *et al.* (2001) 'The efficacy of wrist protectors in preventing snowboarding injuries.', *The American journal of sports medicine*, 29(5), pp. 581–5. Available at: http://www.ncbi.nlm.nih.gov/pubmed/11573916.

Russel, K., Hagel, B. . and Goulet, C. (2010) 'Snowboarding', in Caine, D. ., Harmer, P. ., and Schiff, M. . (eds) *Epidemiology of Injuries in Olympic Sports*, pp. 447–472.

Russell, K., Hagel, B. and Francescutti, L. H. (2007) 'The effect of wrist guards on wrist and arm injuries among snowboarders: a systematic review.', *Clinical Journal of Sport Medicine*, 17(2), pp. 145–50. doi: 10.1097/JSM.0b013e31803f901b.

Ryu, J. *et al.* (1991) 'Functional ranges of wrist motion', *The Journal of hand surgery*, 16(3), pp. 409–19.

Sasaki, K. *et al.* (1999) 'Severity of Upper Limb Injuries in Snowboarding', *Arch Orthop Trauma Surg*, 119, pp. 292–295. Available at:

http://www.scopus.com/inward/record.url?eid=2-s2.0-0344899664&partnerID=tZOtx3y1.

Sasaki, K. *et al.* (1999) 'Snowboarder's wrist: its severity compared with Alpine skiing Journal title: Journal of trauma: injury, infection, and critical care', *Journal of Trauma and Acute Care Surgery*, 46(6), pp. 1059–1061.

Schieber, R. . *et al.* (1996) 'Risk factors for injuries from in-line skating and the effectiveness of safety gear', *The New England journal of medicine*, 335(22), pp. 1630–1635. Available at: http://www.nejm.org/doi/full/10.1056/NEJM199611283352202 (Accessed: 1 October 2014).

Schmitt, K.-U. *et al.* (2012) 'Characterizing the mechanical parameters of forward and backward falls as experienced in snowboarding.', *Sports Biomechanics*, 11(1), pp. 57–72. doi: 10.1080/14763141.2011.637127.

Schmitt, K.-U., Michel, F. and Staudigl, F. (2012) 'Testing Damping Performance and Bending Stiffness of Snowboarding Wrist Protectors', *Journal of ASTM International*, 9(4), pp. 104–204. doi: 10.1520/JAI104204.

Schmitt, K.-U., Spierings, A. B. and Derler, S. (2004) 'A finite element approach and experiments to assess the effectiveness of hip protectors', *Technol. Health Care (Netherlands)*, 12(1), pp. 43–9.

Schuit, S. C. . *et al.* (2004) 'Fracture incidence and association with bone mineral density in elderly men and women: the Rotterdam Study', *Bone*, 34(1), pp. 195–202. doi: 10.1016/j.bone.2003.10.001.

Senner, V. (2015) 'Methodological challenges for biomechanics approaches in winter sports', in *33rd International Conference on Biomechanics in Sports*. Poiters, France.

SIA (2011) *SIA snow sports market, intelligent report*. McLean, VA, USA: Snowsports Industries America Research.

Statistica (2018a) *Estimated number of skier/snowboard visits in the U.S.* Available at: https://www.statista.com/statistics/206544/estimated-number-of-skier-visits-in-the-us-since-2000/.

Statistica (2018b) 'Winter Sports - Statistics & Facts'. Available at: https://www.statista.com/topics/1770/winter-sports/.

Swiss Council for Accident Prevention (bfu) (2012) *STATUS 2012: Statistics on non-occupational accidents and the level of safety in Switzerland, Road traffic, sports, home and leisure*. Berne.

Tan, J.-S. *et al.* (2006) 'Wrist impact velocities are smaller in forward falls than backward falls from standing.', *Journal of biomechanics*, 39(10), pp. 1804–11. doi:

10.1016/j.jbiomech.2005.05.016.

Thermetrics (2016) *Thermal Hand Test System*. Available at: http://www.thermetrics.com/products/partial-manikins/thermal-hand-test-system.

Thoraval, C. *et al.* (2012) 'Epidemiological study applied to the design of wrist guard.', *Computer methods in biomechanics and biomedical engineering*, 15(S1), pp. 272–273. doi: 10.1080/10255842.2012.713637.

Thoraval, C. *et al.* (2013) 'Evaluation of wrist guard effectiveness for snowboarders', *Computer methods in biomechanics and biomedical engineering*, 16 Suppl 1(October 2014), pp. 187–8. doi: 10.1080/10255842.2013.815872.

Tilley, A. R. and Henry Dreyfuss Associates (2002) *The Measure of Man and Woman: Human Factors in Design*.

Tilley, A. R. and Henry Dreyfuss Associates (2002) *The Measure of Man and Woman: Human Factors in Design*.

Toon, D. (2008) *Design and analysis of sprint footwear to investigate the effects of longitudinal bending stiffness on sprinting performance*. Available at: http://medcontent.metapress.com/index/A65RM03P4874243N.pdf%5Cnhttp://ethos.bl.uk/OrderDetails.do?uin=uk.bl.ethos.547392.

Torjussen, J. and Bahr, R. (2006) 'Injuries among elite snowboarders (FIS Snowboard World Cup).', *British journal of sports medicine*, 40, pp. 230–234. doi: 10.1136/bjsm.2005.021329.

Tsui, F. (2010) *Determining impact intensities in contact sports*.

Van Tuyl, J., Burkhart, T. A. and Quenneville, C. E. (2016) 'Effect of posture on forces and moments measured in a Hybrid III ATD lower leg', *Traffic Injury Prevention*. Taylor & Francis, 17(4), pp. 381–385. doi: 10.1080/15389588.2015.1089356.

Ura, D. and Carré, M. (2016) 'Development of a novel portable test device to measure the tribological behaviour of shoe interactions with tennis courts', *Procedia Engineering*. The Author(s), 147, pp. 550–555. doi: 10.1016/j.proeng.2016.06.237.

Waddington, G. *et al.* (2013) 'Does Wearing a Wrist Guard Affect the Site of Wrist Fracture in Snow Sports?', in *Procedia Engineering*, pp. 238–242. doi: 10.1016/j.proeng.2013.07.035.

Wadsworth, P., Binet, M. and Rowlands, A. (2012) 'Prospective study to compare efficacy of different designs of wrist protection for snowboarders', in Johnson, R. J. et al. (eds) *Skiing Trauma and Safety on May 1–7*. Keystone: ASTM International, pp. 17–30. doi: 10.1520/STP104502.

Walker, P. J. *et al.* (2010) 'Design of a force acquisition system for high-energy short-

duration impacts', *Proceedings of the Institution of Mechanical Engineers, Part P: Journal of Sports Engineering and Technology*, 224(2), pp. 129–139. doi: 10.1243/17543371JSET65.

Wells, J. (2016) *How safe is your bicycle helmet?*, *The Independent*. Available at: https://www.telegraph.co.uk/health-fitness/body/how-safe-is-your-bicycle-helmet/ (Accessed: 23 July 2018).

Whiting, W. and Zernicke, R. (2008) *Biomechanics of musculo-skeletal injury*. 2nd edn. Champaign: Human Kinetics Publishers.

Williams, G. L. (2007) 'Improving fit through the integration of anthropometric data into a computer aided design and manufacture based design process'. Available at: http://hdl.handle.net/2134/4328.

Yamauchi, K. *et al.* (2010) 'Characteristics of upper extremity injuries sustained by falling during snowboarding: a study of 1918 cases.', *The American journal of sports medicine*, 38, pp. 1468–1474. doi: 10.1177/0363546509361190.

Yeadon, M. R. (1990) 'The simulation of aerial movement--II. A mathematical inertia model of the human body.', *Journal of biomechanics*, 23(1), pp. 67–74.

Zapata, E. *et al.* (2017) 'An ex vivo experiment to reproduce a forward fall leading to fractured and non-fractured radii', *Journal of Biomechanics*. doi: 10.1016/j.jbiomech.2017.08.013.